

Urban trees and stormwater runoff: The role of rainfall partitioning and transpiration on water regulation at the tree and watershed scales

by

Alireza Nooraei Beidokhti

B.S., Islamic Azad University of Mashhad, 2011

AN ABSTRACT OF A DISSERTATION

submitted in partial fulfillment of the requirements for the degree

DOCTOR OF PHILOSOPHY

Department of Biological and Agricultural Engineering
College of Engineering

KANSAS STATE UNIVERSITY
Manhattan, Kansas

2021

Abstract

Trees provide a variety of ecosystem services to urban communities. In addition to regulating urban microclimate and air quality, providing wildlife habitat, and improving the sense of well-being for people, trees also play a role in regulating the urban hydrologic cycle and thus contribute to the stormwater management. However, the actual effectiveness of preserving or planting trees and the extent to which urban tree systems (which include individual trees to remnant forests located in urban landscapes) contribute to the reduction of runoff volume at various scales is still unclear. This dissertation aimed to answer the overarching question of the extent to which urban tree systems are an effective and scalable approach for regulating the hydrologic response of urban watersheds. To address the question, (1) a meta-data analysis of the existing field studies was conducted to examine the magnitude and drivers of precipitation partitioning and transpiration processes by urban trees, taking into account tree structural characteristics and climatic conditions, at a tree scale, and (2) a mechanistic urban forestry hydrologic model was developed for three study watersheds in the Kansas City metro area, to better clarify the role of urban trees on the reduction of runoff at a watershed scale. At the tree-scale, the results of this analysis indicated that individual urban trees can intercept 10% to 60% of annual precipitation. In addition, the sap flux for studied urban trees ranged from 13.08 to 464.15 $g/cm^2/day$. At the watershed-scale, increasing tree canopy cover from 25% to 100% was predicted to reduce stormwater runoff volume from 6 to 38% for a relatively frequent storm event (25 mm over 24 hours); however, an attendant reduction in an impervious surface area representative of replacing existing impervious surfaces with tree planting pits was required to achieve these volume reductions. By systematically analyzing empirical evidence as well as a modeling approach regarding the potential effectiveness of urban tree systems, this work could

shed some more light on how urban tree systems can be accounted for in stormwater regulatory and management frameworks.

Urban trees and stormwater runoff: The role of rainfall partitioning and transpiration on water
regulation at the tree and watershed scales
by

Alireza Nooraei Beidokhti

B.S., Islamic Azad University of Mashhad, 2011

A DISSERTATION

submitted in partial fulfillment of the requirements for the degree

DOCTOR OF PHILOSOPHY

Department of Biological and Agricultural Engineering
College of Engineering

KANSAS STATE UNIVERSITY
Manhattan, Kansas

2021

Approved by:

Major Professor
Trisha Lynn Moore

Copyright

© Alireza Nooraei Beidokhti 2021.

Abstract

Trees provide a variety of ecosystem services to urban communities. In addition to regulating urban microclimate and air quality, providing wildlife habitat, and improving the sense of well-being for people, trees also play a role in regulating the urban hydrologic cycle and thus contribute to the stormwater management. However, the actual effectiveness of preserving or planting trees and the extent to which urban tree systems (which include individual trees to remnant forests located in urban landscapes) contribute to the reduction of runoff volume at various scales is still unclear. This dissertation aimed to answer the overarching question of the extent to which urban tree systems are an effective and scalable approach for regulating the hydrologic response of urban watersheds. To address the question, (1) a meta-data analysis of the existing field studies was conducted to examine the magnitude and drivers of precipitation partitioning and transpiration processes by urban trees, taking into account tree structural characteristics and climatic conditions, at a tree scale, and (2) a mechanistic urban forestry hydrologic model was developed for three study watersheds in the Kansas City metro area, to better clarify the role of urban trees on the reduction of runoff at a watershed scale. At the tree-scale, the results of this analysis indicated that individual urban trees can intercept 10% to 60% of annual precipitation. In addition, the sap flux for studied urban trees ranged from 13.08 to 464.15 $g/cm^2/day$. At the watershed-scale, increasing tree canopy cover from 25% to 100% was predicted to reduce stormwater runoff volume from 6 to 38% for a relatively frequent storm event (25 mm over 24 hours); however, an attendant reduction in an impervious surface area representative of replacing existing impervious surfaces with tree planting pits was required to achieve these volume reductions. By systematically analyzing empirical evidence as well as a modeling approach regarding the potential effectiveness of urban tree systems, this work could

shed some more light on how urban tree systems can be accounted for in stormwater regulatory and management frameworks.

Table of Contents

List of Figures	xi
List of Tables	xiii
Acknowledgements	xv
Dedication	xvi
Chapter 1 - Introduction	1
1.1 Urbanization and ecosystem services	1
1.2 Runoff issue in urban areas	1
1.3 The role of trees in regulating urban hydrology	2
1.3.1 Interception	3
1.3.2 Transpiration	4
1.4 Modeling hydrologic impacts of urban trees	5
1.5 Trees in urban versus natural environments	6
1.6 Gaps and objectives	9
1.7 Dissertation Organization	11
Chapter 2 - The effects of precipitation, tree phenology, leaf area index, and bark characteristics on throughfall rates by urban trees: a meta-data analysis	12
2.1. Introduction	12
2.2 Method	16
2.2.1 Literature search criteria and data extraction	16
2.2.2 Precipitation partitioning data extraction	17
2.2.3 Tree characteristic data extraction	18
2.2.4 Statistical Analysis	19
2.3 Results	20
2.3.1 Effects of tree phenology on precipitation partitioning	24
2.3.2 Effects of bark characteristics and leaf area index (LAI) on precipitation partitioning	26
2.4. Discussion	32
2.4.1 Study limitations	32
2.4.2 Comparison of precipitation partitioning by rural and urban forest canopies	35

2.4.3 Implications to urban stormwater management	36
2.5 Conclusion	38
Chapter 3 - A preliminary validation of empirical precipitation partitioning models	40
3.1 Introduction.....	40
3.2 Background: Gash and Rutter mechanistic models for estimating interception by forest canopies	41
3.3 Methods	45
3.4 Preliminary Validation Results and Discussion.....	47
3.4.1 Linear regression model performance.....	47
3.4.2 The nonlinear LAI interception rate model validation.....	52
3.5 Conclusion	54
Chapter 4 - The effect of climatic variables on urban trees' transpiration: A Meta data analysis	56
4.1. Introduction.....	56
4.2. Method.....	60
4.2.1 Literature search criteria and data extraction	60
4.2.2 Unifying the data.....	64
4.2.3 Regression and statistical analysis	67
4.3. Results.....	68
4.3.1 Sap flux comparison of different wood anatomy types	70
4.3.2 Correlation behavior of the variables.....	72
4.3.3 Simple linear regression models for modeling sap flux consistent with each independent variable	78
4.3.4 Simultaneous effect of multiple variables on daily sap flux	81
4.4. Discussion.....	83
4.4.1 Assumptions and consequential uncertainties.....	83
4.4.2 Water management	85
4.5. Conclusion	88
Chapter 5 - A modeling approach on the role of trees on the urban runoff management: A case study of three small watersheds in the Kansas City metropolitan area	90
5.1 Introduction.....	90
5.2 Method	94

5.2.1 Watershed descriptions	94
5.2.2 i-Tree Hydro model description and data requirements.....	96
5.2.3 Model calibration and validation	100
5.2.4 Model Scenarios.....	101
5.2.4.1 Tree canopy cover scenarios:.....	102
5.2.4.2 Tree seasonal and evergreenness scenarios	104
5.3 Results.....	105
5.3.1 Model calibration and validation	105
Figure 5-4 Total predicted water flow (m ³ /h) and discharge (m ³ /h) for the study watersheds over the validation time period	107
5.3.2 Tree canopy cover Scenarios	108
5.3.2.1 Design storm event -Water quality (25mm)	108
5.3.2.2 Design storm event - 10 year/24hour (140mm).....	110
5.3.3 LAI Scenario	112
5.3.4 Tree Evergreenness Scenarios	113
5.4. Discussion.....	115
5.5 Conclusion	118
Chapter 6 - Conclusion	121
6.1 Meta-analysis	121
6.2 Modeling.....	125
6.3 Stormwater management implications.....	127
References.....	128
Appendix A - Rainfall partitioning: Characterization of rainfall events, and additional information on canopy structure of the studied trees and their surrounding area	142
Appendix B - Supplemental data for rainfall partitioning analysis	151
Appendix C- Supplemental data for transpiration analysis	152

List of Figures

Figure 1-1 The growing trend of studies from 1995 to July 2020; using keywords interception, urban, and tree.....	7
Figure 1-2 The growing trend of transpiration studies from 1995 to July 2020; using keywords transpiration, urban, and tree	8
Figure 2-1 Regression model analysis for rainfall groups of 0-5 mm (a); 5-25 mm (b), 25-50 mm (c), and >50 mm (d)	25
Figure 2-2 Deciduous-leafless boxplot comparison of the throughfall/precipitation (TH/P) mean ranks of the Rough bark, and Smooth bark trees for rainfall group of 0-25 mm (a); and 25-100 mm (b). Differences in TH/P were significant for both rainfall classes.	27
Figure 2-3 Regression analysis for smooth and rough bark for deciduous leafless trees: rainfall group of 0-25 mm (a), and rainfall group of 25-100 mm (b).....	28
Figure 2-4 Regression analysis for smooth and rough bark for deciduous leafed and evergreen trees: rainfall group of 0-5 mm (a), 5-25 mm (b), 25-50 mm(c), and above 50 mm (d)	29
Figure 2-5 Evergreen and deciduous-leafed boxplot comparison of the throughfall/precipitation (%) mean ranks of the Rough bark, and Smooth bark trees for rainfall group of 0-5 mm (a), 5-25 mm (b), 25-50 mm, and above 50 mm	30
Figure 2-6 The nonlinear regression model on the effect of leaf area index (LAI) on the ratio of throughfall to precipitation (TH/P) for rainfall groups of; 0-5 (a), 5-25 (b), 25-50 (c), and above 50mm (d)	31
Figure 3-1 Measured vs. simulated interception storage for the linear regression model (Equation 3.11)	47
Figure 3-2 Measured vs. simulated interception storage for the multi-linear regression model (Equation 3.12)	48
Figure 3-3 Interception storage vs. gross precipitation for all the events in the independent dataset	51
Figure 3-4 Measured vs. simulated interception rate for LAI interception, Gash, Rutter, and WetSpa models	53
Figure 4-1 The boxplot comparison of daily sap flux for studied wood anatomy groupings for full dataset analysis (a) and non-limiting water analysis (b)	72

Figure 4-2 Daily data illustrating correlations between pairs of the following variables: sap flux (g/cm ² /day), Solar radiation (W/m ²), temperature (°C), and VPD (Pa) for diffuse-porous wood anatomy group for full dataset (a) and non-limiting water (b)	73
Figure 4-3 Daily data illustrating correlations between pairs of the following variables: sap flux (g/cm ² /day), Solar radiation (W/m ²), temperature (°C), and VPD (Pa) for Ring porous wood anatomy group for full dataset (a) and non-limiting water (b)	74
Figure 4-4 Daily data illustrating correlations between pairs of the following variables: sap flux (g/cm ² /day), Solar radiation (W/m ²), temperature (°C), and VPD (Pa) for conifer wood anatomy group for full dataset (a) and non-limiting water (b)	75
Figure 4-5 Regression models and coefficient of determination relating to studied wood anatomy groupings for full dataset analysis, and non-limiting water analysis.....	78
Figure 5-1- Land Cover distribution of surveyed watersheds	96
Figure 5-2 Example of IN05 watershed with 25% tree canopy cover increase for an application of scenario 1 (Top panel) and scenario 2 (bottom panel)	103
Figure 5-3 Total predicted water flow (m ³ /h) and discharge (m ³ /h) for the study watersheds over the calibration time period	107
Figure 5-4 Total predicted water flow (m ³ /h) and discharge (m ³ /h) for the study watersheds over the validation time period	107
Figure 5-5 Total volume reduction; comparison of watersheds in all levels of urbanization for a water quality (25mm) storm water design event in an application of both Scenario; Note, TU02-S1 underlies TH03_S1, and TU02_S2 underlies TH03_S2	109
Figure 5-6- Total volume reduction; comparison of watersheds in all levels of urbanization for a 10 year 24 hour (140mm) storm water design event in the application of both Scenario ..	111
Figure 5-7 Monthly total volume runoff reduction in percentage for residential (TU02) watershed	114
Figure 5-8 Monthly total volume runoff reduction in percentage for residential/commercial (TH03) watershed	114
Figure 5-9 Monthly total volume runoff reduction in percentage for industrial/commercial (IN05) watershed	115

List of Tables

Table 2-1 Average interception and stemflow (as reported over the specified study period) for urban tree canopy partitioning studies	21
Table 2-2 Summary statistics of throughfall values for various rainfall groups in studied tree types	24
Table 2-3 Multiple linear regression model of the effect of precipitation and LAI on throughfall values	31
Table 2-4 Standard regression coefficient result to identify the importance of LAI and precipitation for each rainfall group	32
Table 3-1- The results of the best linear equation fit along with R^2 , and RMSE as statistical criteria for evaluated models.....	49
Table 3-2- The results of the best linear equation fit along with R^2 , and RMSE as statistical criteria for evaluated models.....	52
Table 4-1 Urban tree transpiration studies identified through literature search. The spatial scale over which tree water use was reported included (1) sap flux across the outer 2 cm, J_o , (2) sap flux across the entire active sapwood area, J_s and (3) depth of water transpired per projected canopy area, EC. All studies used heat dissipation methods	61
Table 4-2- Summary of studied environmental variables including vapor pressure deficit (VPD), solar radiation (R_s), and temperature (Temp), and studied wood anatomy groups for each evaluated study; ✓: variable included in the study, ✗: variable was not included in the study	67
Table 4-3- Urban species maximum transpired water in sap flux ($g\ H_2O$ per cm^2 of sapwood area per day) and water use ($Kg\ H_2O$ per tree per day) for various characteristics including DBH (diameter of breast height in cm), PCA (projected canopy area in m^2), height (in m) , and SWA (sapwood area in cm^2) for diffuse porous wood anatomy grouping	68
Table 4-4- Urban species maximum transpired water in sap flux ($g\ H_2O$ per cm^2 of sapwood area per day) and water use ($Kg\ H_2O$ per tree per day) for various characteristics including DBH (diameter of breast height in cm), PCA (projected canopy area in m^2), height (in m) , and SWA (sapwood area in cm^2) for ring porous wood anatomy grouping.....	69

Table 4-5- Urban species maximum transpired water in sap flux (g H ₂ O per cm ² of sapwood area per day) and water use (Kg H ₂ O per tree per day) for various characteristics including DBH (diameter of breast height in cm), PCA (projected canopy area in m ²), height (in m) , and SWA (sapwood area in cm ²) for conifer wood anatomy grouping.....	70
Table 4-6- Statistical summary of variables including sap flux (g/cm ² /day), the temperature (°C), VPD (kPa), and solar radiation (W/m ²) for specified wood anatomy groupings.	71
Table 4-7- P-values and Spearman's rho for all the studied variables including sap flux (J _s), solar radiation, Temperature (Temp), and VPD over various wood anatomy groupings and soil water conditions.	76
Table 4-8 Simple linear regression results for studied wood anatomy groupings.....	80
Table 4-9- Multiple linear regression model results for studied variables including sap flux (J _s), temperature (Temp), solar radiation (R _s), and VPD across the wood anatomy groupings ..	81
Table 5-1- Study Watershed Characteristics.....	95
Table 5-2- Model inputs and related sources	99
Table 5-3- hydrologic parameters values attained through calibration process for current watershed conditions.....	105
Table 5-4- Nash-Sutcliffe Efficiency (NSE) ratios attained for study watersheds through model calibration process	106
Table 5-5- Watershed comparison for an example of 100% tree canopy over impervious surface cover for a water quality design storm event in the application of Scenarios 1&2	110
Table 5-6 Watershed comparison for an example of 100% tree canopy cover structures for a 10yr/24hr design storm event in the application of Scenario 1&2	112
Table 5-7 The effect of wide-range variation of LAI in stormwater runoff reduction for various levels of urbanization	113
Table 5-8 Yearly average of total runoff reduction; a comparison of all watershed area covered by evergreen trees with existing condition for the study watersheds	115
Table A.6-1 - Canopy structure, landscape, and rainfall features of final selected studies based on an event-based rainfall evaluation.....	147

Acknowledgements

This work has definitely been a challenge that could not have been accomplished without the assistance of many individuals. My deepest gratitude goes to Dr. Trisha Moore for her guidance and unconditional support throughout my doctoral program. While being far from family, she not only supported me as an advisor, but also as an encouraging family member. Words cannot express my gratitude, and, I sincerely thank Dr. Moore for everything that she has done for me. I would like to thank my dissertation chairman, Dr. Walter Dodds, and the rest of my committee members Dr. Mary Kirkham, Dr. Aleksey Sheshukov, and Dr. Charles Barden for their time and efforts. Dr. Kirkham provided excellent feedback that helped me broaden my research perspectives, and her profound knowledge and expertise in this area of research have always led me throughout my work. I am also grateful for the knowledge I gained while attending my advisor and my committee members' doctoral classes, as well as conducting research with them. Finally, I would like to thank my family and friends for all of the support that they gave me over the last few years.

Dedication

To my loving parents, Hossein and Ghodsieh, for their endless love.

In the memory of my father, whose unconditional love, kindness, and unwavering support always inspired me to work towards achieving my highest goals.

To my beautiful sister Shadi for always raising my spirits.

And to my lovely little nieces, Niayesh, and Yekta, and all my family and friends

Chapter 1 - Introduction

1.1 Urbanization and ecosystem services

Urban areas have rapidly grown, which is caused by increases in the number of people in these settings in recent decades. Urban planners and policymakers try to develop strategies to respond to this challenge. An established ecosystem framework (Millennium Ecosystem Assessment 2005) helps to identify the benefits of the natural environment to the urban population along with proposed planning recommendations (Kabisch, 2015). The ecosystem service framework categorizes the benefits of ecosystems for human society into the four classifications including provisioning (food, water, timber, and fiber) regulating (affecting climate, floods, disease, wastes, and water quality), cultural (recreational, aesthetic, and spiritual benefits), and supporting services (soil formation, photosynthesis, and nutrient cycling). Urban green spaces provide ecosystem services that can effectively oppose environmental problems caused by the increasing urban population (Bolund & Hunhammar, 1999). These services include air pollutant removal (Jim & Chen, 2008), urban heat island mitigation (Tan et al., 2016), energy consumption reduction (Z. H. Wang et al., 2016), urban noise reduction (Fang & Ling, 2003), increasing in carbon sequestration (Nowak & Crane, 2002), stormwater management advantages (Stovin et al., 2008a), preventing biodiversity loss through habitat provision for various species (Niemelä, 1999), and improving mental and physical health through stress reduction (Taylor et al., 2015)..

1.2 Runoff issue in urban areas

One of the most significant ecological issues associated with urbanization is the high percentage of impervious cover. The high percentage of urban settings impervious cover impacts hydrological processes, which, in consequence, causes the increase in the volume, peak rate, and

duration of surface runoff (Kalnay & Cai, 2003). Traditionally, gray infrastructure such as subsurface pipe networks were implemented to overcome this problem. Gray infrastructure collection systems are categorized into two groups; combined and separate. Combined sewer systems carry stormwater and sanitary sewage in the same conveyance construction, while separate sewer systems utilize separate pipes (Adam Berland et al., 2017). Both systems, however, face issues due to limited capacity, and improvement in these systems does not fully solve the surface runoff issue in urban areas. More recently, green infrastructure and green spaces have been introduced to the field of stormwater management due to the benefits and services they provide. This term is described as an interconnected network of greenspace that conserves natural ecosystem values and functions and provides associated benefits to human populations (Benedict & McMahon, 2012). Green infrastructure includes greening strategies to deal with the problems caused by urbanization and landscape change. Green infrastructure can be used to describe “engineered” vegetated systems such as rain gardens and bioretention systems, to vegetated streetscapes, to natural and semi-natural urban forests and wetlands (Kim & Park, 2016).

1.3 The role of trees in regulating urban hydrology

Trees are a critical component of green infrastructure in many cities as they play an essential role in providing ecosystem services. Among the services urban trees provide is stormwater runoff regulation. Above ground, trees intercept and evaporate incident precipitation to reduce runoff timing and volume. Trees may also reduce runoff by enhancing infiltration processes below ground and subsequently returning water stored in the soil profile to the atmosphere via transpiration. The following sections describe interception and transpiration processes in greater detail.

1.3.1 Interception

Canopy interception refers to the total amount of water stored on canopy surfaces (e.g., leaves, stems, branches) and evaporated from them. This value can be calculated by subtracting the amount of throughfall and stem-flow from the total precipitation. Throughfall is the proportion of rainfall that passes through or drips from the canopy to the ground. On the other hand, stem-flow runs along the stem and trunk of the tree to the ground at the tree's base. Stemflow and throughfall may infiltrate or become runoff, and it depends on characteristics of the soil and landscape of the environment around the tree. Meteorological variables and tree characteristics are the main drivers of the interception rate (Xiao et al., 2000; Zabret et al., 2018). Different trees vary based on tree size, health, leaf characteristics including canopy architecture, area, texture, angle, and bark features (Van Stan et al., 2015a). In a study of twenty species, coniferous trees showed a better ability to store water on their surface compared to broadleaf deciduous trees (Xiao & McPherson, 2016). Livesley et al. (2014) reported an interception rate of 29% and 44% of annual rainfall for two individual trees of the same species. Different interception rates were reported by Van Stan et al. (2015) for trees of the same size but with differing canopy architectures. Asadian & Weiler (2009) considered the effect of tree health in their study in which healthier trees were shown to intercept more rainfall. They assigned either poor or good categories to each tree based on the tree crown condition and the density of the foliage. Increased leaf area index (LAI) has been associated with higher rainfall interception rates in urban studies (Baptista et al., 2018; Beidokhti & Moore, 2019; Huang et al., 2017; Yang et al., 2019). Rainfall and meteorological variables such as rainfall intensity, duration, temperature, wind speed affect the interception rate. Less extreme rainfall events resulted in

higher interception rates than more intense, rainfall events (Van Stan et al., 2015a; Xiao, 2000; Xiao & McPherson, 2016, 2011b; Zabret et al., 2018; Zabret & Šraj, 2019).

1.3.2 Transpiration

Through transpiration, trees remove the water stored in the soil and send it back to the atmosphere through stems and leaves. This process also improves the capacity of the soil for water storage, and therefore, may improve initial soil infiltration rates. Environmental variables such as temperature, vapor pressure deficit, wind, soil moisture, and light, along with tree characteristics such as canopy density and type of species control the transpiration process. Soil-water status and condition of underlying soils can also influence transpiration rates. For example, Fair et al. (2012) evaluated the impact of soils with different bulk density on transpiration by a red maple tree. For trees grown in compacted soils, the transpiration rate was 70-80% lower compared to soil with greater porosity. The higher volumetric water content for less compacted soil was declared as the reason for higher transpiration rate. Kjelgren & Montague (1998) evaluated the influence of the landscape around the tree on the transpiration rate in Carbondale, IL, United States. They showed that in a pear tree placed in a parking lot, the water loss per unit of leaf area was almost 25% higher than the tree planted in the turfgrass. They theorized that microclimatic differences in surface temperature and long-wave radiation fluxes between these two landscapes could cause differences in transpiration rate. In a study performed in Beijing, China, LAI was shown to be an essential factor in impacting the transpiration rate (Wang et al., 2012). They observed a linear growing trend on daily transpiration (EC mm/day) by increasing in LAI values. The transpiration was highly variable among various species in a study done by Pataki et al., (2011) in Los Angeles, California. The transpiration rate varied between species from less than 0.5 mm per projected canopy area per tree to more than 2 mm. They also found a

significant difference between the transpiration rates for non-irrigated trees versus irrigated ones. In contrast, Chen et al., (2011) found no significant relationship between transpiration rates and soil water content. They stated that the ability of tree roots to access deep water caused no reduction in transpiration during a short drought period.

1.4 Modeling hydrologic impacts of urban trees

To the best of our knowledge, most of the measured field studies in urban settings are performed at a tree scale. Though, from a stormwater management standpoint, we are more interested in the impact of trees on urban management issues at larger scales such as a watershed or a city scale. However, due to the distinctive characteristics of individual trees and urban conditions, it is not easily possible to generalize the results at a tree scale in a measured study to larger scales. Therefore, urban modelling studies have been utilized to evaluate the effect of urban trees on runoff management. Efforts to quantify the aggregate impact of tree-scale processes at the scale of urban watersheds have relied on a variety of process-based and empirical models. In a more process-based modeling approach, the specialized forest interception models from Gash (1979) and Rutter et al. (1975), were compared to empirical/conceptual model which is an adapted solitary tree version of the Water and Energy Transfer between Soil, Plants and Atmosphere model (WetSpa) by Smets et al. (2019). Results based on two single tree setups showed that WetSpa outperformed Gash and Rutter models for rainfall events $> 10\text{mm}$ in predicting interception storage of a single tree. A water balance deterministic model was calibrated and validated using field experiment data to assess the capability of tree pits to mitigate runoff in from small ($< 0.05\text{ Ha}$) but highly impervious urban areas. The results of this study revealed that even in heavily urbanized areas with low conductivity soils, a 90% reduction in annual runoff is achievable (Grey et al., 2018). At the

watershed to city-scale, several studies have examined the potential influence of urban tree canopy on urban hydrology through modeling approaches such as the Curve Number method (Cronshey et al., 1985), in which interception and other tree-mediated hydrological processes are indirectly represented. For example, Sanders (1986) found that increasing the tree canopy cover in Dayton, Ohio by 22% could reduce the stormwater runoff by 7% based on the curve number method. Likewise, Yao et al. (2015) applied the curve number method to evaluate the effect of canopy cover increase on runoff reduction on a city scale in Beijing, China. Outcomes showed a 30% yearly reduction in runoff by adding approximately 11% of tree canopy cover. Matteo et al.,(2006) studied the watershed-wide ability of street and riparian buffering in urban to reduce runoff. They used a distributed/lumped parameter watershed model called generalized watershed loading function (GWLF) to simulate the watershed processes based on daily times steps weather data and water balance calculations. Results indicated that watershed stormwater runoff would be decreased through the location-specific application of riparian and street buffers. Others have adopted modeling approaches in which hydrologic processes associated with urban trees are explicitly represented. For example, Mittman (2009) examined the impact of the spatial distribution of vegetation using a spatially-distributed, process-based model called Regional Hydro-Ecological Simulation System (RHESSys). The results exhibited that, although riparian forests may provide better reduction of peak flow than upslope forests, upslope forests may provide a more significant reduction of runoff volumes.

1.5 Trees in urban versus natural environments

According to Scopus, a substantially higher number of studies have evaluated interception in natural forests and rural areas relative to urban areas. More than two thousand studies were found using keywords; tree, and interception, while only about 100 studies were

recognized using keywords urban, tree, and interception. As indicated in Figure 1.1, there is a growing trend in urban tree studies in which interception is a key word. Although not each of these studies entailed quantifying interception rates, the increasing publishing rate may indicate growing interest and/or recognition of hydrological roles played by trees in urban settings.

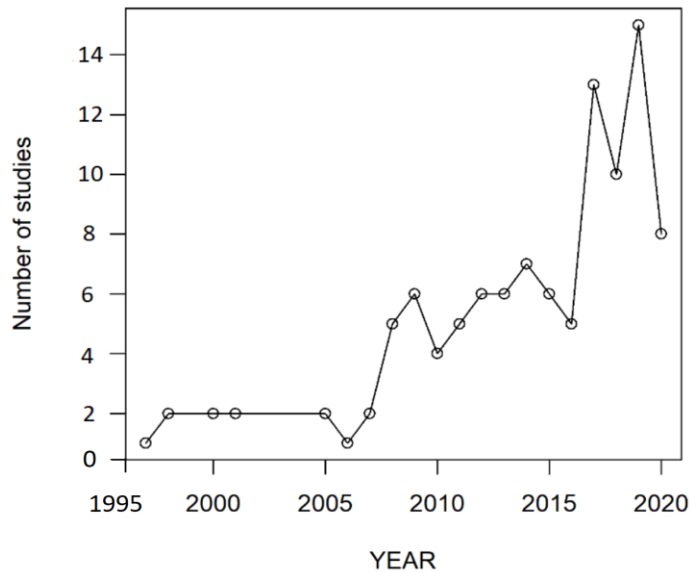


Figure 1-1 The growing trend of studies from 1995 to July 2020; using keywords interception, urban, and tree

The plantations of trees for urban areas are substantially different from natural forests both in arrangement and conservation methods. Therefore, more significant variability in the number of tree species exists in urban areas as compared to natural forests. There is less interaction between trees in urban areas as opposed to natural forests in which trees are isolated. This isolation causes less interface of intercepted water between trees (e.g. the leaf drip of one tree onto the adjacent tree). Meteorological variables differ in urban areas compared to natural forests. Wind can alter the distribution of rainfall in urban trees. Due to the angle through which

the rainfall is delivered to the tree, significant measurement errors might occur by mixing the rainfall and throughfall in the collection system in open-grown trees. Variation in leaf and stem surfaces due to open-grown condition in contrast with the interaction in the natural forest, as well as microclimate effects on urban trees due to inherent differences between urban and natural environment are also considered as reasons for differences in rainfall partitioning between urban and natural forests.

A similar search in Scopus using the keywords “tree” and “transpiration” revealed more than 5,600 applicable studies. However, only 158 of these corresponded to tree transpiration in urban areas. Figure 1.2 displays a growing trend of the studies associated with tree transpiration in the urban environment, which, as with interception studies, may reflect a growing interest in the effects of tree transpiration on urban water budgets.

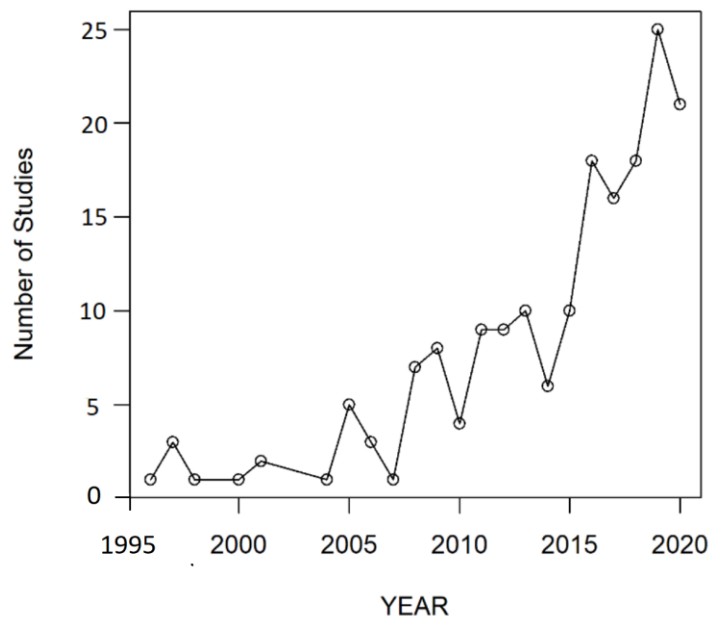


Figure 1-2 The growing trend of transpiration studies from 1995 to July 2020; using keywords transpiration, urban, and tree

Similar to interception, the tree transpiration is also likely to differ in urban areas in comparison with natural forests. The urban heat island affects the air temperature and vapor pressure deficit in urban areas relative to surrounding areas. Therefore, even the same species in natural forests may have different behavior, due to being exposed to a broader range of temperature and vapor pressure deficit (Bush et al., 2008), when they are planted in urban settings (Clark & Kjølsgren, 1990). Due to high impervious cover and compacted soils in urban areas, hydrological processes change, which in consequence, may influence soil water content as a major driver of tree transpiration (Craul, 1985; Hölscher et al., 2005). Additionally, there is a significant difference between species composition in urban areas as opposed to natural forests. In general, human cultivated species, nonnative, and invasive plants are more common in urban areas (Hahs et al., 2009; Walker et al., 2009).

1.6 Gaps and objectives

As mentioned in the previous section, trees have been less studied in urban areas compared to their rural counterpart and measured field studies were mostly performed on the scale of a tree. Although from a stormwater management standpoint, information is required on larger scales such as a watershed or a city, it is not easy to generalize the outcomes of an individual studied tree to all the trees. Models are developed to evaluate the effects of urban trees and urban greening on larger scales; however, variability in tree species and structures have made it challenging to assign single features to all groups of trees. Also, too detailed input data may cause complication in the model and render it inapplicable for stormwater management and policymaking purposes.

More specifically, insufficient information exists on the influence of both rainfall and canopy characteristics on rainfall partitioning components. While precipitation is a significant

driver in rainfall partitioning components, given the inherent discrepancies between natural and urban forest, it is not clear to what extent this factor can play a role in the rainfall partitioning of urban areas. Moreover, the impact of tree phenology, canopy and bark characteristics on the relationship between precipitation and rainfall partitioning components lacks in urban environments.

Although trees' transpiration has been indicated to have a significant effect on transmitting water from soil to the atmosphere, it is not clear how this transpired water varies among different species with differences in wood anatomies in urban areas.

On a large scale (e.g. watershed and city scales), existing studies have evaluated the effect of canopy cover on stormwater and runoff reduction in urban settings (Maco & McPherson, 2002; E. Gregory McPherson et al., 2011; G. E. McPherson et al., 2008; Service et al., 2008; Stovin et al., 2008b; J. Wang et al., 2008a). However, it has remained unclear how strategic canopy cover variation might affect the runoff volume reduction in different applications of urban areas. Besides, it is unknown how tree phenologic and canopy density (e.g. LAI) may be useful in reducing runoff in these settings.

This dissertation aims to highlight the role of trees on stormwater management in urban areas. More particularly, on a tree scale, how rainfall partitioning and transpiration processes vary in urban environments as well as how meteorological and tree characteristics may influence these two processes. Similarly, a process-based model was applied to better understand the aggregate hydrologic effects of increasing tree canopy cover at the small ($< 10 \text{ km}^2$) urban watershed scale across a range in landuse pattern and development intensity. The potential to further optimize urban hydrological responses by selecting trees with different phenological characteristics and canopy density was also explored.

The results of this work may help stormwater managers and policymakers to have a better understanding of the role of trees as a component in urban greening and green infrastructure plus providing them practical and simplified equations to estimate the extent to which trees can be practically credited and integrated in stormwater management programs.

1.7 Dissertation Organization

To achieve the objectives of the study, this work is organized to assess the effect of urban trees on both tree and watershed scales. In Chapter 2, the ability of urban trees to partition rainfall to throughfall and other components is evaluated through a meta-data analysis of experimental partitioning data collected at the scale of individual trees. A preliminary validation of the empirical rainfall partitioning equations resulting from this meta-data analysis is presented in Chapter 3. Similarly, in Chapter 4, a meta-data analysis is presented to evaluate the water-use ability of urban trees on a tree scale. Subsequently, in Chapter 5, and on a watershed scale, the effect of varying canopy cover on runoff reduction for various levels of urbanization is appraised. Finally, in the Chapter 6, the overall result of the study is presented as a conclusion.

Chapter 2 - The effects of precipitation, tree phenology, leaf area index, and bark characteristics on throughfall rates by urban trees: a meta-data analysis

2.1. Introduction

The urban forest, which includes street and park trees in public places, trees in residential yards and other privately-owned spaces, and remnant forest interspersed throughout urban developments, has gained increasing attention worldwide as a component of green stormwater infrastructure. Impervious surface cover in urban and suburban areas as well as the increase in the extreme events due to climate change (e.g. Tavakol et al., 2020a, 2020b) are linked to high volumes of stormwater runoff, flooding, water quality degradation, and other hydrological impacts. Trees can help counter such impacts in urban watersheds by delaying runoff through rainfall interception, soil infiltration, and transpiration processes (e.g., Berland et al., 2017; Kuehler et al., 2017). A better understanding of processes through which runoff can be reduced by urban trees could broaden recognition of hydrological services provided by urban trees and incentivize tree preservation and planting as part of meeting stormwater management goals (Baró et al., 2019; Hepcan & Hepcan, 2017; Livesley et al., 2016; E.G. McPherson et al., 2011; X. Wang et al., 2018).

Among the most widely studied processes through which urban tree canopies may regulate stormwater runoff are precipitation partitioning processes. As represented in Equation 2.1, precipitation (P) falling on tree canopies may be partitioned among throughfall (TH), interception (I) or stemflow (SF).

Equation 2.1

$$P = TH + I + SF$$

Here, the units are in "mm", and throughfall refers to the amount of rainfall that reaches the ground through the canopy, with or without contacting canopy surfaces. Interception is the amount of rainfall remaining on tree canopy surfaces and is evaporated after or during a rainfall event. Stemflow refers to precipitation that is delivered to the base of the tree via the trunk. As indicated by recent reviews on the topic (Berland et al., 2017; Cappiella et al., 2016; Kuehler et al., 2017), the extent to which urban forests may reduce the volume of stormwater runoff by interception or infiltrating rainfall at the base of the tree via stemflow is a growing area of interest to stormwater managers.

Seminal precipitation partitioning studies in rural forests described rainfall partitioning processes as a function of rainfall characteristics, meteorological factors, tree characteristics, and the interface between these elements (Gash, 1979; Rutter et al., 1975). Similarly, meteorological and vegetation characteristics have been identified as the most influential factors on rainfall partitioning in open-grown trees in urban areas (Crockford & Richardson, 2000; Staelens et al., 2008; Xiao et al., 2000; Xiao & McPherson, 2011). Meteorological variables explain the variability in rainfall partitioning through the influence of rainfall amount, duration and intensity, raindrop size, velocity and the number of raindrops (Levia et al., 2019; Magliano et al., 2019; Nanko et al., 2006; Zabret et al., 2018; Zabret & Šraj, 2018, 2019), and climate variables such as wind speed and direction, air temperature and humidity, net radiation (Bezák et al., 2018; Šraj et al., 2008; Van Stan et al., 2014; Zabret & Šraj, 2019). Vegetation characteristics of different species likely describe discrepancies in rainfall partitioning fates observed during similar precipitation events (Dietz et al., 2006; Staelens et al., 2008; Xiao et al., 2000; Xiao & McPherson, 2016) through leaf

area, leaf storage capacity, leaf characteristics (e.g. leaf architecture, and leaf morphology), and contribution of stems and branches (Kuehler et al., 2017). The influence of meteorological variables relative to vegetation characteristics was claimed to be more influential in urban areas (Tobaa & Ohtaa, 2005). Additionally, the amount of rainfall has been found to be the most influential variable among rainfall characteristics (Zabret et al., 2018).

The majority of rainfall interception studies have been conducted in rural forest ecosystems in climates ranging from arid and semi-arid to tropical. Rainfall interception by hardwood deciduous trees of the eastern United States was reviewed by Helvey & Patric (1965), who produced two regression models for winter and summer periods. Their analysis indicated a similar throughfall rates (90% of precipitation) for both winter and summer periods from which can be inferred 10% of rainfall was converted to interception or stemflow. Others have reported interception losses ranging from 10 to 50% of total precipitation as a function of forest characteristics and climate (Roth et al., 2007). In a review of selected studies from around the globe, Carlyle-Moses and Gash (2011), reported coniferous forest interception rates ranged from 16 to 45%), while hardwood forests ranged from 19 to 40%, and mixed and tropical forests ranged from 14 to 19%, and 6 to 32% respectively. In a meta-analysis of rainfall partitioning field studies representing 68 woody plant species in drylands, average interception, throughfall, and stemflow accounted for 24, 69.8, and 6.2% of total rainfall, respectively (Magliano et al., 2019). The authors noted that the proportion of throughfall increased along an increasing rainfall gradient observed across sites included in the analysis, while the proportion of stemflow and interception decreased.

While potential rates of interception or throughfall in urban tree canopies can be inferred from studies in rural settings, observations from rural forests may not translate directly to urban tree systems. The canopies of rural forests are generally characterized by a closed growth form as

opposed to more open canopy growth of urban forests (Macinnis-Ng et al., 2014; Marin et al., 2000; Sadeghi et al., 2016; Staelens et al., 2008). In addition, urban ecosystems have a unique climate which may lead to differences in the rainfall partitioning and therefore differences in the generation of runoff relative to natural forests (Alberti, 2008; Dobbs et al., 2014; McDonnell et al., 1997). There is a growing body of precipitation partitioning studies conducted in urban settings; however, there has not yet been a concerted effort to quantitatively synthesize the findings from urban studies to characterize expected ranges in canopy interception. Such synthesis would aid in quantifying the hydrological benefits of urban tree systems such as their impact on runoff reduction and could support stormwater managers interested in integrating urban tree systems in runoff management programs (Beidokhti & Moore, 2019; A. Berland et al., 2017; Gregory McPherson, 1992; Kuehler et al., 2017; X. Liu & Chang, 2019).

Insufficient and unknown information includes the effect of both rainfall and canopy characteristics on the relationship between precipitation and rainfall partitioning components in urban areas. It has been indicated that rainfall amounts can affect rainfall partitioning components; however, given morphological differences between rural and urban tree canopies, the extent to which precipitation partitioning responds to various rainfall amounts in urban areas is still unclear. Moreover, in many studies, evergreen trees intercepted more rainfall than deciduous trees, although the influence of the leaf-on and leaf-off period was not considered. Similarly, an understanding of bark and canopy characteristics (e.g. LAI) effect on the relationship between precipitation and rainfall partitioning components lacks in urban areas.

The objective of this study was to quantitatively describe relationships between rainfall characteristics and rainfall partitioning in urban tree canopies. We also aimed to evaluate the effect of tree characteristics – including phenological differences, bark roughness and canopy density (as

described by the leaf area index, or LAI) on partitioning processes and interactive effects with rainfall depth. More specifically, we aimed to answer the following questions:

- 1- How does tree phenology (evergreen versus deciduous; deciduous leafless versus leafed periods) affect precipitation-throughfall relationships?
- 2- Does bark roughness exert a significant effect on throughfall rates in urban settings?
- 3- To what extent does canopy LAI influence precipitation partitioning?

To answer these questions, we performed a meta-regression analysis of existing precipitation partitioning studies conducted in urban areas. The results are intended to deliver a general understanding between the patterns of precipitation-throughfall relationships in urban forests as compared to their rural counterparts based on a tree scale, event-based analysis. It also provides useful information for stormwater managers and policymakers to account for potential runoff reductions gained by preserving trees or planting new trees in urban developments.

2.2 Method

2.2.1 Literature search criteria and data extraction

A literature search using scholarly database search engines – including ISI Web of Knowledge, Scopus, and Google Scholar – was performed to identify relevant peer-reviewed studies published. Additional papers were identified from the reference lists of selected studies. A combination of the search keywords Urban, Tree, and Interception returned over 100 studies. To achieve the objective of this study, candidate papers were required to meet the following criteria: Firstly, only papers in peer-reviewed journals were analyzed. Secondly, papers with field studies were chosen (modeled studies were not considered). Thirdly, our focus was exclusively confined to measured studies of open-grown trees, which are most representative of trees grown in an urban

context. Eight studies were identified that met all of these criteria. In practice, interception is not directly measured. Rather, it is inferred based on the difference between measured precipitation, throughfall and stemflow values. Methods utilized to measure throughfall and stemflow components of rainfall partitioning were variable across the studies. Throughfall measurement methods included point measurements taken below the tree canopy using randomly placed rain gauges, linear troughs constructed from zinc-aluminum or PVC materials, area-based measurements using trapezoidal-shaped polyethylene sheets, or a combination of these methods. Stemflow was generally measured by wrapping tubing or other flexible material in a spiral around the bole of the tree to collect stemflow and direct it to a container or rain gauge at the base of the tree to be measured. Of the eight studies identified herein stemflow was measured in six, while in two others it was either neglected or assumed based on literature values. This inconsistency in the measurement of stemflow between studies could cause an error in estimating the true value of interception, as interception rates reported in the studies in which stemflow was not measured may reflect a combination of neglected stemflow and interception, particularly on an event basis. Therefore, we decided to conduct our analysis using throughfall values rather than interception values since all studies reported measured throughfall values.

2.2.2 Precipitation partitioning data extraction

Reported precipitation, throughfall, stemflow (when available) and interception depths were extracted from each study on an event basis. When these data were presented in graphs or other figures, the Web-Plot-Digitizer 4.1 tool (Ankit Rohatgi, 2019) was used to extract the essential numerical data. We acknowledge that the duration and/or the intensity of each rainfall event along with a host of other meteorological variables likely influence partitioning among throughfall, interception and stemflow. However, the majority of studies did not report event

duration or intensity; therefore, this analysis is limited to precipitation depth only. Each rainfall event was categorized into different groups according to depth: 0-5 mm, 5-25 mm, 25-50 mm, and >50 mm. These classifications roughly followed the distribution of rainfall events compiled in this dataset (see Appendix A). To verify that selected rainfall classes were appropriate for the analysis, we also plotted throughfall rate (as a percent of total-precipitation) versus precipitation and ran a linear regression model to assure the effect of precipitation depth was not significant when throughfall was normalized by the precipitation depth for all rainfall groups (see Appendix A).

2.2.3 Tree characteristic data extraction

Tree canopy and bark characteristics (e.g. crown shape, leaf density, leaf and bark roughness, stem and branch angle) can vary widely between and within species and, as reviewed previously, likely play a role in precipitation partitioning (e.g. Berland et al. 2017). There was a lack of consistency in the types of tree characteristics reported among the surveyed studies. Therefore, this analysis is limited to those characteristics reported among enough studies to include in the statistical analyses described in Section 2.2, and included tree phenology, bark texture and leaf area index (LAI). To understand how seasonal dynamics may influence precipitation partitioning by urban trees, each tree in the dataset was classified as either evergreen or deciduous. Precipitation partitioning data reported for deciduous trees was divided further into leaf-on and leaf-off periods. Each tree was then assigned to a bark texture category: rough or smooth. The majority of studies compiled for this analysis reported bark texture as either rough or smooth and, when provided, this same classification was adopted for this analysis. When bark texture was not provided by the study authors, additional literature review was performed using tree identification resources (Burns & Honkala, 1990b, 1990a; Santos Alves et al., 2014) to classify the bark according to the tree species given in the study. The third tree characteristic that we were able to

extract from enough studies was LAI, which describes the tree canopy density through a dimensionless number defined as one-sided green leaf area per unit ground area. While LAI varies over the course of the growing season, studies reporting LAI only reported a single value representative of the leaf-on period; thus, this analysis was limited to single values of LAI as reported by the studies compiled.

2.2.4 Statistical Analysis

Due to non-normal distributions of throughfall data within each rainfall grouping, the nonparametric Kruskal-Wallis with Dunn post-hoc was used to test for significant differences in throughfall among evergreen, deciduous-leafed and deciduous-leafless trees within each of the four rainfall classes. A linear regression analysis model was developed to describe the relationship between throughfall depth and rainfall event depth for evergreen, deciduous/leafed, and deciduous leafless trees. Multiple linear regression models were then developed to examine relationships between throughfall depth and available meteorological (precipitation depth) and tree morphological (LAI) data. The standardized regression coefficients method was used to identify the most important variable in multiple linear regression models. All the statistical analyses were performed using R-Studio. The readxl, basictrendline, pastecs, Hmisc, and FSA were utilized as user library packages for our analyses.

The influence of bark characteristics on precipitation partitioning was analyzed by first testing for significant differences in throughfall rates between bark types via the Kruskal-Wallis test and then characterizing throughfall rates as a function of rainfall depth via linear regression models grouped by bark type. Both of these statistical tests were conducted within the same rainfall groupings (0-5, 5-25, 25-50, and above 50 mm) used to examine differences in partitioning by tree phenology.

We performed an analysis to evaluate the effect of LAI on precipitation partitioning within specified rainfall classifications of 0-5, 5-25, 25-50, and greater than 50 mm. These analyses were limited to partitioning data for evergreen and deciduous-leafed trees (deciduous trees during the leaf-off period were assumed to have LAIs close to zero and were therefore not included) from the subset of studies in which LAI was reported (5 out of 8; see Appendix A). Although LAI varies over seasonal and annual scales, studies reporting LAI reported a single LAI value, typically corresponding to the peak of the growing season. As the first step in evaluating LAI impact on rainfall partitioning the total amount of throughfall during the leaf-on season in each study was divided by the total amount of precipitation to obtain an overall % throughfall rate for each tree with LAI data within each rainfall depth classification. This was done in an effort to normalize the effects of precipitation depth on observed throughfall depths (as discussed in 2.2.2, there was no significant relationship between % throughfall and rainfall depth within any of the four rainfall classifications) so that the influence of LAI could be assessed more directly. The effect of LAI on % throughfall within each rainfall depth classification was analyzed through a nonlinear regression model. A multiple linear regression model was also developed to evaluate the relative effects of precipitation and LAI on observed throughfall values. Following a multiple linear regression model, we developed a standard regression coefficient which normalizes the various independent variables with respect to their range of variation. This helps to understand which of the independent (precipitation depth and LAI) variables exerted a greater effect on the dependent variable (throughfall).

2.3 Results

Average interception and stemflow rates reported by studies meeting selection criteria are presented in Table 2.1. This dataset represents urban canopy precipitation data collected in four

different continents (North and South America, Australia, and Europe) across a wide range in climate (semi-arid to tropical). The dataset included observations from evergreen trees (n = 10) and deciduous trees during both leaf on (n = 4) and leaf off periods (n =4), thus enabling the effects of tree phenology on precipitation partitioning in urban areas to be analyzed. Additional study details, including tree characteristic variables, are provided in the Appendix A . In addition to the variables explored in this analysis (evergreenness, bark roughness, LAI), information regarding the landscape context in which trees were located was also extracted from studies. While all trees in this analysis were located in an urban area, their landscape context varied. For example, individual trees were located on a university campus, the streets of residential, industrial, or commercial areas, and in urban parks (see Appendix A). This variability in the landscape setting may have impacted rainfall partitioning due to differences in microclimate. However, we did not include landscape context as an explanatory variable in this analysis.

Table 2-1 Average interception and stemflow (as reported over the specified study period) for urban tree canopy partitioning studies

Study	Location	Tree Type	Study period	Climate (Köppen climate classification)	Interception%	Stemflow%
Xiao et al., 2000	Davis, California, US	<i>Pyrus calleryana</i> Deciduous *n=1	Dec 1996, 1997, and Jan-June 1998	Csa	15	8
Xiao et al., 2000	Davis, California, US	<i>Quercus suber</i> Evergreen n=1	Dec 1996, 1997, and Jan - June 1998	Csa	27	15

Guevara-Escobar et al., 2007	Queretaro City, Queretaro Mexico	<i>Ficus benjamina</i> Evergreen n=1	July - Oct 2005	Bsk	59.5	2.4
Asadian & Weiler, 2009	Vancouver, British Columbia, Canada	<i>Pseudotsuga menziesii</i> Evergreen n=3	Oct 2007 - June 2008	Cfb-Csb	49	N_M
Asadian & Weiler, 2009	Vancouver, British Columbia, Canada	<i>Thuja plicata</i> Evergreen n=3	October 2007 - June 2008	Cfb-Csb	61	N_M
Xiao & McPherson, 2011	Oakland, California, US	<i>Citrus limon</i> Evergreen n=1	2005-2007 during rainy seasons	Csb	27	2.1
Xiao & McPherson, 2011	Oakland, California, US	<i>Liquidambar styraciflua</i> Deciduous n=1	2005-2007 during rainy seasons	Csb	14.3	4.1
Xiao & McPherson, 2011	Oakland, California, US	<i>Ginkgo biloba</i> Deciduous n=1	2005-2007 during rainy seasons	Csb	25.2	1
Livesley et al., 2014	Melbourne, Victoria, Australia	<i>Eucalyptus nicholii</i> Evergreen n=1	25 May - 31 Oct 2009	Cfb	44	0.2
Livesley et al., 2014	Melbourne, Victoria, Australia	<i>Eucalyptus saligna</i> Evergreen n=1	25 May - 31 Oct 2009	Cfb	29	1.8
Véliz-Chávez et al., 2014	Queretaro City, Queretaro Mexico	<i>Ficus Benjamina</i> Evergreen n=1	2005 (summer and fall), and 2006 (spring, summer, and fall)	Bsk	65	2.1

Zabret et al., 2018	Ljubljana, Slovenia	<i>Betula pendula</i> Roth Deciduous n=not specified	January 2014 - June 2017	Cfb	45	1.2
Zabret et al., 2018	Ljubljana, Slovenia	<i>Pinus nigra</i> Arnold Evergreen n=not specified	January 2014 - June 2017	Cfb	72	0.02
Nytch et al., 2019	San Juan, Puerto Rico	<i>Calophyllum antillanum</i> Evergreen n=6	Sep -Nov	Af	16.7	N_M
Nytch et al., 2019	San Juan, Puerto Rico	<i>Albizia procera</i> Deciduous n=3	Sep - Nov	Af	22.7	N_M

*n= Number of individual trees of the specified species assessed in the study; N_M = Refers to studies in which stemflow is neglected or interception + stemflow included in interception; Af = Wet equatorial climate; Bsk = Tropical and subtropical steppe climate; Csa, Csb = Mediterranean climate; Cfb = Marine west coast climate

A total of 396 events across 8 different studies was evaluated. Of these, 81 events, corresponding to 3 different studies, were performed on deciduous trees during leafless periods. A total of 71 events for deciduous-leafed trees were extracted from 3 different studies. More data were available for the evergreen tree type with a total of 244 events extracted from 7 different studies. In the case of leafless deciduous trees, out of a total of 2607 mm of rainfall, 1915.25 mm fell through the canopy as throughfall. This implies a 73% throughfall rate. Similarly, the rate of throughfall for deciduous trees over the leafed period was 72% (1454.1 mm of throughfall out of total precipitation of 2007.6 mm). Evergreen trees had an overall throughfall rate of 63% (2709.95 mm of throughfall out of 4291.05 mm total rainfall), which was almost 10% less compared to the other two groups.

2.3.1 Effects of tree phenology on precipitation partitioning

Table 2.2 provides summary statistics for throughfall amounts reported for evergreen, deciduous-leafed, and deciduous-leafless trees within each rainfall depth grouping. There was no statistically significant difference between throughfall depths reported for evergreen and deciduous-leafed trees within any of the rainfall depth categories. Throughfall depths reported for evergreen trees were significantly lower than leafless deciduous trees for rainfall classifications of 5 – 25 mm ($p= 2.01 \times 10^{-6}$) and 25-50 mm ($p= 0.004$). Measured throughfall depths for leafed deciduous trees were significantly lower than leafless deciduous trees only for rainfall classification of 5-25 mm ($p= 1.01 \times 10^{-3}$).

Table 2-2 Summary statistics of throughfall values for various rainfall groups in studied tree types

Tree type	Mean [SD] 0-5 mm	Mean [SD] 5-25 mm	Mean [SD] 25-50 mm	Mean [SD] Above 50 mm
Evergreen throughfall (mm)	1.1 [1.03] n=81	6.69 [5.15] ** n=99	23.03 [9.04] ** n= 46	48.54 [16.3] n=17
Deciduous-leafed throughfall (mm)	1.01 [0.91] n=9	7.32 [4.9] ** n=29	27.28 [9.41] n=21	55.01 [21.19] n=12
Deciduous-leafless throughfall (mm)	1.24 [1.06] n=31	13.34 [6.21] n=29	31.55 [4.91] n=13	61.82 [12.16] n=8

n= Number of throughfall values; [SD] = Standard deviation; **= Significantly different from deciduous-leafless trees

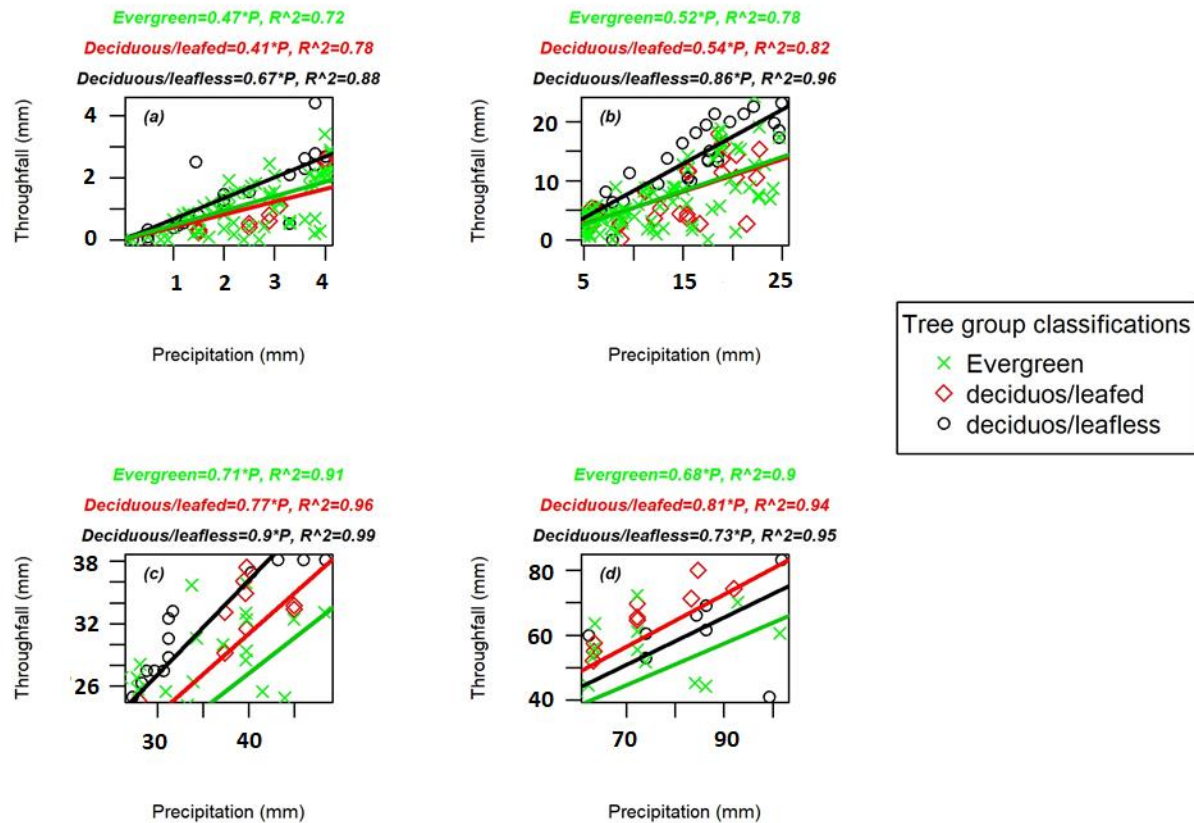


Figure 2-1 Regression model analysis for rainfall groups of 0-5 mm (a); 5-25 mm (b), 25-50 mm (c), and >50 mm (d)

Precipitation depth was a significant predictor ($p < 0.05$) of throughfall observed throughfall depths for all tree types in every rainfall classification (Figure 2.1). The high magnitude of R^2 for almost all regression equations indicates the ability of precipitation depth to explain the majority of variability in throughfall rates, particularly for rainfall classes higher than 5 mm.

As can be seen in Figure 2.1, throughfall rates during small rainfall events (< 5 mm) were on the order of 67% for leafless deciduous trees. This observation implies that in the absence of leaves, trees' stems and branches may intercept and/or direct precipitation to the base of the tree via stemflow 33% of the rainfall amount for such small events. For the same rainfall group

classification, the average increase in throughfall value per unit precipitation in deciduous-leafed period and evergreen trees was 41% and 47% respectively.

For the rainfall amounts falling between 5-25 mm, the average increase in throughfall value per unit precipitation was as high as 86% for leafless deciduous trees, reflecting interception and/or stemflow rates of 14%. In contrast, evergreen and deciduous-leafed trees exhibited throughfall rates of 52% and 54%, respectively, for this rainfall class. For rainfall amount classification of 25-50mm, evergreen trees had throughfall rates of 70% compared to 77% for deciduous leafed trees and 90% of for deciduous leafless trees. For the studied group of rainfall values above 50mm, almost 68% of rainfall reached to the ground as throughfall for evergreen trees. Also, deciduous leafless trees with 73% of the throughfall rate showed a greater ability on intercepting rainfall as compared to its leafed counterpart with a throughfall rate value of 81%.

2.3.2 Effects of bark characteristics and leaf area index (LAI) on precipitation partitioning

Since phenology-related effects on precipitation partitioning were only detected between deciduous leafless and evergreen/deciduous leafed trees, the effects of bark roughness were analyzed first for deciduous leafless trees and then for evergreen and deciduous leafed trees together. In the case of deciduous leafless trees, rainfall classifications were combined to 0-25 and 25-100 mm due to a lack of data across all rainfall groupings for leafless trees. Rainfall categories of 0-5, 5-25, 25-50, and above 50 mm were maintained for the evergreen/deciduous leafed group. A statistical comparison between smooth and rough barked deciduous trees during leafless periods indicated significant differences in throughfall rates for both rainfall groups evaluated (Figure 2.2). In the 0-25 mm rainfall class, observed throughfall rates were significantly lower for rough-barked trees ($p = 6.9 \times 10^{-8}$). Similarly, significantly lower throughfall depths (and, hence, higher

interception and stemflow rates) were observed for rough-barked trees in the 25-100 mm rainfall category ($p=0.03$; Figure 2.2).

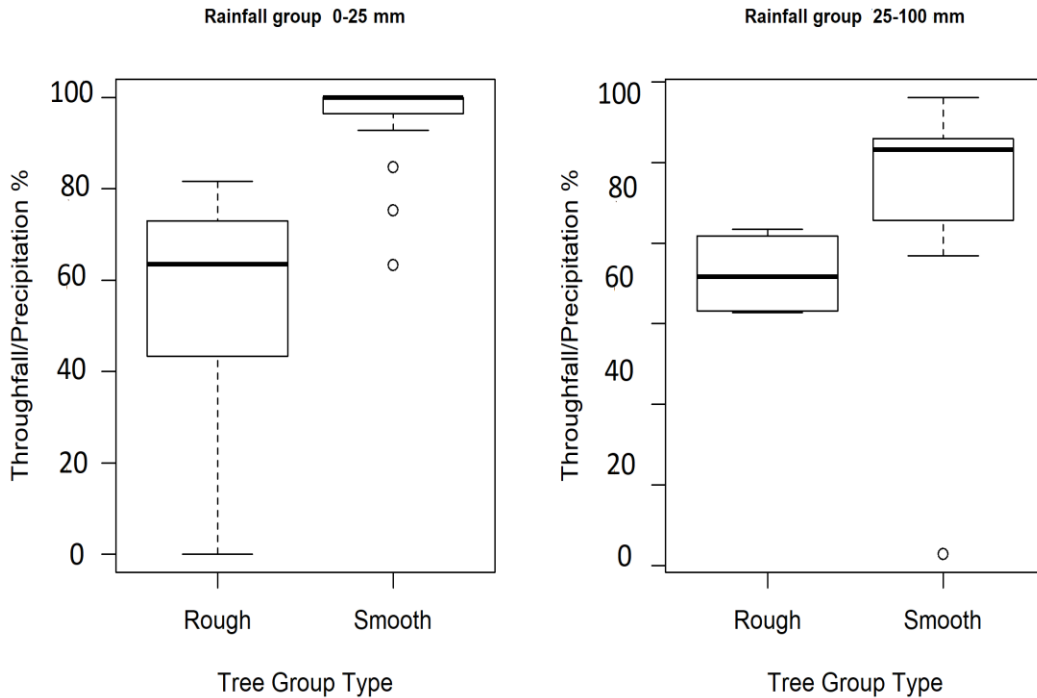


Figure 2-2 Deciduous-leafless boxplot comparison of the throughfall/precipitation (TH/P) mean ranks of the Rough bark, and Smooth bark trees for rainfall group of 0-25 mm (a); and 25-100 mm (b). Differences in TH/P were significant for both rainfall classes.

Figure 2.3 provides the regression model along with equations and coefficient of determination for deciduous leafless trees for 0-25 mm and 25-100 mm rainfall groups. For the rainfall group of 0-25 mm, higher rates of throughfall were observed for smooth bark (95%) compared to rough bark trees (73%). In the 25-100 mm group, throughfall rates for both smooth and rough bark trees follow a similar trend.

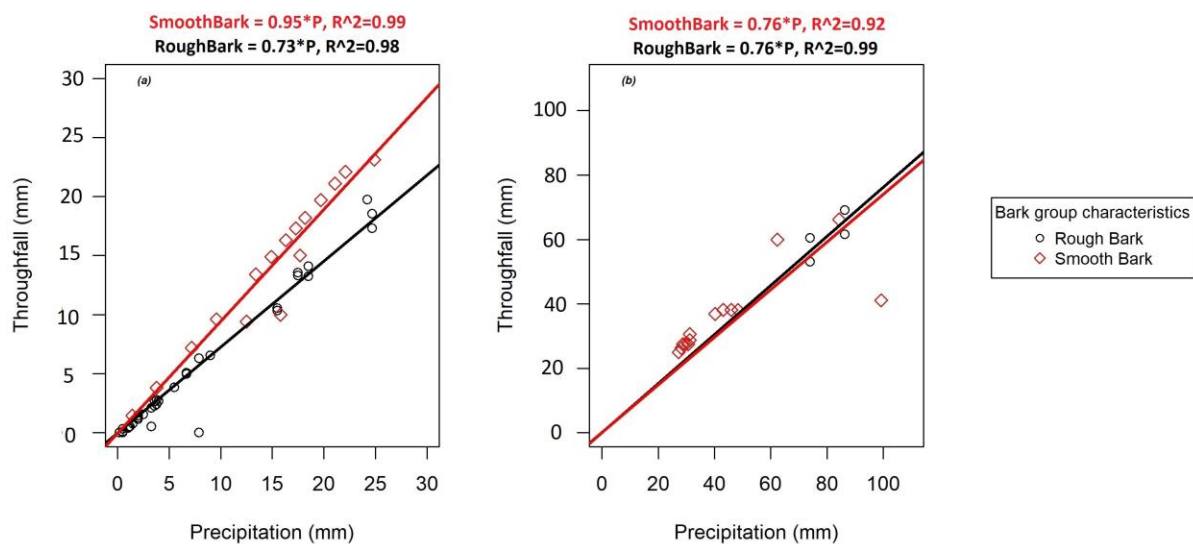


Figure 2-3 Regression analysis for smooth and rough bark for deciduous leafless trees: rainfall group of 0-25 mm (a), and rainfall group of 25-100 mm (b)

Owing to the lack of significant difference in throughfall depths observed between evergreen and deciduous-leaved trees, these two tree groupings were combined prior to performing a similar analysis of bark texture. Figure 2.4 displays regression models and coefficients of determination for evaluated rainfall groups. In the 25-50 mm rainfall group, smooth and rough bark exhibited similar throughfall rates (71% and 72%, respectively). Counter to expectations though, throughfall rates for rough bark were numerically higher than throughfall rates for smooth bark across all other rainfall groupings. These differences were only significant for rainfall classes of 5-25 mm ($p=0.01$) and above 50 mm ($p= 0.03$). The other two rainfall classes (0-5 mm and 25-50 mm) exhibited no statistically significant differences (Figure 2.5).

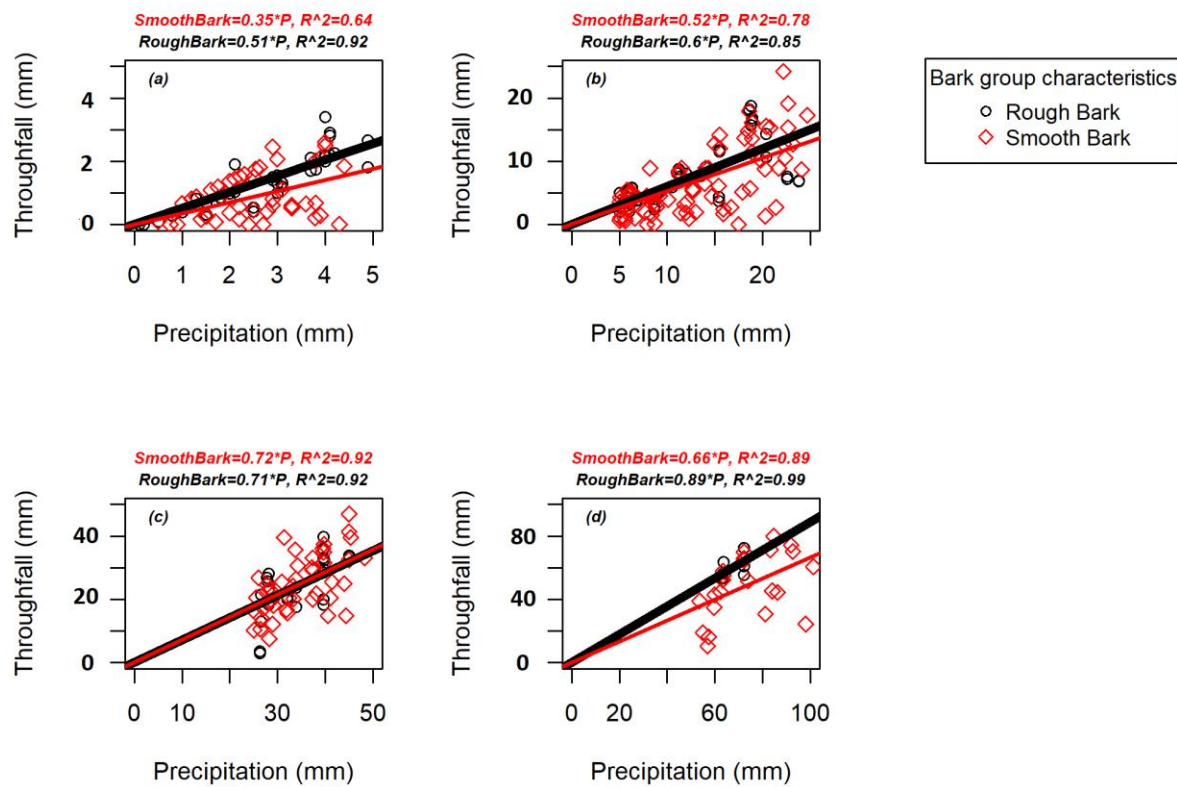


Figure 2-4 Regression analysis for smooth and rough bark for deciduous leafed and evergreen trees: rainfall group of 0-5 mm (a), 5-25 mm (b), 25-50 mm(c), and above 50 mm (d)

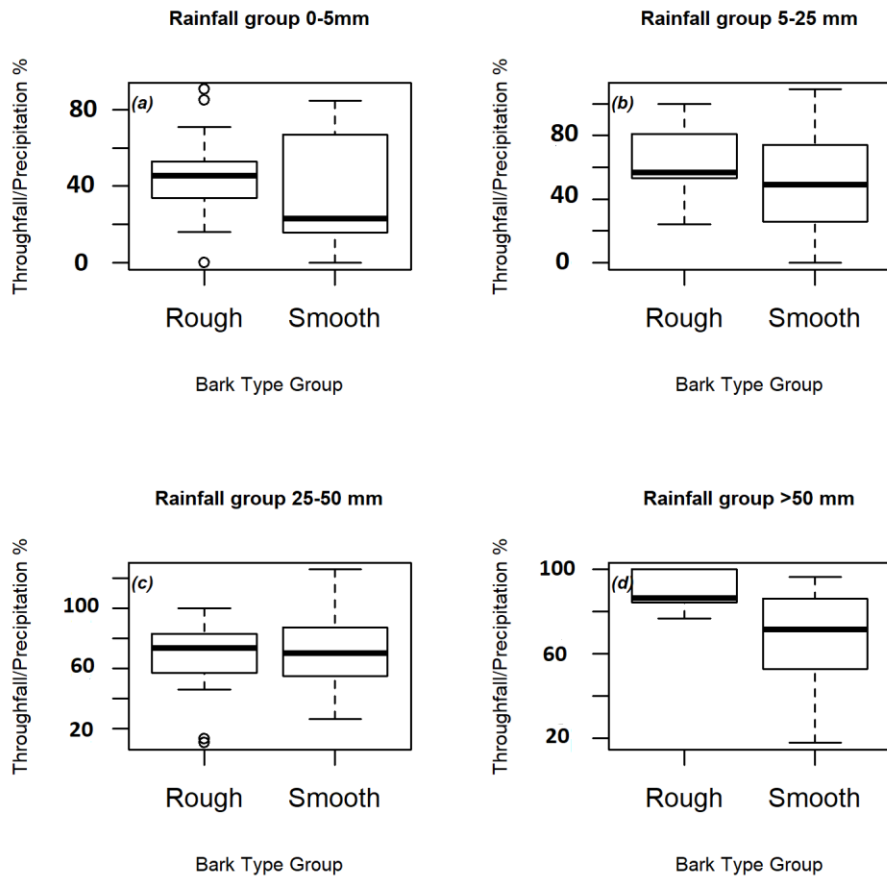


Figure 2-5 Evergreen and deciduous-leaved boxplot comparison of the throughfall/precipitation (%) mean ranks of the Rough bark, and Smooth bark trees for rainfall group of 0-5 mm (a), 5-25 mm (b), 25-50 mm, and above 50 mm

As depicted in Figure 2.6, an inverse relationship was observed between overall throughfall rates (that is, the ratio of total throughfall to total precipitation in each study) and LAI. This relationship appeared to be non-linear and was best explained through a logarithmic relationship. As indicated by the value of the slope terms in in each rainfall grouping, it seems that LAI exerts a greater influence on throughfall rates for higher rainfall values.

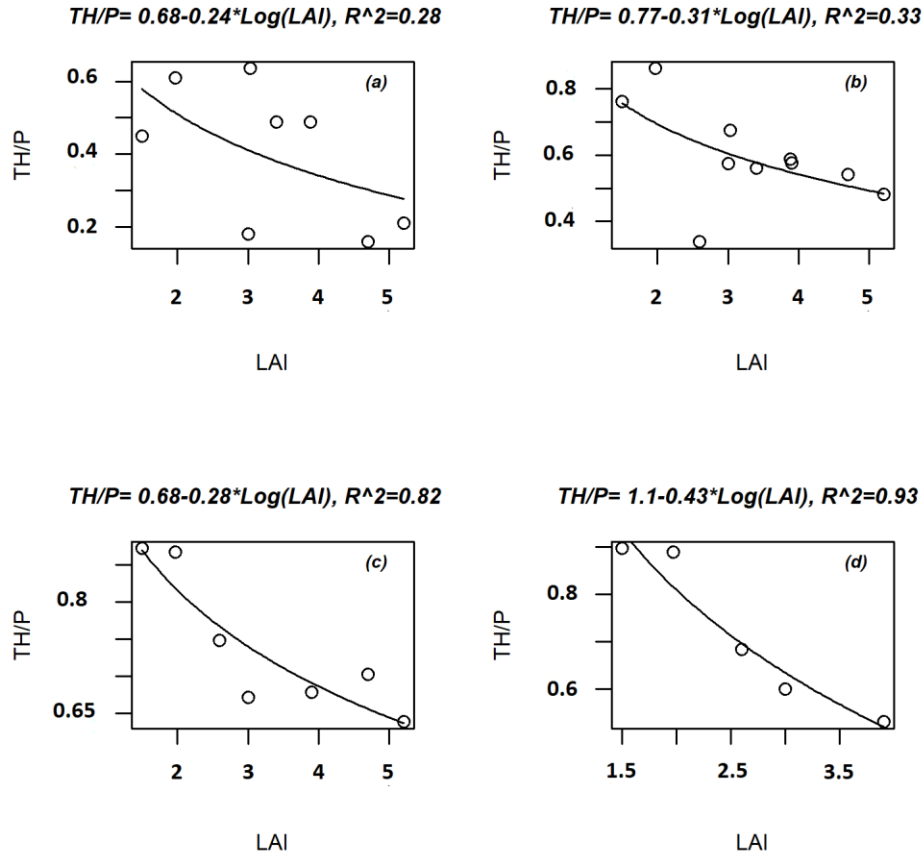


Figure 2-6 The nonlinear regression model on the effect of leaf area index (LAI) on the ratio of throughfall to precipitation (TH/P) for rainfall groups of; 0-5 (a), 5-25 (b), 25-50 (c), and above 50mm (d)

The simultaneous effects of precipitation depth and LAI on throughfall depths in urban tree canopies was examined through a multiple linear regression model (Table 2.3). As expected, precipitation and LAI exhibited positive and inverse relationships with throughfall, respectively.

Table 2-3 Multiple linear regression model of the effect of precipitation and LAI on throughfall values

Rainfall group (mm)	Precipitation coefficient	LAI coefficient	Coefficient of determination (R^2)	P-value
0-5 *n= 74	0.56	-0.08	0.48	$2.4 * 10^{-11}$

5-25 n= 102	0.68	-1.09	0.58	2.2*10 ⁻¹⁶
25-50 n= 57	0.77	-2.51	0.43	8.3*10 ⁻⁸
>50 n= 29	0.79	-12.2	0.47	9.2*10 ⁻⁵

*n= Number of data points for each rainfall group

The value of coefficients in the multiple linear regression model also suggest LAI becomes more influential on precipitation partitioning as the rainfall amount increases. The standard coefficient regression model supports this supposition by indicating an increasing effect of LAI for higher rainfall values (Table 2.4). As can be observed from the table, precipitation depth exerts the greatest influence on throughfall depth when the rainfall amount falls between 5 – 25 mm. While the relative influence of precipitation is greater than LAI for rainfall groups below 50 mm, LAI may exert a greater control on the amount of rainfall partitioned between throughfall versus interception/stemflow than precipitation when rainfall amount is above 50 mm.

Table 2-4 Standard regression coefficient result to identify the importance of LAI and precipitation for each rainfall group

Rainfall group (mm)	Precipitation coefficient	LAI coefficient
0-5	0.69	-0.06
5-25	0.76	-0.21
25-50	0.59	-0.31
>50	0.57	-0.62

2.4. Discussion

2.4.1 Study limitations

The meta-analysis approach adopted for this study provides insights to the relative magnitude of precipitation partitioning processes in urban tree canopies and to the relative effects of precipitation depth, bark roughness, and LAI. However, the results of these analyses

should be interpreted in light of various study limitations. Many of these limitations stem from the relatively small number of studies (8) published to date in which precipitation partitioning by urban tree canopies has been measured. Owing to this relatively small dataset, we were unable to include numerous variables that likely are important determinants of precipitation partitioning. For example, although most of the evaluated studies were conducted during rainy seasons, some were conducted over a long-term period with both rainy and non-rainy seasons included. Rainfall events in different seasons and in different geographic areas represented in this analysis are certain to occur with different intensity and under differing meteorological conditions. However, the only variable included in this study to characterize rainfall events was rainfall depth. This analysis was limited to rainfall depth because few studies also reported rainfall intensities or other meteorological variables. Unaccounted for heterogeneity in meteorological variables across studies may cloud interpretation of any of our analyses. As noted previously, differences in landscape context may influence urban microclimates and, hence, precipitation partitioning processes. The dataset in our study was too small to include landscape features in the analysis but investigating the effect of different urban landscapes on rainfall partitioning warrants additional research.

Canopy structure is a broad concept that includes a variety of factors such as characteristics of the trunk and bark, branches, leaves, and overall shape of the tree. In this analysis, we used LAI as a quantitative descriptor of canopy structure as it was the most common metric of canopy density reported across the collection of studies analyzed herein. However, LAI is just one aspect of canopy structure that may play a role in precipitation partitioning. For example, stem, leaf and branch angles, which were not quantified in most studies and were not considered in this analysis, are thought to be important determinants of stemflow and throughfall

(e.g., Livesley et al., 2014). Other features, such as canopy shape, can be described by a range of qualitative descriptors, but our study was limited in including such factors due to the relatively small size of the dataset and lack of reporting in studies reviewed. We did attempt to consider bark texture by qualitatively characterizing the bark of trees in this dataset as “rough” or “smooth.” There may be error in these groupings as not all trees have merely rough or smooth bark. For example, bark texture may change from relatively smooth in young trees and become rough as a tree matures. In some tree species, bark texture changes throughout the course of the growing season as bark is sloughed off. Results of the bark roughness analysis for evergreen and deciduous leafed trees were somewhat inconclusive and may reflect inaccuracies in bark roughness categories. Alternatively, these results may indicate that leaf surfaces play a greater role in determining the fate of incipient precipitation when leaves are present. The effect of bark texture followed expectations for deciduous trees during leafless periods, with more throughfall generated under smooth-barked trees. This result indicates that, even though stemflow may be higher for smooth barked trees (e.g., Livesley et al., 2014), rough-barked trees tend to intercept more precipitation, leading to lower throughfall rates below rough-barked, leafless canopies. Despite these limitations and unaccounted for heterogeneity in the climate and landscape context in which this set of 8 studies was conducted, precipitation depth emerged as an important control on precipitation partitioning, explaining over 70% of variability in observed throughfall depths for small and large rainfall events, regardless of tree phenological conditions. We note that, the number of data points for each rainfall group (i.e., 0-5m, 5-25 mm, 25-50 mm and > 50 mm) was not evenly distributed. This non-homogeneity of data availability between rainfall groups may have influenced the result. In general, more data were available for evergreen compared to deciduous leafed and deciduous leafless trees. Also, more data existed for rainfall groups below

25 mm. Therefore, we are more confident about the results obtained for evergreen trees and rainfall groups below 25 mm. Additional measurements of throughfall and stemflow within urban deciduous tree canopies, particularly for rainfall amounts exceeding 25 mm, could improve future efforts to characterize the effects of tree phenological factors on rainfall partitioning.

2.4.2 Comparison of precipitation partitioning by rural and urban forest canopies

Comparison between the results of this study with similar analyses in rural forest ecosystems, where the majority of precipitation partitioning studies have been conducted, is of interest to understand the extent to which the results of such studies could be generalized to open grown, urban forest canopies. As averaged over the study period for individual urban trees included in the dataset compiled herein, interception rates ranged from 14 to 72%. Various reviews from rural forests suggest an overlapping, though perhaps narrower range in overall interception rates (10 to 50%) (Barbier et al., 2009; Carlyle-Moses and Gash, 2011; Magliano et al., 2019; Roth et al., 2007). In a review of rainfall interception by hardwoods of the eastern United States, Helvey & Patric (1965) produced regression models for winter (leafless) and summer (leafed) periods to describe throughfall rates as a function of precipitation depth on an event basis. Their regression models – which spanned a comparable range in precipitation depth as our study - indicated throughfall represented 90% of precipitation for both winter and summer periods. The rate of change of throughfall in response to precipitation for urban trees ranged as analyzed herein was 0.4 to 0.8 for deciduous leafed trees and 0.7 to 0.9 for deciduous leafless trees. Therefore, a comparison between the results from studies in rural forest ecosystems to the results of this analysis suggest urban trees have a higher capacity to intercept rainfall compared to their rural counterparts.

2.4.3 Implications to urban stormwater management

We posed three research questions to gain insight to factors that affect precipitation partitioning by urban trees. In the following section, these questions are discussed in the context of the meta-analysis conducted here along with potential implications to stormwater management in urban landscapes.

How does tree phenology affect precipitation-throughfall relationships? The meta-analysis conducted herein indicates a higher interception average for evergreen trees relative to deciduous trees in urban areas. This observation makes sense as evergreen trees retain their foliage throughout the year. However, this generalization does not account for other factors, such as seasonal timing of precipitation, amount of rainfall, and canopy characteristics. Due to variations in canopy characteristics, some deciduous trees might intercept more rainfall than evergreen trees during a leaf-on period. Therefore, if runoff issues are of greatest concern during periods in which deciduous trees have their leaves on, maintaining deciduous trees with dense canopies may provide similar (or better) stormwater runoff management benefits than evergreen trees even if the latter show a better ability to intercept rainfall on an annual basis. For regions in which wet periods coincide with the non-growing season, evergreen trees are likely to provide greater stormwater runoff reduction benefits. A result of this study showed a better ability of deciduous leafless trees on intercepting rainfall as compared to its leafed counterpart for large rainfall events (above 50 mm). However, this result is counter intuitive and might be associated with the small dataset. Therefore, it could raise a future study question to more particularly investigate the capability of stems and branches on rainfall interception for large rainfall values.

Does bark roughness exert a significant effect on throughfall rates in urban settings?

Although bark characteristics are likely to influence stemflow (e.g., Barbier et al., 2009; Van

Stan et al., 2015)., our analysis suggests bark roughness may also influence throughfall, particularly during leaf-off periods. In this analysis, differences in throughfall rates below smooth- and rough-barked trees were not only statistically significant; they are also of a magnitude potentially relevant to stormwater management (difference in median value nearly 40% for events < 25 mm and 15% for events > 25 mm; Figure 2.2). By comparison, the influence of bark roughness for evergreen and deciduous leafed trees was less conclusive and somewhat counterintuitive as rough-barked trees were found to have significantly higher throughfall rates than smooth-barked trees within rainfall classes of 5-25 mm and > 50 mm. This result may indicate that other canopy characteristics (e.g., leaf density) play a greater role during leafed periods such that the effects of bark roughness are less evident .However, we should also consider that underlying causes such as the small number of data points, unevenly distribution of data points within each class across the different tree groupings (see Supplementary Information), intensity of rainfall, differences in other rainfall characteristics, and canopy characteristics may affect this result. Overall, additional studies are required to determine the influence of bark and branch characteristics on rainfall partitioning in urban tree canopies.

To what extent does canopy LAI influence precipitation partitioning? Intuitively, denser tree canopies, which are characterized by higher LAI values, are expected to intercept more rainfall. Our analysis supported this supposition, particularly for precipitation values exceeding 25 mm. LAI is dynamic over time, while it is regularly reported as a constant variable. However, we were able to detect an effect of LAI on precipitation partitioning even though our analysis was limited to a single LAI value as reported in individual studies. Therefore, we performed our analyses based on our interpretation of the results on LAI support using trees with higher LAI to reduce runoff volumes in urban areas, particularly for storms greater than 25 mm.

Even though some studies claim that the impact of meteorological factors, specifically rainfall characteristics, on rainfall partitioning overcomes the effect of canopy structure (Tobaa & Ohtaa, 2005; Zabret et al., 2018) more studies are needed to evaluate this assertion. Our results show that for rainfall amounts above 50 mm, the effect of LAI as one component in canopy structure, exerts a greater influence on observed throughfall rates than rainfall depth. This result suggests that, from a stormwater management standpoint, selected tree species and/or maintaining trees in ways that promote dense, vertically structured canopies is beneficial. Similarly, our results also indicated that trees with different phenology type can significantly differ in partitioning the rainfall if rainfall values fall between a range of 5-25 mm. This outcome suggests that runoff management policies could specify desired tree characteristics (e.g., high leaf density, rough bark if deciduous) to promote runoff reduction benefits.

2.5 Conclusion

We analyzed how throughfall in urban tree canopies varies with changes in rainfall amounts for rainfall classifications of 0-5 mm, 5-25 mm, 25-50 mm, and above 50 mm for a total of 396 events. These data were compiled from studies conducted on four different continents in a wide variety of climates. Also, the influence of bark characteristics and LAI on the amount of rainfall that reaches the ground as throughfall for various rainfall classifications in different phenological groupings was evaluated. The throughfall rate was significantly higher for deciduous-leafless trees than evergreen trees for 5-25 and 25-50 mm rainfall classes. Similarly, deciduous-leafless trees showed significantly higher throughfall rates compared to deciduous-leafed trees for rainfall class of 5-25 mm. Significantly lower throughfall rates were observed for rough-barked deciduous trees than smooth-barked during leafless periods. LAI also influenced throughfall values, with the strongest effects observed for rainfall groupings > 25 mm. While the

influence of precipitation amount on throughfall values was more influential for rainfall groups below 50 mm, LAI exerted a greater effect on observed throughfall values relative to precipitation depth for rainfall depths exceeding 50 mm. An average across all the rainfall group regression models showed a mean throughfall coefficient values of 0.59, 0.63, and 0.79 for evergreen, deciduous leafed, and deciduous leafless trees. This result was comparable to the only other event-based meta-data analysis of which we were aware, in which Helvey and Patric (1965) reported throughfall regression model coefficients of 0.9 for both summer and winter periods in hardwood rural forests of the eastern United States. However, their study was performed on a stand scale as opposed to our study which was done on a single tree scale. Observed differences between our analysis of urban trees and similar analysis conducted in rural forests warrant additional study of precipitation partitioning by urban forests. Apparently lower throughfall rates (and corresponding higher interception and/or stemflow) in our analysis could correspond to effects of unique microclimates on open-grown tree in various urban landscapes; however, more in-depth research is required to evaluate the extent of which urban microclimate or other conditions affect partitioning of rainfall.

Chapter 3 - A preliminary validation of empirical precipitation partitioning models

3.1 Introduction

The regression models developed in Chapter 2 to estimate rainfall partitioning by urban tree canopy utilized LAI and/or rainfall depth as the only predictive variables. However, as discussed in Chapter 2, meteorological variables, along with canopy characteristics, play an essential role in rainfall partitioning by trees. Inclusion of additional meteorological and canopy variables was not possible in the context of the meta-analysis described in Chapter 2 and remains a limitation of statistical models produced through this meta-analysis. In contrast, mechanistic models aim to mathematically represent physical and biological processes that control precipitation partitioning and could therefore be assumed to provide a more accurate estimate of canopy interception and throughfall across widely ranging canopy and meteorological conditions. Pioneering work in this area was completed by Rutter et al. (1971), who developed a numerical model that is widely recognized as the first mechanistic canopy partitioning model. The Gash model, which followed a few years later, is an analytical adaptation of the Rutter model (Gash, 1979). Numerous other process-based canopy partitioning models have been proposed since then (Linhoss & Siegert, 2016; Schellekens, 2000; J. Wang et al., 2008b), but even these more recent models tend to represent refinements of the original Rutter and Gash models.

While the primary goal of the meta-regression analysis described in Chapter 2 was to characterize variability in event throughfall/interception by urban tree canopies and attribute variability to measured variables, a secondary outcome of this work was the development of statistical models that could be integrated in urban hydrological models or used in stormwater management planning. Although relatively easy to use, the estimation accuracy is questionable

given the limitations of such regression models. Therefore, in this section, we aimed to validate our models' accuracy using an independent dataset and compare their performance to the established Rutter and Gash mechanistic interception models. More specifically, we extracted data from Smets et al., (2019), who, in addition to measuring throughfall and stemflow by urban trees, compared measured data with canopy interception rates predicted by Gash, Rutter, and Wetspa models. This independent dataset helped to not only examine the performance of empirical models presented in Chapter 2 but also to compare their performance to the most reliable models in the literature.

In the next section, additional background material regarding the Gash and Rutter mechanistic models is presented. Next, the independent dataset against which the meta-regression precipitation partitioning models were presented in Chapter 2 were validated is discussed, as is the process by which model performance was evaluated (Section 3.3). Results and discussion of model performance are presented in Section 3.4 followed by concluding remarks regarding insights to meta-regression models and their future development.

3.2 Background: Gash and Rutter mechanistic models for estimating interception by forest canopies

Rutter equation (Rutter et al., 1971) uses a conceptual canopy water balance presented in Linhoss et al.,(2016) as follows.

Equation 3.1

$$(1 - p - p_t) \int R dt = \int D dt + \int E dt + \Delta C$$

The trunk water balance is also presented in equation 3.2.

Equation 3.2

$$p_t \int R dt = Sf + \int E_t dt + \Delta C_t$$

The rate of the drainage from the canopy can be calculated as:

Equation 3.3

$$D_c = D_s \exp [b(C - S)] \quad C \geq S$$

$$D_c = 0 \quad C < S$$

Evaporation from the canopy is obtained from:

Equation 3.4

$$E_c = E_p \frac{C}{S} \quad C < S$$

$$E_c = E_p \quad C \geq S$$

Stemflow is presented as:

Equation 3.5

$$Sf = C_t - S_t \quad C_t \geq S_t$$

$$Sf = 0 \quad C_t < S_t$$

And evaporation from the trunk is shown as:

Equation 3.6

$$E_t = \epsilon E_p \frac{C}{S} \quad C_t < S_t$$

$$E_t = \epsilon E_p \quad C_t \geq S_t$$

\bar{R} is the mean rainfall rate, p is the free throughfall coefficient, p_t is the stemflow coefficient, S is maximum canopy storage capacity, S_t is trunk storage capacity, C is actual canopy storage, E_p is potential evaporation (Monteith, 1965), E_c is evaporation from the canopy, E_t is evaporation from the trunk, ϵ describes the evaporation from the trunk as a

proportion of the evaporation from the saturated canopy, D_C is the rate of water dripping from the canopy, D_s is the rate of water dripping from the canopy when canopy storage capacity has been reached, b is an empirical drainage parameter, and I is interception. Fitted parameters in the model equations (b , ϵ , and S) were calibrated with empirical measurements from a Corsican pine stand (*Pinus negra*).

The Gash model considers rainfall events as discrete events, in which canopy interception can be estimated as a function of the amount of rainfall required to saturate the canopy as follows (Gash et al., 1995):

Equation 3.7

$$P'_G = - \frac{\bar{R}}{\bar{E}_C} \frac{S}{C} \ln\left(1 - \frac{\bar{E}_C}{\bar{R}}\right)$$

Where P'_G is the depth of rainfall needed to saturate the canopy, S is the canopy storage capacity, C is the canopy cover, \bar{R} is the mean rainfall rate for saturated canopy conditions, and \bar{E}_C is the mean evaporation rate during rainfall.

Equation 3.8

$$I_C = C \cdot P_G \quad \text{for } P_G < P'_G$$

$$I_C = C \cdot P'_G + \left(C \cdot \frac{\bar{E}_C}{\bar{R}}\right) (P_G - P'_G) \quad \text{for } P_G > P'_G$$

In which I_C and P_G are interception and gross rainfall, respectively.

As shown above, key differences between the Rutter and Gash models lie in the computational approach; the Rutter model estimates rainfall interception by running a continuous water balance, whereas the analytical Gash method assumes discrete wetting, saturation, and drying phases to incorporate the different water balance components. Also, Gash considers rainfall events as separate events. Among their similarities is the inclusion of a canopy storage

(S) variable as an important characteristic of the canopy. In addition, these models were developed and are typically applied at the forest stand scale as opposed to the tree-scale at which most urban tree canopy data is collected. In contrast, in interception module within the WetSpa hydrological model has been adapted to simulate interception by a solitary tree. WetSpa is a physically-based, distributed hydrological model used to estimate the water and energy transfer between soil, plants, and atmosphere across a range in spatial scales. In WetSpa Extension, interception is defined as a function of the rainfall rate reaching to the canopy. For rainfall rates greater than canopy storage capacity versus rainfall rates below or equal to canopy storage capacity, the interception can be shown as (Y. B. Liu & De Smedt, 2004):

Equation 3.9

$$I_i(t) = I_{i,0} - SI_i(t - 1) \quad \text{for } P_i(t) > I_{i,0} - SI_i(t - 1)$$

$$I_t(t) = P_i(t) \quad \text{for } P_i(t) < I_{i,0} - SI_i(t - 1)$$

Where $I_i(t)$ is the interception loss at the unit area (cell) I over the time interval (mm), $I_{i,0}$ is the cell interception storage capacity (mm), $SI_i(t - 1)$ is the cell interception storage at time step $t-1$ (mm), and $P_i(t)$ is the cell precipitation amount (mm). Furthermore, the mass balance of interception storage at a pixel cell can be calculated as:

Equation 3.10

$$SI_i(t) = SI_i(t - 1) + I_i(t) - EI_i(t)$$

In which $SI_i(t - 1)$ and $SI_i(t)$ are cell interception storage at time step $t-1$ and t (mm), $EI_i(t)$ is the cell evaporation from interception storage (mm). $EI_i(t) = 0$ when interception storage is zero, or during the storm event. $EI_i(t) = SI_i(t - 1)$ under the condition of $P_i(t) = 0$ and $E_P > SI_i(t - 1) > 0$, in which E_P is the potential evaporation (mm). And $EI_i(t) = E_P$ for the rest conditions.

3.3 Methods

This preliminary validation of the empirical regression equations included two components. First, an independent dataset not included in the meta-analysis described in Chapter 2 was identified on which to test the performance of the regression models developed herein to reproduce measured interception depths. This dataset is documented in Smets et al., (2019), who measured throughfall and stemflow in the urban environment of Brussels, the capital of Belgium. The Belgium climate is classified as a temperate oceanic climate (Cfb) according to the Köppen climate classification system (Kottek et al., 2006). Measurements were made on two deciduous trees – Norway maple (*Acer platanoides L.*) and Small-leaved lime (*Tilia cortada Mill.*)- of similar height (Norway maple = 47; Small-leaved lime = 46) and trunk diameter (Norway maple = 8.92; Small-leaved lime = 8.79). The average leaf area (cm²) for the Norway maple and small-leaved lime were 90.36 and 41.41, respectively. While LAI was measured periodically during the study period, it was 3.6 and 4.8 under full-leaf conditions for Norway maple and small-leaved lime, respectively. The average yearly rainfall for the area was between 750 to 850 mm, and during the study period about 60 events were analyzed with precipitation ranging from almost 0 to 18 mm. Using linear regression models for deciduous/leafed trees (Chapter 2, Figure 2.1), and multi-linear regression models (Chapter 2, Table 2.3), interception depth for each precipitation partitioning event reported by Smets et al. (2019) was predicted. These regression models are presented here for reference in Equations 3.11 (linear regression) and 3.12 (multi-linear regression):

Equation 3.11

$$TH = 0.41 * P \quad \text{for } 0 < P \leq 5 \text{ mm}$$

$$TH = 0.54 * P \quad \text{for } 5 < P \leq 25 \text{ mm}$$

Equation 3.12

$$TH = 0.56 * P - 0.08LAI \quad \text{for } 0 < P \leq 5 \text{ mm}$$

$$TH = 0.68 * P - 1.09LAI \quad \text{for } 5 < P \leq 25 \text{ mm}$$

TH, P, and LAI represent throughfall, precipitation, and leaf area index, respectively.

A nonlinear relationship between LAI and throughfall to precipitation (TH/P) rate was also developed in Chapter 2 as given in Equation 3.13.

Equation 3.13

$$\frac{TH}{P} = 0.68 - 0.24 \log LAI \quad \text{for } 0 < P \leq 5 \text{ mm}$$

$$\frac{TH}{P} = 0.77 - 0.31 \log LAI \quad \text{for } 5 < P \leq 25 \text{ mm}$$

The ratio of throughfall to precipitation (TH/P) was modeled throughfall using LAI data presented in Smets et al. (2019) using Equations 3.13 and then compared to actual TH/P ratios calculated for measured throughfall and precipitation data reported by Smets et al. (2019). To facilitate comparison with mechanistic models, the interception to precipitation rate was computed by subtracting the TH/P ratio from one for both measured and modelled data. Note that the measured stemflow in the Smets et al. (2019) study was negligible, so we assumed interception was equal to precipitation minus throughfall. The interception rate for measured interception storage was then plotted against the simulated interception storage for both the non-linear models presented in Equation 3.13.

The second component of this preliminary validation entailed comparing the predictive performance of our regression models with the performance of three mechanistic approaches for modeling interception (Gash, Rutter and WetSpa – refer to Section 3.2 for model background

information) which were also applied by Smets et al. (2019). The performance of the Gash, Rutter, and WetSpa models was compared to the interception models presented in Equations 3.11, 3.12 and 3.13 using the coefficient of determination (R^2) and root mean squared errors (RMSE) as statistical criteria.

3.4 Preliminary Validation Results and Discussion

3.4.1 Linear regression model performance

Figures 3.1 and 3.2 show the best linear fit between measured interception depths reported by Smets et al. (2019) and interception as predicted by the linear regression model (precipitation as the predictive variable), and multi-linear regression model (precipitation and LAI as the predictive variables), respectively.

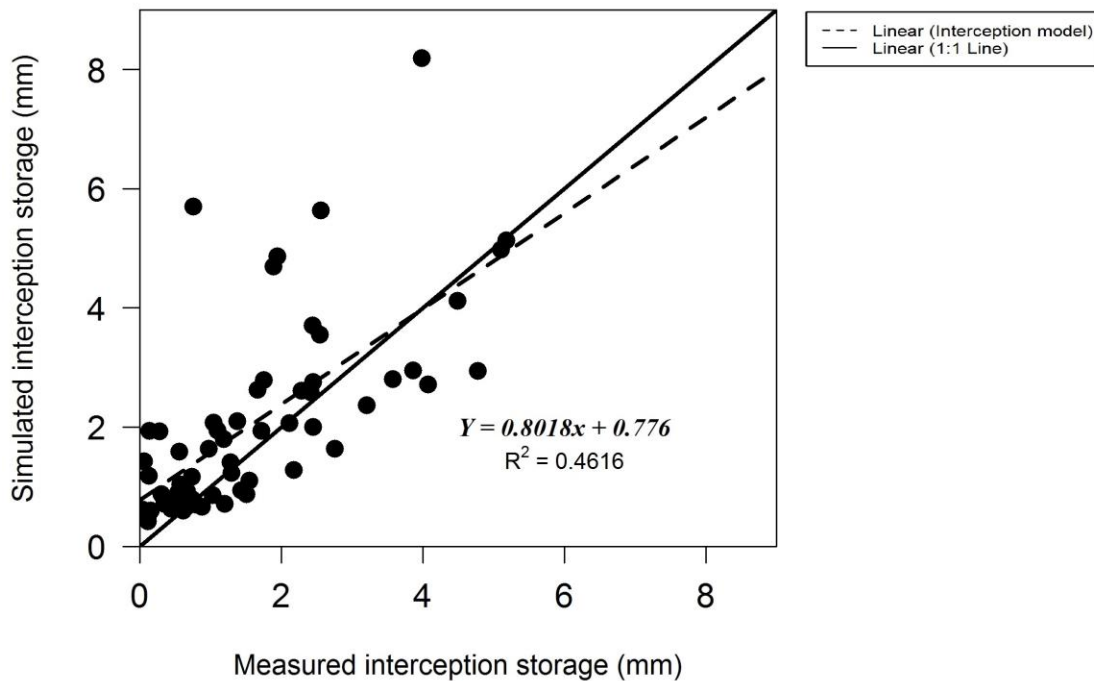


Figure 3-1 Measured vs. simulated interception storage for the linear regression model (Equation 3.11)

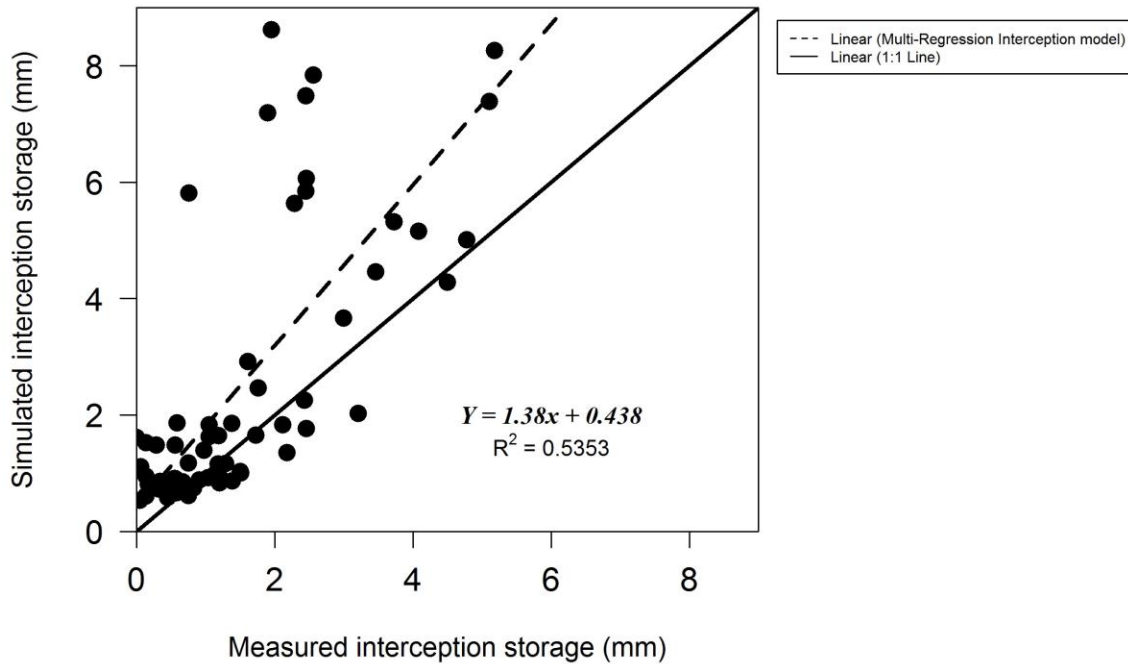


Figure 3-2 Measured vs. simulated interception storage for the multi-linear regression model (Equation 3.12)

A comparison between Figures 3.1 and 3.2 indicates a better coefficient of determination (R^2) for the multi-linear regression model; however, the root mean square error (RMSE) is less for the linear regression model (Table 3.1). Additionally, the linear regression model had a slope closer to one and tended to slightly over predict the interception up to values of four mm, and underpredict for interception values above four mm. In contrast, the multi-linear regression model consistently over predicted the intercepted rainfall. The higher precipitation coefficient in estimating the throughfall for multi-linear regression model compared to linear regression model implies that multi-linear regression might have a lower interception value. However, as results

oppose this expectation, we may conclude that the effect of LAI causes an overprediction of the interception in the multi-linear regression model. This over prediction could be correlated to the limited number and range of LAI with which the multi-linear regression was developed. While Smets et al., (2019) included LAI below 1 to 6, the LAI values with which the multiple-linear regression model was created, ranged from 1.5 to 5.8.

A comparison of the performance of the regression models developed herein with the process-based Gash, Rutter and Wetspa models applied by Smets et al. (2019) is presented in Table 3.1. The Gash model outperformed other models with the highest R^2 (0.6) and the lowest RMSE (0.89). The linear regression equation (Equation 3.11) had the lowest R^2 with a value of 0.46 and the second highest RMSE (1.28). The highest value for RMSE belonged to the multi-linear regression model (Equation 3.12) with a value of 2.06. Although the regression models developed herein performed worse than process-based models on the basis of R^2 and RMSE, the closest slope to one was observed for the linear regression interception model.

Table 3-1- The results of the best linear equation fit along with R^2 , and RMSE as statistical criteria for evaluated models

Model	Intercept	Slope	R^2	RMSE
Gash	0.81	0.63	0.6	0.89
Rutter	1.24	0.49	0.5	1.05
WetSpa	0.95	0.66	0.59	0.95
Statistical model (linear regression)	0.78	0.8	0.46	1.28
Statistical model (multi-linear regression)	0.44	1.38	0.53	2.06

Figure 3.3 presents interception storage versus gross precipitation for all the evaluated models. A linear interception model developed from data measured by Smets et al. (2019) is also shown for all the precipitation events occurred in the study. The linear regression model developed in Chapter 2 performed similarly to the mechanistic models used in the Smets et al.

(2019) study. While the mechanistic models all over predict, and under predict the interception storage for rainfall values below and above 8 mm, the linear regression model tends to over predict interception for rainfall values below 13 mm and under predict for rainfall values greater than 13 mm. As can be seen in Figure 3.3, for rainfall events above 11 mm, the linear regression model has the closest performance to linear fit between the gross precipitation and measured interception compared to other models. In contrast, mechanistic models performance performing weaker, relative to the linear fit between gross precipitation and measured interception, as precipitation increases beyond 11 mm. From a stormwater management standpoint, this may indicate the better ability of linear regression models, as runoff issues mostly occurs for higher rainfall values.

Figure 3.3 also illustrates the tendency of the multi-linear regression model to overpredict interception storage. However, for interception storage above 3 mm, this model tends to fit the upper envelop of the interception values. Higher interception storage could be related to higher canopy density (higher LAI). This might imply that, for potential rainfall amounts generating interception storage more than 3 mm, if the canopy is relatively dense (LAI is greater than 1.5 (i.e., within the range of LAI upon which this model was developed), this model might have a good performance. However, the limitation of data with which this model was developed prevented us from developing a model based on a wider range of LAI, with lower values included.

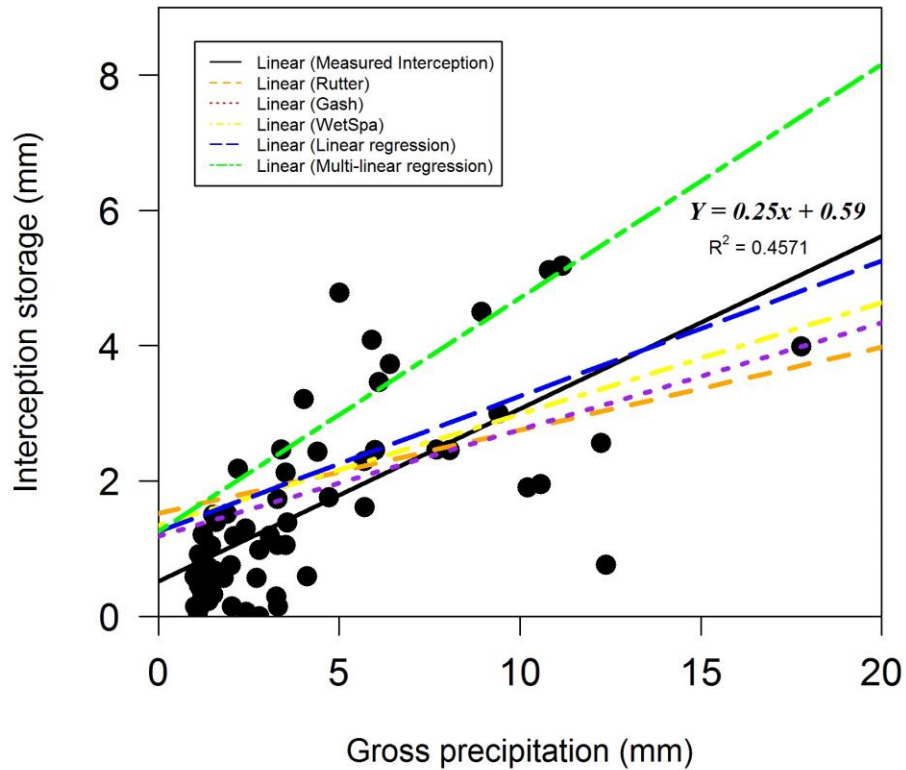


Figure 3-3 Interception storage vs. gross precipitation for all the events in the independent dataset

These results likely demonstrate tradeoffs between model accuracy and model complexity. The empirical models developed herein only used precipitation (linear regression interception model) or precipitation and LAI (multi-linear regression model) as predictive variables whereas the Gash, Rutter, and WetSpa models require considerably more input variables (over 10). Nevertheless, while the performance of these simplistic regression equations was not as good as mechanistic models based on the metrics assessed, they came to within 12 to 44% of the best-performing mechanistic model on the basis of R^2 and RMSE, respectively.

3.4.2 The nonlinear LAI interception rate model validation

Figure 3.4 shows the measured vs. simulated interception rate in percentage for LAI interception rate, Gash, Rutter, and WetSpa models, respectively. The best-fit equation, along with R^2 and RMSE, are also presented in the figures and are summarized below in Table 3.2.

Table 3-2- The results of the best linear equation fit along with R^2 , and RMSE as statistical criteria for evaluated models

Model	Intercept	Slope	R^2	RMSE
Gash	38.6	0.4	0.1745	29.2
Rutter	52.8	0.42	0.07	46.6
WetSpa	38.99	0.59	0.1745	39.8
Non-linear LAI interception rate model	33.8	0.12	0.17	24.72

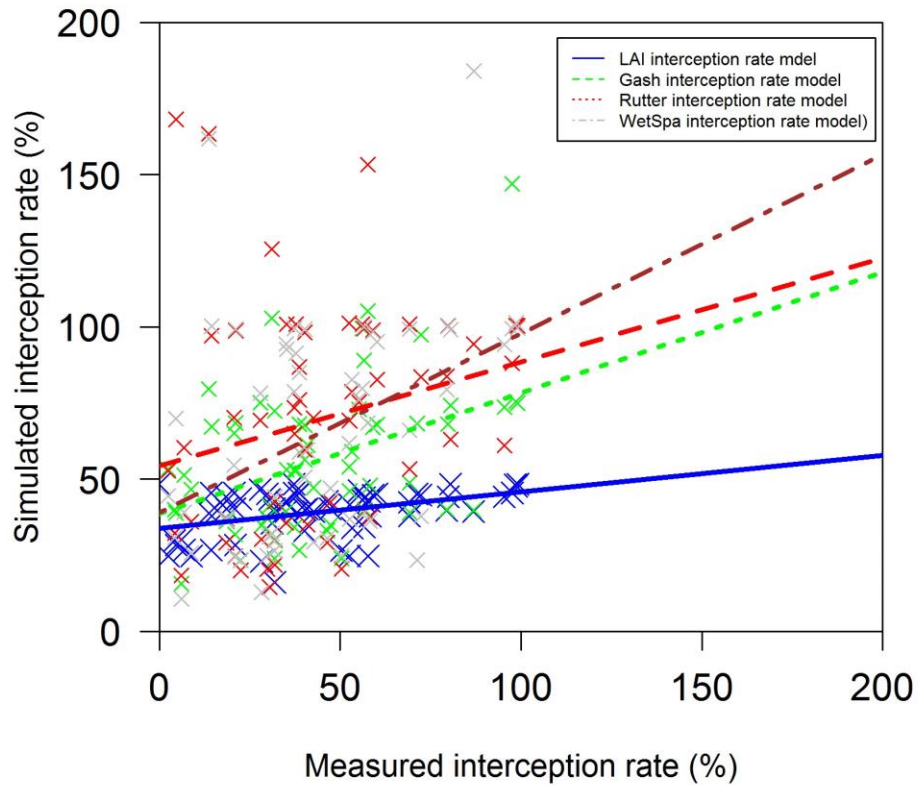


Figure 3-4 Measured vs. simulated interception rate for LAI interception, Gash, Rutter, and WetSpa models

The result based on the Figure 3.4 suggests that the non-linear, LAI-based model developed through the meta-regression in Chapter 2 may perform similarly, if not better, than the most common mechanistic interception models in the literature. This result may imply that LAI exerts a nonlinear influence (since the linear LAI-based model failed to perform as well as mechanistic models) and/or that LAI provides a reasonable surrogate for canopy variables included in mechanistic models. For example, canopy storage is a main predictive variable in both the Gash and Rutter models; however, difficulty to measure or otherwise accurately assign a

value to this uncertain parameter could also contribute to the comparatively poor fit of mechanistic models.

3.5 Conclusion

Preliminary results imply that, from a stormwater management standpoint, using the empirical models developed in Chapter 2 of this dissertation can give a reasonable estimate of interception. At the same time, they are fast and straightforward enough to apply due to a smaller number of inputs that are also relatively easy to measure or estimate. Furthermore, canopy storage capacity is considered as the main driver in estimating interception for conventional models in the literature. This factor is not easy to estimate and vary for individual species. Although, the developed models in this study could not incorporate this factor (due to the non-reporting of this variable for candidate studies in section 2.1), not having this variables included in the model made it possible to easily generalize the results of this study from a tree scale to larger scales such as city or watershed.

Overall, the preliminary validation of the empirical interception models developed in Chapter 2 against the independent dataset from Smets et al. (2019) indicated these models can perform comparably to mechanistic interception models. The linear regression model had the closest performance to the linear measured interception fit compared to all the other studies for rainfall values above 11 mm. Additionally, although multi-linear regression constantly over predicted the interception storage, it indicated a tendency to fit the upper envelop for interception storage above 3 mm compared to other evaluated models. The overprediction of this model might be relevant to the limited range of LAI using which the model was developed. However, the achievement of a good fit for higher interception storage might suggest the ability of model for trees with relatively high LAI values. These observations are preliminary in nature as model

performance is only assessed on a single dataset with a relatively small number of data points (60). Furthermore, our empirical models included four different rainfall groupings, including 0-5, 5-25, 25-50, and above 50 mm, but the validation dataset only contained data below 25 mm. Also, for each rainfall group classification, three different empirical equations were developed for evergreen, deciduous/leafed, and deciduous/leafless trees separately. Nevertheless, the validation dataset only provided data for deciduous/leafed trees. Therefore, future studies and more datasets are required to better examine the validity of empirical interception models presented in chapter 2 and better assess their potential to account for rainfall interception by urban trees in stormwater management applications.

Chapter 4 - The effect of climatic variables on urban trees'

transpiration: A Meta data analysis

4.1. Introduction

Urbanization is rapidly growing, and hence destruction in nature is inevitable. Approaches are needed to make this cause and effect circumstance compatible. Urban trees are progressively considered as a constituent of urban management strategies (Berland & Hopton, 2014; Galeniefs, 2017; Kuehler et al., 2017). Thus, using trees in urban areas not only simulates natural processes but also helps to overcome common issues such as excessive runoff (Armson et al., 2013; Bijoor et al., 2012; Seitz & Escobedo, 2008; Soares et al., 2011; Xiao & Mcpherson, 2011). Tree transpiration is a component of total evapotranspiration by which trees can provide a variety of services, including mitigation of runoff (Carlyle-Moses et al., 2020; Gotschet al., 2018; Pataki et al., 2011). Therefore, understanding the capacity of urban trees together with environmental variables affecting the transpiration rate seems vital.

Numerous methods have been utilized in natural forests to estimate the whole-tree transpiration including weighing lysimeters, large-tree porometers, ventilated chambers, radioisotopes, stable isotopes, and an array of heat dissipation methods (Wullschleger et al., 1998a). However, tree transpiration rates in urban areas may differ from rates observed in natural forests due to disparities in tree structure, spacing and associated microclimate, and species composition. Urban settings have significant amounts of impervious cover and compacted soils that affect the tree transpiration through changes in the hydrological process and soil water content (Bruijnzeel, 2004; Depietri et al., 2012; Livesley et al., 2016; Whitford et al., 2001). Air temperature and vapor pressure deficit (VPD) are different from those in the natural forest, mainly due to urban heat island (Chen et al., 2012; Kjergren & Montague, 1998; Wang et al., 2011). Non-

native, invasive, and human cultivated species are more frequently found in urban areas, which lead to species composition variation between urban and natural forests (Bush et al., 2008; Peters et al., 2010).

Heat dissipation methods to measure sap flow are commonly used in studies measuring urban tree transpiration rates. This approach is an empirical method for measuring sap flux density in trees, where two conifers and one ring-porous hardwood species were used by the Grainer (1987) to develop the method. In this technique, two sensors (one heated probe and one unheated) are installed radially into the sapwood area of a tree bole at 2 cm depth. The upper probe is supplied with a constant electric voltage and the difference in temperature between the two probes is monitored. The sap flux density is dependent on the temperature difference with which higher temperature difference corresponds to higher sap flux density. The sap flux (J_s) is calculated as Equation 4.1:

Equation 4.1

$$J_s = \left(\frac{\Delta T_m - \Delta T}{\Delta T} \right)^{1.231}$$

Equation 4.1 is adapted from Grainer (Granier, 1987) in which sap flux is shown as J_s in $\text{g H}_2\text{O}/\text{m}^2/\text{s}$, ΔT_m ($^{\circ}\text{C}$) is the maximum nighttime temperature difference between the heated and unheated sensors, and ΔT is the mean temperature difference between sensors.

The sap flux measurement method typically only measures the outer 2 cm of the sapwood area; however, nonuniformities across the rest of the sapwood area preclude linear extrapolation to the tree scale. Some researchers have accounted for such heterogeneity in sap flux across the sapwood area by installing multiple heat probes at various depths (Ford et al., 2004; James et al.,

2002) . It is more common, however, to apply regression models such as developed by Pataki et al. (Pataki et al., 2011) to extrapolate the sap flux throughout the entire active sapwood area.

Tree transpiration varies due to differences in physiological characteristics of various species and climatic factors in urban areas. Some studies evaluated the physiological characteristics of trees through different classifications based on the same genre, plant functional category, and wood anatomy (Peters et al., 2010; Rana et al., 2020; Litvak et al., 2011; Bush et al., 2008). In contrast, other studies focused on the transpiration of individual species (Chen et al., 2011; Litvak et al., 2011; Pataki et al., 2011b; Riikonen et al., 2016; Wang et al., 2012). Also, climate variables, as significant transpiration drivers, were examined differently across the studies. In general, most studies investigated climatic factors by introducing soil water content, VPD, light energy (in various forms), and temperature as the most commonly measured, influential variables in urban studies. Wang et al. (2012) grouped various independent environmental variables into a single evaporative demand index. The results showed a saturation response of canopy transpiration by an increase in the defined index. Soil water content was a significant tree transpiration driver, mainly for studies in which water limitation periods existed (Pataki et al., 2011b; Tirpak et al., 2018). VPD behaved in disparate ways across the studies. Chen et al. (2011) indicated a decrease in canopy conductance by an increase in VPD. An increase in VPD in some studies showed a saturation response to sap flux (Litvak et al., 2011; Peters et al., 2010). Other studies showed sap flux sensitivity to VPD; however, the degree of sensitivity to individual species was not equal (Litvak et al., 2011; Pataki et al., 2011b; Rana et al., 2020). The effect of light energy was shown in different forms, such as total radiation or photosynthetically active radiation, and was positively correlated to temperature. A rise in these two variables corresponded to an increase in sap flux. Nevertheless, the level of sap flux sensitivity in response to these variables was diverse.

Despite all the stated efforts in the literature to explain the behavior of the transpired water in urban trees, discrepancies in the reported units of transpired water across the studies made it difficult to compare the water use among different species in various climates. Besides, a solitary unit allows us to scale up species differences in transpiration from a single tree to a neighborhood or city scale.

Additionally, a few studies have categorized their species into major classifications schemes such as wood anatomy. But it is ambiguous to what extent transpired water varies across this type of grouping, and how limited and non-limited water periods can affect this classification. Studies have been done in different climates, which has led to wide variability in the range of both dependent and independent variables across the studies. Also, explanatory variables have indicated inconsistent and sometimes opposing effects on transpired water from one study to another. Moreover, the simultaneous impact of descriptive variables, together with their interactive relationship, remains unclear.

To fill these gaps, we aimed to provide an informative holistic study to elucidate substantial differences in tree transpiration based on various wood anatomies [diffuse-porous angiosperms, ring-porous angiosperms, and gymnosperms (conifer wood trees with only conifer wood and no vessels)], while incorporating a single unit to scale up tree water use. In addition, we attempted to describe quantitatively relationships between climatic variables and transpiration rates to anticipate better the pattern of water use in varied urban environments. More specifically, we designed our work to answer the following questions:

- 1- To what extent does sap flux vary in response to different wood anatomy groupings with and without the impact of water-limited conditions?

- 2- What is the transpiration response to climatic variables for different wood anatomy groupings?
- 3- How the concurrent influence of environmental variables drives the sap flux pattern for various wood anatomy groupings.

To answer these questions, we performed a meta-regression analysis of existing tree transpiration studies conducted in urban areas. The outcomes are intended to provide a broader understanding of the water use by urban trees across a range of environmental conditions on a daily basis for various wood anatomy groupings while describing its relationship with environmental variables for each based on daily values. It also delivers information for stormwater managers and policymakers to enhance their decision-making and advance their policies to optimize water use and manage runoff in the urban environment.

4.2. Method

4.2.1 Literature search criteria and data extraction

A search of published literature was performed to identify peer-reviewed studies reporting transpiration rates for urban trees. The primary search utilized the ISI Web of Knowledge, Scopus, and Google Scholar search engines. Additional papers were identified through reference lists of selected studies. The selected papers met the following requirements: Firstly, the analysis was confined to peer-reviewed journal papers. Secondly, we only focused on papers with field measurements and did not consider modeled studies. Thirdly, we limited our emphasis to studies reporting transpiration data on a daily time scale for trees located in urban areas. Six studies were identified (Table 4.1). All studies utilized similar heat dissipation methods to measure sap flux as an indicator of transpiration rate. Data related to tree water use (reported as sap flux and/or whole

tree water use), tree characteristics, and meteorological variables were extracted from each study on a daily time scale. Due to dissimilar study objectives, a wide range of variability existed in the procedures with which transpired water was reported, the study period, and selection of tree species and landscape setting. Although the total evaluated studies were limited to six, it includes 40 different tree species across three different continents, ranging from semi-arid to warm-summer humid continental (Dfb), hot-summer humid continental (Dfa), monsoon-influenced hot-summer humid continental (Dwa), warm-summer Mediterranean (Csb), humid subtropical (Cfa) köppen climate classifications.

Table 4-1 Urban tree transpiration studies identified through literature search. The spatial scale over which tree water use was reported included (1) sap flux across the outer 2 cm, J_o , (2) sap flux across the entire active sapwood area, J_s and (3) depth of water transpired per projected canopy area, EC. All studies used heat dissipation methods

Study	Species	Wood anatomy	Location and Study periods	Environmental variables measured ^a	Reported transpiration unit
Bush et al. (2008)	<i>Platanus acerifolia</i>	Diffuse-porous	Salt Lake valley metropolitan area, June to September	Temp, VPD, SWC, RH	J_s (g/cm ² /day)
	<i>Acer platanoides</i>	Diffuse-porous			
	<i>Populus fremontii</i>	Diffuse-porous			
	<i>Gleditsia triacanthos</i>	Ring-porous			
	<i>Quercus gambelii</i>	Ring-porous			
Peters et al. (2010)	<i>Quercus rubra</i>	Ring-porous	Minneapolis-Saint Paul metropolitan area, April to October	PAR, Temp, VPD, SWC	J_s (g/cm ² /day)
	<i>Picea glauca</i>	Conifer wood			
	<i>Picea pungens</i>	Conifer wood			
	<i>Pinus strobes</i>	Conifer wood			
	<i>Quercus rubra</i>	Ring-porous			
	<i>Fraxinus pennsylvaniaca</i>	Ring-porous			
	<i>Tilia Americana</i>	Diffuse-porous			
	<i>Picea abies</i>	Conifer wood			
	<i>Pinus nigra</i>	Conifer wood			
	<i>Pinus Sylvestris</i>	Conifer wood			
<i>Ulmus pumila</i>	Ring-porous				
<i>Ulmus thomasii</i>	Ring-porous				
	<i>Juglans nigra</i>	Diffuse-porous			

Chen et al. (2011)	<i>Cedrus deodara</i>	Conifer wood	Dalian City, Liaoning province, China, July to September	Rs, Temp, VPD, REW	EC (mm/m ² /day)
	<i>Zelkova schneideriana</i>	Ring-porous			
	<i>Metasequoia glyptostroboides</i>	Conifer wood			
	<i>Euonymus bungeanus</i>	Diffuse-porous			
Pataki et al. (2011)	<i>Platanus hybrida</i>	Diffuse-porous	Los Angeles metropolitan area, Mid-July to November	VPD	J _o (g/cm ² /day)
	<i>Platanus racemose</i>	Diffuse-porous			
	<i>Pinus canariensis</i>	Conifer wood			
	<i>Jacaranda mimosifolia</i>	Diffuse-porous			
	<i>Malosma laurina</i>	Diffuse-porous			
	<i>Ulmus parvifolia</i>	Ring-porous			
	<i>Sequoia sempervirens</i>	Conifer wood			
	<i>Brachychiton discolor</i>	Ring-porous			
	<i>Brachychiton populneus</i>	Ring-porous			
Litvak et al. (2011)	<i>Eucalyptus grandis</i>	Diffuse-porous	Los Angeles basin, California, May to December	VPD, PAR	J _o (g/cm ² /day)
	<i>Coast redwood</i>	Conifer wood			
Rana et al. (2020)	<i>Olea europea</i>	Diffuse-porous	Bari, southern Italy, January to December	VPD, Temp, Rs, CWSI	EC (mm/m ² /day)
	<i>Citrus sinensis</i>	Diffuse-porous			
	<i>Eriobotrya japonica</i>	Diffuse-porous			
	<i>Cupressus arizonica</i>	Conifer wood			
	<i>Pinus pinea</i>	Conifer wood			
	<i>Ailantum altissima</i>	Ring-porous			
	<i>Celtis australis</i>	Ring-porous			
<i>Quercus ilex</i>	Semi-ring to diffuse-porous				

^a Environmental variables abbreviated as Temp (temperature), PAR (photosynthetically active radiation), VPD (vapor pressure deficit), RH (relative humidity) Rs (total solar radiation), SWC (soil water content), REW (relative extracted water), CWSI (crop water stress index).

To find the relationship between tree transpiration and explanatory variables, data were first extracted from selected studies. When these data were presented in graphs or other figures, the Web-Plot-Digitizer 4.1 tool (Ankit Rohatgi, 2019) was used to extract measured data points. Following previous work on the role of tree functional traits on transpiration in natural forests (e.g., Lockaby et al., 2013), species were classified according to their wood anatomies, including diffuse-porous, ring-porous, and conifer wood trees. In the case of trees described as semi-ring porous, which indicated sapwood pores that exhibit a mix of both ring porous and diffuse porous characteristics (e.g., *Q. ilex*), the tree was assigned to the ring-porous group in analyses in which wood anatomy was used as a descriptive variable.

Vapor pressure deficit, solar radiation, temperature, and soil water content were the most commonly measured variables across the studies. Among these variables, soil water content was not always stated with a single way of measurement. In some studies, the absolute soil water content was reported; in others, a relative value was given. This relative value either corresponded to the normalized value of soil water content according to maximum and minimum values or a soil water content relative to the maximum measured value during the studied period. We were not able to convert given soil moisture data to a common value across all studies (e.g., absolute measures to relative or relative to absolute) with the soil water content data provided; thus, analysis to find the direct relationship between (relative or absolute) soil water content and transpired water was not feasible. However, we were able to evaluate the influence of water-limited conditions on tree transpiration by conducting two separate analyses. In the first, all data, including the water-limited periods, were used to analyze the relationship between explanatory variables and transpired water. In the second analysis, an investigation was done through each study to remove the periods in which the soil water conditions of the trees were limiting; the relationship between transpired

water and explanatory variables was done across the data under non-limiting water conditions. Unless an exact water-limited period was indicated, assumptions were made to identify this period according to indices and information provided in each study. In particular, assumptions were made about the soil type in the studies by Chen et al. (2012) and Peters et al. (2010), where the water-limited period was considered to be for REW values below 25% and SWC values below 20%, respectively. Species were considered to be in a water-limited period, if they were labeled as unirrigated (study by Pataki et al., 2011). The trees were assumed to be in a limiting-water period if the CWSI was below 50% (study by Rana et al., 2020). Bush et al. (2008) indicated the exact limited-water period, and as stated by Litvak et al. (2011), soil water content remained high during the entire study period.

4.2.2 Unifying the data

The next step was to unite the different approaches and units through which variables were represented. The value of tree transpiration was reported in different units including sap flux for the active sapwood area of the tree (J_s in $\text{g}/\text{cm}^2/\text{day}$), sap flux for the outer two centimeters of the active sapwood area (J_o in $\text{g}/\text{cm}^2/\text{day}$), and the total transpired water per projected canopy area (EC in $\text{mm}/\text{m}^2/\text{day}$). We unified the collected transpired water of each study to the unit of sap flux ($\text{g}/\text{cm}^2/\text{day}$). Other options for reporting this variable include transpired water per tree or projected canopy area (Chen et al., 2011; Martin et al., 1997; Wullschleger et al., 1998b; Wullschleger et al., 2000). Reporting the transpired water on a tree scale fails to consider the effect of tree size's characteristics such as the trunk, sapwood depth, and projected canopy area. Even though two single trees of the same species might have the same sap flux, the reported transpired water per tree might significantly vary due to differences in size. Reported transpired water per projected canopy area could also fail to identify species

differences. Denser tree canopies might transpire a higher amount of water; however, the projected canopy area defines the projected canopy cover on the ground, which misses the density of the canopy. Furthermore, two single trees within the same species group might have the same sap flux rate per unit of the sapwood area. Variations in the sapwood area and projected canopy sizes cause a significant difference in the reported transpired water on a projected canopy area basis. In general, with no unique relationship between tree and canopy size, reported transpired water falls short of identifying the differences between various species. The following assumptions and calculations were made to convert transpiration measurements reported as J_o and EC to J_s . Studies with reported transpired water as EC were examined to find the average canopy cover area and sapwood area for each tree species. EC was multiplied by the projected canopy area, and the resulting transpired water was then divided by the sapwood area to attain the transpired water as J_s . In the case of studies that reported transpiration in terms of J_o , we utilized equations from Pataki et al. (2011) for angiosperms (i.e., flowering plants including ring-porous and diffuse-porous trees; Equation 4.2) and gymnosperms (i.e., non-flowering plants including conifers; Equation 4.3) to account for the non-linear relationship between sap fluxes in the outer 2 cm (where sap flow tends to be highest) and as averaged across the rest of the sapwood area to obtain the J_s based on the reported J_o

Equation 4.2

Angiosperm
$$J_i/J_o = 1.033 \exp \left[-0.5 \left(\frac{x - 0.09963}{0.4263} \right)^2 \right]$$

Equation 4.3

Gymnosperms
$$J_i/J_o = 1.257 \exp \left[-0.5 \left(\frac{x + 0.3724}{0.6620} \right)^2 \right]$$

Here, J_i/J_o is the ratio of the sap flux at an arbitrary depth i (cm) and sap flux in the outer 2 cm (J_o) at relative sapwood depth x (where x is the ratio of depth i to the total sapwood depth). For each tree species, J_i was calculated in two-centimeter increments along the sapwood depth and then multiplied by the sapwood area of the given increment to obtain sap flux as g/day. Incremental values of sap flux in g/day were then summed to obtain sap flux across the entire sapwood area. Finally, the sum was divided by the total sapwood area to obtain J_s in units of g/cm²/day.

Another variable to unify was radiated energy from the sun. Studies reported this variable as either photosynthetically active radiation (PAR) in Mol/m²/day or solar radiation (R_s) in W/m². Firstly, it is essential to make a distinction between incoming R_s and PAR. R_s consist of visible and near-infrared radiation, while PAR is only visible radiation between 400 to 700 nm. Along the solar radiation spectrum, three ranges exist which are ultraviolet, visible (i.e., PAR), and infrared. Across these ranges, infrared radiation makes up 49.4%, visible light provides 42.3%, and ultraviolet radiation makes up about 8% of the total solar radiation (Bigelow et al., 1998). PAR is usually expressed in μ mols of photons/m²/s, but it can be converted to W/m². By using Planck's equation (Risken, 1996) to get the total energy of a μ mol of photons, PAR can be transformed to in W/m² to μ mols/m²/s, as follows:

Equation 4.4

$$\text{PAR} (\mu\text{mols/m}^2/\text{s}) = \text{PAR}(\text{W/m}^2) * 4.638$$

Knowing the proportional energy of PAR to the total solar radiation and with the help of Equation 4.4, we calculated the total solar radiation for studies with the reported daily PAR, so that the radiated energy from the sun was reported as single total solar radiation unit (R_s).

Other measured variables, including VPD, temperature, and soil water content, were reported in uniform units across the studies.

4.2.3 Regression and statistical analysis

In our first statistical analysis, the Spearman correlation between all the studied variables was assessed. We then ran a single linear regression model to evaluate the isolated effect of each independent variable on sap flux. Next, a multiple linear regression was utilized to assess the simultaneous effect of the independent variables on sap flux. Because individual studies did not necessarily evaluate all the variables (Table 4.2), a single, robust multiple linear regression model was not possible to develop. Therefore, where needed, two separate multiple linear regression models were created: the first incorporated the highest number of data points and studies, and the second reflected the best fitted models as indicated by R^2 value.

The analyses were completed separately for each of the three wood anatomy groups (diffuse-porous, ring-porous, and conifer wood) and applied to both the full dataset (the water-limited period was included in the dataset) and non-limiting water period (the limited-water period was removed from the dataset). The difference in average sap flux was statistically compared for the three different wood anatomy groupings using the Wilcox Rank test. All the statistical analyses were performed using R-Studio. The readxl, basictrendline, pastecs, Hmisc, and FSA were utilized as user library packages for our analyses.

Table 4-2- Summary of studied environmental variables including vapor pressure deficit (VPD), solar radiation (Rs), and temperature (Temp), and studied wood anatomy groups for each evaluated study; ✓: variable included in the study, ✗: variable was not included in the study

	VPD	Rs	Temp	Studied wood anatomy groups
Bush et al. (2008)	✓	✗	✓	diffuse-porous, ring-porous
Peters et al. (2010)	✓	✓	✓	diffuse-porous, ring-porous, conifer wood
Chen et al. (2011)	✓	✓	✓	diffuse-porous, ring-porous, conifer wood
Pataki et al. (2011)	✓	✗	✗	diffuse-porous, ring-porous, conifer wood

Litvak et al. (2011)	✓	✓	×	conifer wood
Rana et al. (2020)	✓	✓	✓	diffuse-porous, ring-porous, conifer wood

4.3. Results

Table 4.3 indicates the variability in the maximum rate of different urban species to transpire water per day. At the tree scale, *Fraxinus pennsylvanica* had the highest transpired water with 227.2 kg/day. In contrast, *Malsoma laurina* presented a rate of 1.5 kg/day, which was the lowest across the studied urban trees. The average water use was 73.3 kg/day, with a standard deviation of 63.0.

Using the scale of a unit of sapwood area, the highest sap flux belonged to *Euonymus bungeanus*, with a value of 464.15 g/cm²/day. Also, *Malsoma laurina* had the lowest sap flux with a rate of 13.08 g/cm²/day.

Table 4-3- Urban species maximum transpired water in sap flux (g H₂O per cm² of sapwood area per day) and water use (Kg H₂O per tree per day) for various characteristics including DBH (diameter of breast height in cm), PCA (projected canopy area in m²), height (in m) , and SWA (sapwood area in cm²) for diffuse porous wood anatomy grouping

Species	DBH (cm)	PCA (m ²)	Height (m)	Sap flux (g H ₂ O cm ⁻² d ⁻¹)	SWA (cm ²)	Water use (kg H ₂ O tree ⁻¹ day ⁻¹)	Reference
<i>Tilia americana</i>	22.8	28.1	12.8	356.42	365.27	130.2	Peters et al. 2010
<i>Euonymus bungeanus</i>	19.3	14.39	5.6	464.15	51.44	23.9	Chen et al. 2011
<i>Platanus acerifolia</i>	25	-	-	448.32	445.51	199.73	Bush et al., 2008
<i>Acer platanoides</i>	26.5	-	-	354.09	489.33	173.27	Bush et al., 2008
<i>Populus fremontii</i>	30.3	-	-	362.02	428.51	155.13	Bush et al., 2008
<i>Juglans nigra</i>	40.8	96.4	15	264	542.87	143.3	Peters et al. 2010
<i>Platanus racemosa</i>	36.8	-	-	57.5	872.48	50.2	Pataki et al. 2011
<i>Platanus hybrida</i>	56.8	-	-	96.8	1054.5	102	Pataki et al. 2011

<i>Jacaranda mimosifolia</i>	14.5	-	-	70.5	165.1	11.6	Pataki et al. 2011
<i>Malsoma laurina</i>	12.1	-	-	13.08	114.9	1.5	Pataki et al. 2011
<i>Eucalyptus grandis</i>	67	-	-	151.4	679.3	102.8	Pataki et al. 2011
<i>Olea europaea</i>	33.5	-	-	53.5	625	33.4	Rana et al. 2020
Citrus and Eriobotrya	15.6	-	-	46.6	225	10.5	Rana et al. 2020
Average	30.85	46.3	11.13	210.64	466.09	87.5	

For tables 4-3 to 4-5: *Tree characteristics and sap flux or transpiration rates are presented as an average across identified species and correspond to an average for each column

Table 4-4-Urban species maximum transpired water in sap flux (g H₂O per cm² of sapwood area per day) and water use (Kg H₂O per tree per day) for various characteristics including DBH (diameter of breast height in cm), PCA (projected canopy area in m²), height (in m), and SWA (sapwood area in cm²) for ring porous wood anatomy grouping

Species	DBH (cm)	PCA (m ²)	Height (m)	Sap flux (g H ₂ O cm ⁻² d ⁻¹)	SWA (cm ²)	Water use (kg H ₂ O tree ⁻¹ day ⁻¹)	Reference
<i>Gleditsia triacanthos</i>	20.8	-	-	160.73	176.93	28.44	Bush et al., 2008
<i>Quercus gambelii</i>	13.5	-	-	133.7	94.12	12.58	Bush et al., 2008
<i>Quercus rubra</i>	21.4	-	-	202.11	178.22	36.02	Bush et al., 2008
<i>Brachychiton discolor</i>	52	-	-	102.8	447.3	46	Pataki et al. 2011
<i>Brachychiton populneus</i>	38	-	-	118.7	309.6	37	Pataki et al. 2011
<i>Ulmus parvifolia</i>	28.9	-	-	64.14	655	42	Pataki et al. 2011
<i>Ailantum altissima</i> + <i>Celtis australis</i> + <i>Quercus Ilex</i> *	30.7	-	-	267.4	667.5	178.5	Rana et al. 2020
<i>Zelkova schneideriana</i>	13.9	56.58	5.3	260.1	18.99	4.9	Chen et al. 2011
<i>Fraxinus pennsylvanica</i>	49.1	101.6	19.4	185	1228.36	227.2	Peters et al. 2010
<i>Quercus rubra</i>	42.9	85.1	20.8	244	232.41	56.7	Peters et al. 2010
<i>Ulmus pumila</i> + <i>Ulmus thomasi</i> *	47.6	79.45	16.9	191.9	394.08	75.6	Peters et al. 2010
Average	32.62	80.68	15.6	220.25	400.23	67.72	

Table 4-5- Urban species maximum transpired water in sap flux (g H₂O per cm² of sapwood area per day) and water use (Kg H₂O per tree per day) for various characteristics including DBH (diameter of breast height in cm), PCA (projected canopy area in m²), height (in m) , and SWA (sapwood area in cm²) for conifer wood anatomy grouping

Species	DBH (cm)	PCA (m ²)	Height (m)	Sap flux (g H ₂ O cm ⁻² d ⁻¹)	SWA (cm ²)	Water use (kg H ₂ O tree ⁻¹ day ⁻¹)	Reference
<i>Picea glauca</i> + <i>Picea pungens</i> *	16.7	8.05	9.7	144.7	148.72	21.5	Peters et al. 2010
<i>Pinus strobes</i>	15.2	28.7	10.3	215.7	178.32	38.5	Peters et al. 2010
<i>Picea abies</i> + <i>Picea glauca</i> *	39.8	36.15	16.9	220.6	494.2	109	Peters et al. 2010
<i>Pinus nigra</i> + <i>Pinus Sylvestris</i> *	31.2	26	14.55	189.2	590.17	111.7	Peters et al. 2010
<i>Cedrus deodara</i>	17.3	16.56	7.03	408.3	33.99	13.9	Chen et al. 2011
<i>Metasequoia glyptostroboides</i>	19.3	4.8	11.6	178.5	36.63	6.5	Chen et al. 2011
<i>Cupressus arizonica</i> + <i>Pinus pinea</i> *	49.6	-	-	100	1122	112.2	Rana et al. 2020
<i>Sequoia sempervirens</i>	48.4	52.5	18	80.3	506.68	40.7	Litvak et al. 2011
<i>Pinus canariensis</i>	54.9	-	-	44.3	1895.8	84	Pataki et al. 2011
Average	32.49	24.68	12.58	175.73	556.28	59.78	

4.3.1 Sap flux comparison of different wood anatomy types

A statistical summary of the variables used in the analysis for all the studied wood anatomy groups for both full dataset and non-limiting water groups, one and two, is presented (Table 4.4). As can be seen, data were not evenly distributed between different groups. In general, more data were available for conifer wood compared to diffuse and ring-porous groups. Ring-porous group had a higher median sap flux than other two wood anatomy groupings for both full dataset and non-water limiting water groups. In addition, diffuse-porous group had almost the same median sap flux as conifer wood group in the full dataset water group, whereas for the non-limiting water group, this median was higher for ring-porous group.

Table 4-6- Statistical summary of variables including sap flux (g/cm²/day), the temperature (°C), VPD (kPa), and solar radiation (W/m²) for specified wood anatomy groupings.

Wood anatomy	Mean [SD]* Sap flux (g/cm ² /day)	Mean [SD] Temperature (°C)	Mean [SD] VPD (kPa)	Mean [SD] Solar radiation (w/m ²)
Diffuse-porous full dataset	92.08 [91.08] **n= 2371	19.04 [6.75] n= 1574	1.3 [0.87] n= 2395	180.8 [87.4] n= 1299
Ring-porous full dataset	93.22 [30.91] n= 2381	19.05 [6.62] n= 1751	1.4 [0.91] n= 2237	180.6 [84.8] n= 1484
Conifer full dataset	68.35 [40.35] n= 2791	18.6 [6.2] n= 1349	1.1 [0.73] n=2724	183.7 [75.5] n= 2138
Diffuse-porous non-water limiting	102.23 [96.88] n=1815	18.8 [7] n=1274	1.3 [0.91] n= 1946	154.9 [78] n= 999
Ring-porous non-water limiting	90.76 [30.23] n= 1725	19.6 [6.5] n= 1568	1.5 [0.92] n= 2054	180.8 [83.5] n= 1303
Conifer non-water limiting	63.82 [38.55] n= 2157	18.1 [6.1] n= 1256	1.06 [0.71] n= 2482	179.8 [74] n= 2045

* SD= standard deviation shown in the brackets; ** n= number of data points for each group

Figure 4.1 shows a boxplot comparison of reported sap flux observations for each wood anatomy grouping. For the full dataset, the sap flux for ring-porous wood was significantly higher than that for the conifer wood or the diffuse-porous wood ($p=2.2 \times 10^{-16}$). For the same group, sap fluxes for diffuse-porous and conifer woods were also significantly different ($p=2.89 \times 10^{-5}$). Similarly, under non-limiting water conditions, ring-porous wood exhibited significantly higher sap fluxes than diffuse-porous wood ($p=1.84 \times 10^{-8}$). Likewise, when water-limiting periods were removed, a significant difference was observed in conifer wood compared to ring- and diffuse-porous wood groupings ($p=2.2 \times 10^{-16}$). Although ring-porous trees exhibited higher sap fluxes overall, the maximum sap flux rates reported for conifer and diffuse-porous species far exceeded those reported for ring-porous species. As indicated by the overlap in reported environmental drivers (Table 4.4), this result may reflect the influence of various mechanisms employed by trees to regulate water movement during stressful periods.

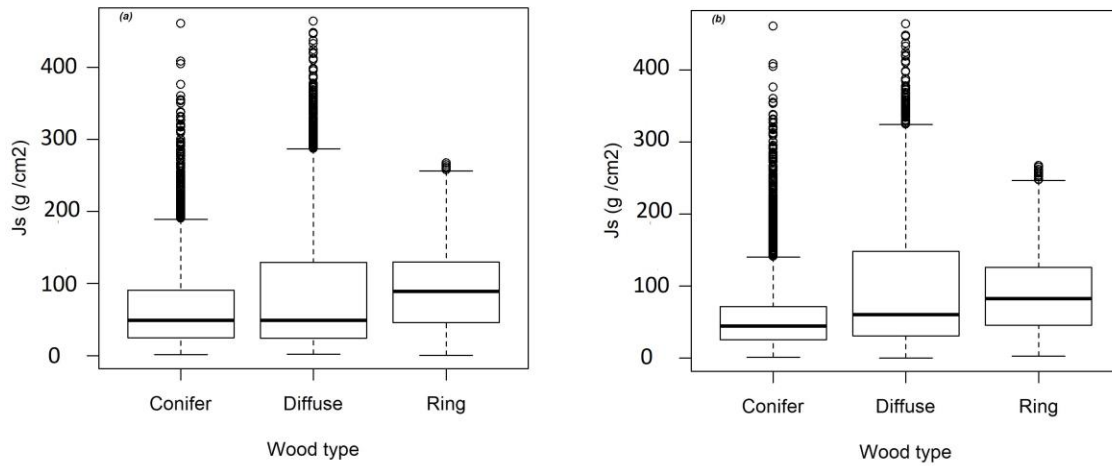


Figure 4-1 The boxplot comparison of daily sap flux for studied wood anatomy groupings for full dataset analysis (a) and non-limiting water analysis (b)

4.3.2 Correlation behavior of the variables

Figures 4.1 to 4.3 show the relationship between sap flux and environmental variables for diffuse-porous, ring-porous, and conifer wood anatomy groupings. Associated Spearman correlation coefficients and corresponding p-values for each correlation set are presented in Table 4.5.

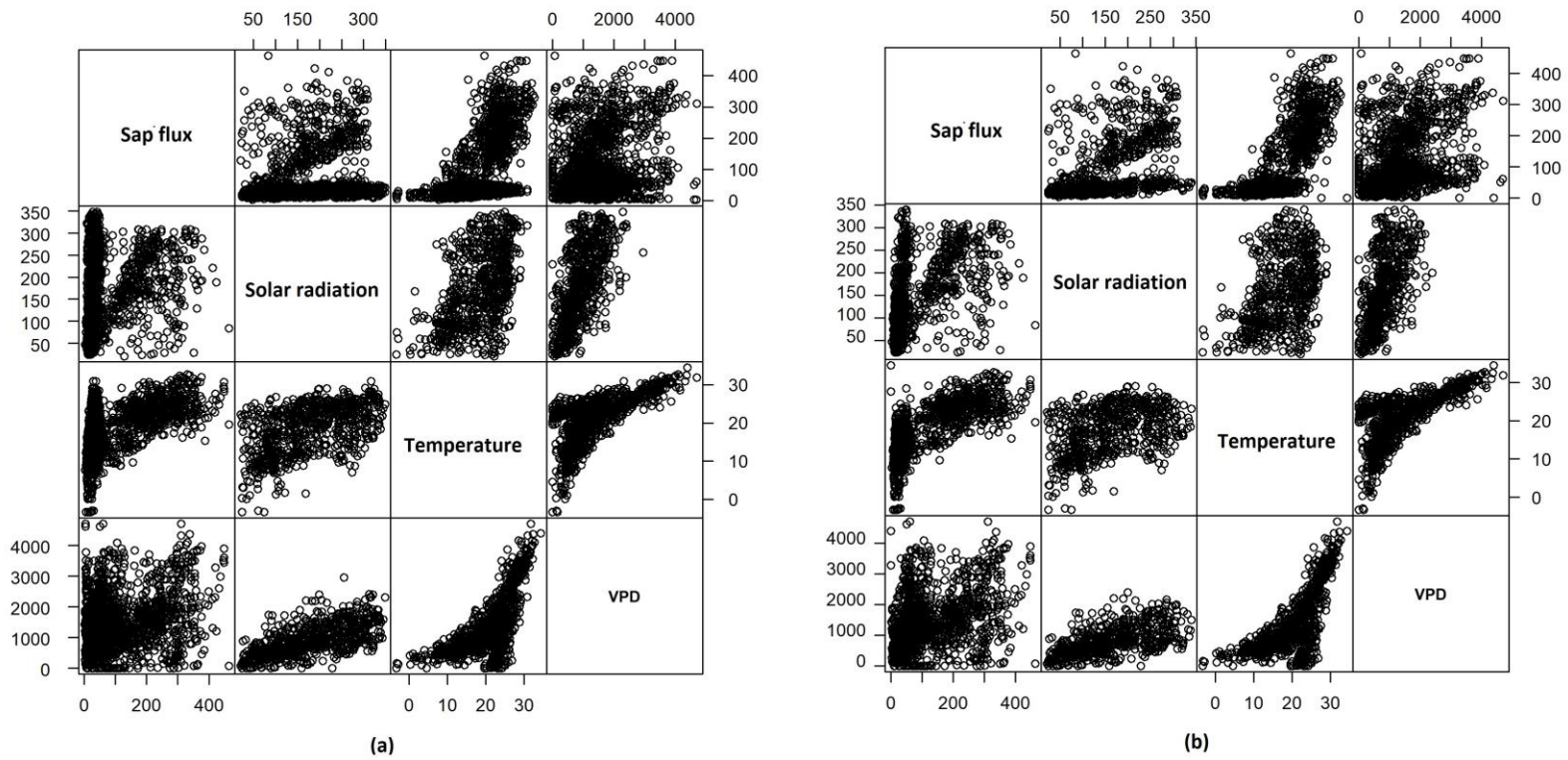


Figure 4-2 Daily data illustrating correlations between pairs of the following variables: sap flux ($\text{g}/\text{cm}^2/\text{day}$), Solar radiation (W/m^2), temperature ($^{\circ}\text{C}$), and VPD (Pa) for diffuse-porous wood anatomy group for full dataset (a) and non-limiting water (b)

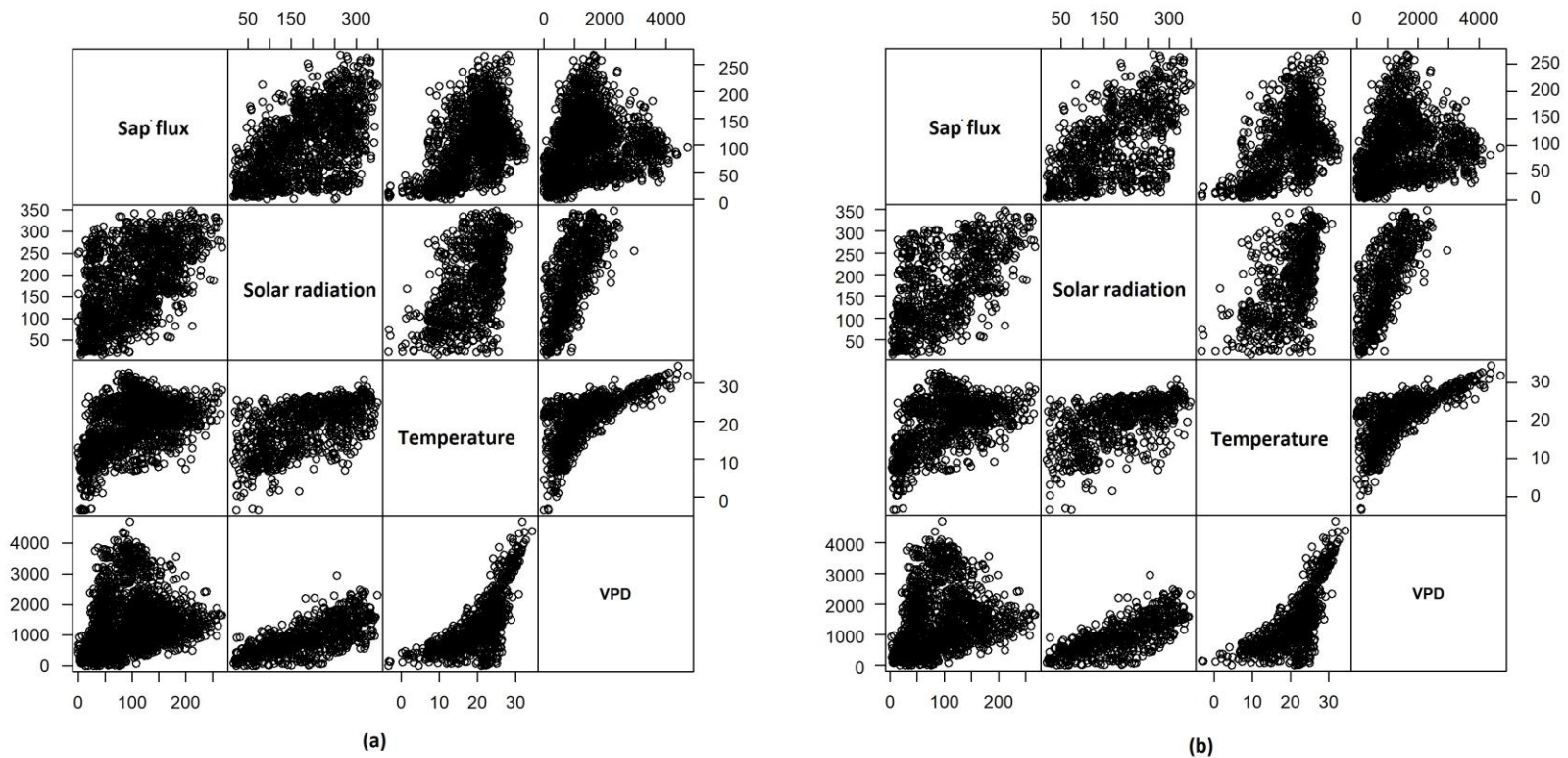


Figure 4-3 Daily data illustrating correlations between pairs of the following variables: sap flux ($\text{g}/\text{cm}^2/\text{day}$), Solar radiation (W/m^2), temperature ($^{\circ}\text{C}$), and VPD (Pa) for Ring porous wood anatomy group for full dataset (a) and non-limiting water (b)

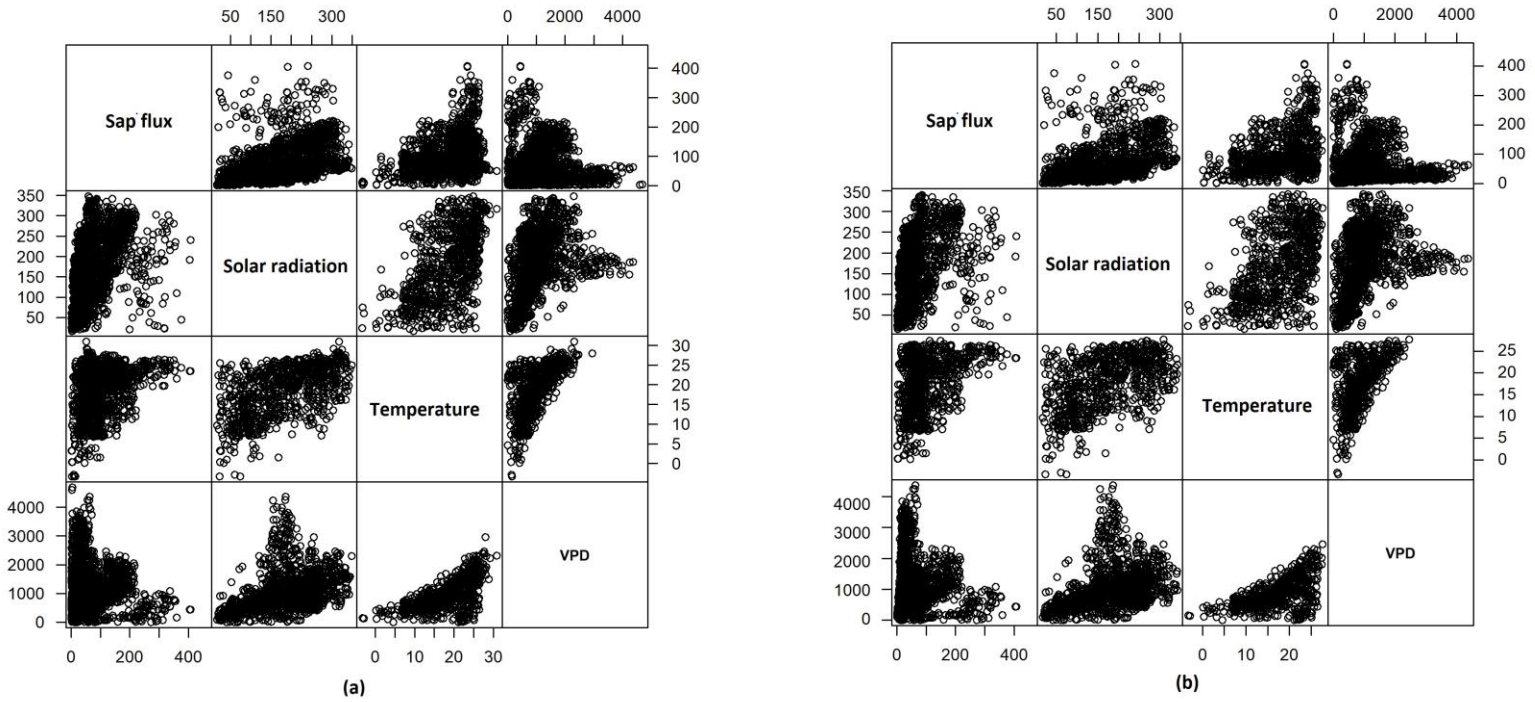


Figure 4-4 Daily data illustrating correlations between pairs of the following variables: sap flux (g/cm²/day), Solar radiation (W/m²), temperature (°C), and VPD (Pa) for conifer wood anatomy group for full dataset (a) and non-limiting water (b)

Table 4-7- P-values and Spearman's rho for all the studied variables including sap flux (J_s), solar radiation, Temperature (Temp), and VPD over various wood anatomy groupings and soil water conditions.

Diffuse porous: full dataset	J_s	0.22	0.56	0.36	Diffuse porous: non-limiting water	J_s	0.56	0.78	0.53
	p= 1.8×10^{-15}	Solar radiation	0.58	0.71		p= 2.2×10^{-16}	Solar radiation	0.49	0.67
	p= 2.2×10^{-16}	p= 2.2×10^{-16}	Temp	0.77		p= 2.2×10^{-16}	p= 2.2×10^{-16}	Temp	0.75
	p= 2.2×10^{-16}	p= 2.2×10^{-16}	p= 2.2×10^{-16}	VPD		p= 2.2×10^{-16}	p= 2.2×10^{-16}	p= 2.2×10^{-16}	VPD
Ring porous: full dataset	J_s	0.56	0.49	0.34	Ring porous: non-limiting water	J_s	0.57	0.49	0.35
	p= 2.2×10^{-16}	Solar radiation	0.55	0.75		p= 2.2×10^{-16}	Solar radiation	0.55	0.78
	p= 2.2×10^{-16}	p= 2.2×10^{-16}	Temp	0.73		p= 2.2×10^{-16}	p= 2.2×10^{-16}	Temp	0.71
	p= 2.2×10^{-16}	p= 2.2×10^{-16}	p= 2.2×10^{-16}	VPD		p= 2.2×10^{-16}	p= 2.2×10^{-16}	p= 2.2×10^{-16}	VPD
Conifer wood full dataset	J_s	0.29	0.39	-0.001	Conifer wood non-limiting water	J_s	0.37	0.38	-0.04
	p= 2.2×10^{-16}	Solar radiation	0.51	0.54		p= 2.2×10^{-16}	Solar radiation	0.46	0.52
	p= 2.2×10^{-16}	p= 2.2×10^{-16}	Temp	0.44		p= 2.2×10^{-16}	p= 2.2×10^{-16}	Temp	0.37
	p= 0.93	p= 2.2×10^{-16}	p= 2.2×10^{-16}	VPD		p= 0.08	p= 2.2×10^{-16}	p= 2.2×10^{-16}	VPD

Across all wood anatomy groupings, removing flux measurements during water-limited conditions caused an increase in the correlation between sap flux and all the evaluated independent variables. Of these variables, temperature exhibited the strongest correlation with observed sap fluxes in the diffuse-porous group. The relative strength of correlation between sap flux and VPD or solar radiation differed across the full dataset and non-limiting water groups; while VPD exhibited a stronger correlation with sap flux in the full dataset, solar radiation exhibited a stronger correlation with sap flux under non-limiting water conditions.

Correlations between sap fluxes and environmental variables reported for ring-porous wood were weakest for VPD. In contrast, correlations between sap flux the other two variables (temperature and solar radiation) were similar. Unlike diffuse-porous trees, removing observations during water-limited periods did not have any significant effect on Spearman rho values.

In the case of conifer wood, temperature exhibited a stronger correlation with sap flux compared to solar radiation for the full dataset. The correlation between temperature and sap flux remained almost unchanged under non-limiting water conditions; however, solar radiation and sap flux correlations were strengthened for non-limiting water conditions. In conifer wood, sap flux did not exhibit any relationship with VPD in either the full dataset or the non-limiting water group.

In all wood anatomy groupings, environmental variables were similarly related. VPD was positively correlated to both temperature and solar radiation. Also, as the temperature increased, the upper limit for VPD magnitude was raised for all the evaluated woods.

While the measured sap flux over the surveyed studies for diffuse-porous wood passed the value of $400 \text{ g/cm}^2/\text{day}$, this value remained below $300 \text{ g/cm}^2/\text{day}$ for the ring-porous wood grouping. The scatterplots for the correlation between sap flux and VPD for ring-porous group (Figure 4.3) showed a maximum sap flux of $160 \text{ g/cm}^2/\text{day}$ for VPD values above almost 2.5 kPa .

Similarly, in the conifer wood, the sap flux stayed below 100 and 220 $g/cm^2/day$ for 2.2 and 1.2 kPa VPD values, respectively (Figure 4.4).

4.3.3 Simple linear regression models for modeling sap flux consistent with each independent variable

As can be seen in Figure 4.5, independent variables, including VPD, solar radiation, and temperature, were plotted against sap flux across the wood anatomy groupings. The results of regression models, developed separately for each variable in each group, are provided in Table 4.6.

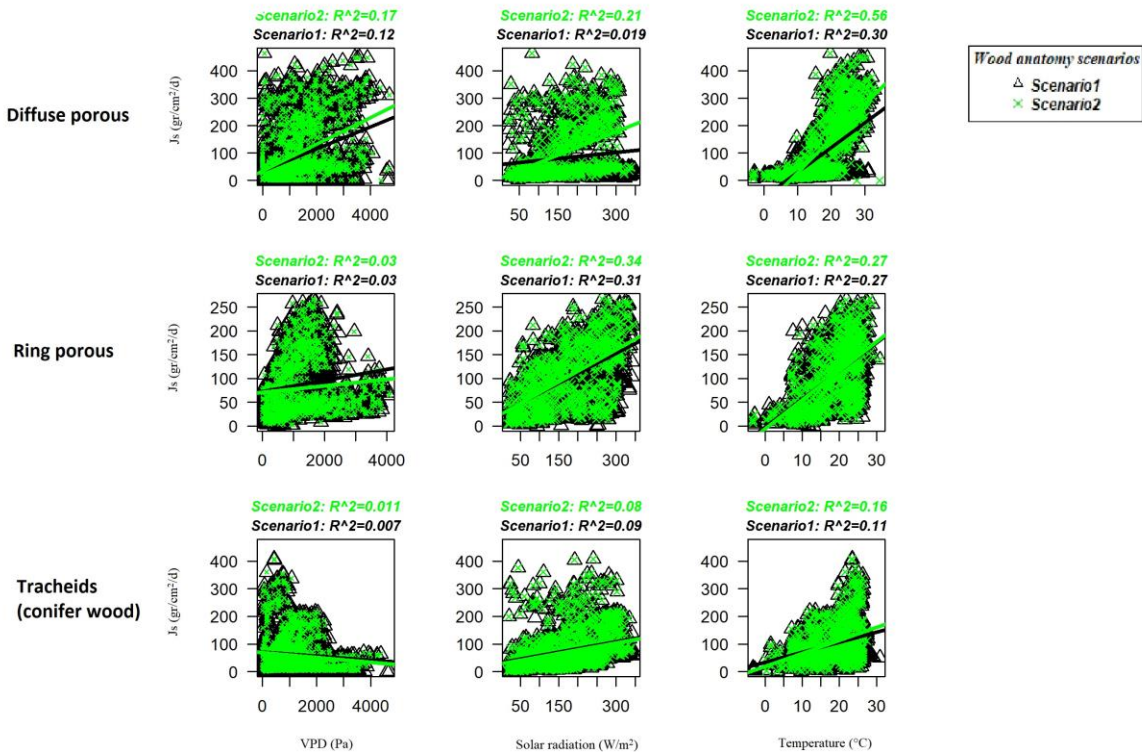


Figure 4-5 Regression models and coefficient of determination relating to studied wood anatomy groupings for full dataset analysis, and non-limiting water analysis

Although there was a significant linear relationship between VPD and sap flux ($p < 0.05$) for all the evaluated of wood anatomy groupings and analyses, the coefficient of determination

was not significant. It is not possible to do a comparison within the environmental variables by their slopes, unless they are all normalized with respect to their range of variation. However, a comparison across the wood anatomy groupings for each environmental variable indicated that for both VPD and temperature diffuse-porous wood was the most affected group by variation in these variables, whereas the conifers grouping was the least influenced. In contrast, the highest impact of solar radiation occurred on the ring-porous group, followed by the conifer and diffuse-porous groupings.

In the full dataset group, both temperature and solar radiation were statistically significant predictors of sap fluxes in all wood anatomy groups, although neither explained a majority of observed variability in sap fluxes. In the case of ring-porous wood, solar radiation and temperature explained similar amounts of variability in observed sap fluxes with R^2 values of 0.31 and 0.27, respectively. Similarly, solar radiation and temperature explained similar levels of variability (albeit very low) in the conifer sap fluxes with R^2 values of 0.09 and 0.11, respectively. In the case of diffuse-porous wood, temperature provided greater predictive power ($R^2 = 0.30$) compared to VPD ($R^2 = 0.13$) or solar radiation ($R^2 = 0.02$).

Table 4-8 Simple linear regression results for studied wood anatomy groupings

Variable	Wood anatomy	Full dataset				Non-limiting water			
		Equation		Adjusted R ²	P-value	Equation		Adjusted R ²	P-value
		Intercept	Slope			Intercept	Slope		
VPD	Diffuse porous	33.7	0.04	0.13	2.2*10 ⁻¹⁶	34.9	0.05	0.2	2.2*10 ⁻¹⁶
	Ring porous	72.2	0.01	0.04	2.2*10 ⁻¹⁶	69.71	0.01	0.03	3.78*10 ⁻¹⁴
	Conifer wood	69.9	-0.007	0.005	0.0001	68.5	-0.008	0.008	1.45*10 ⁻⁵
Temperature	Diffuse porous	-59.4	9	0.3	2.2*10 ⁻¹⁶	-95.6	12.5	0.56	2.2*10 ⁻¹⁶
	Ring porous	15.6	4.7	0.27	2.2*10 ⁻⁶	14.95	4.7	0.27	2.2*10 ⁻¹⁶
	Conifer wood	34.4	3.6	0.11	2.2*10 ⁻¹⁶	18.5	4.71	0.16	2.2*10 ⁻¹⁶
Solar radiation	Diffuse porous	58.1	0.15	0.02	5.01*10 ⁻⁷	6.65	0.57	0.21	2.2*10 ⁻¹⁶
	Ring porous	26.4	0.42	0.31	2.2*10 ⁻¹⁶	24.1	0.45	0.34	2.2*10 ⁻¹⁶
	Conifer wood	32.5	0.25	0.09	2.2*10 ⁻¹⁶	28.9	0.25	0.08	2.2*10 ⁻¹⁶

Under non-limiting water conditions, with the removal of water-limited periods, the temperature coefficient of determination for diffuse-porous, and conifer wood groups increased to 0.56, and 0.16, respectively. Slope values also increased, indicating an enhanced response in flux rates to temperature under adequate water conditions. In contrast, both the response to and predictive power of temperature remained the same for the ring-porous group even when limiting water conditions were removed. While no improvement in the solar radiation coefficient of determination value was observed by removing water limited periods in the conifer wood group, this criterion improved the values for diffuse and ring-porous groups to 0.21 and 0.34, respectively. Coefficient values also increased, particularly in the case of diffuse-porous trees, again suggesting an enhanced sap flux response to solar radiation in the absence of water limited conditions.

4.3.4 Simultaneous effect of multiple variables on daily sap flux

The results of the multiple regression model are shown in Table 4.7. As can be seen, the influence and kinds of variables vary across the wood anatomy groupings.

Table 4-9- Multiple linear regression model results for studied variables including sap flux (Js), temperature (Temp), solar radiation (Rs), and VPD across the wood anatomy groupings

Wood anatomy groups	Equation	R ²	Number of data points	Number of studies
Diffuse-porous full dataset	$J_s = -40.4 + 5.1Temp + 0.05VPD$	0.35	1434	4
Ring-porous full dataset (highest number of data points)	$J_s = 15.6 + 4.7Temp$	0.27	1689	4
Ring-porous full dataset (highest performance)	$J_s = -6.15 + 2.82Temp + 0.12Rs + 0.04VPD$	0.46	1288	3
Conifer Full dataset (highest number of data points)	$J_s = -34.3 + 0.29Rs - 0.01VPD$	0.1	1971	4
Conifer full dataset (highest performance)	$J_s = -50.9 + 6.4Temp + 0.77Rs - 0.03Temp \cdot Rs$	0.21	1318	3

Diffuse-porous non-limiting water	$J_s = -82.4 + 9.7\text{Temp} + 0.03\text{VPD}$	0.58	1047	4
Ring-porous non-limiting water (highest number of data points)	$J_s = 14.95 + 4.7\text{Temp}$	0.27	1068	4
Ring-porous non-limiting water (highest performance)	$J_s = -6.15 + 5.1\text{Temp} + 0.05\text{VPD}$	0.53	786	3
Conifer Non-limiting water (highest number of data points)	$J_s = -33.3 + 0.29R_s - 0.01\text{VPD}$	0.1	1616	4
Conifer non-limiting water (highest performance)	$J_s = -32.6 + 5.3\text{Temp} + 0.53R_s - 0.01\text{Temp} * R_s$	0.24	895	3

There was a marked improvement in the coefficient of determination in diffuse-porous wood groupings by removing limited water periods. While the R^2 was equivalent to 0.35 in the full dataset, it increased to 0.58 under non-limiting water conditions. However, as with simple linear regression models, there was not a substantial improvement in predictive power by removing water limited periods for ring-porous or conifer wood anatomies.

In general, temperature seemed to be the most influential variable in all wood anatomy groupings since the highest R^2 corresponded to the models in which this variable was incorporated. In the ring-porous wood group, the mere use of temperature as an independent variable best described the variability in sap flux, if the highest possible data points were included. However, the best fit with the highest R^2 was achieved when the all VPD, temperature, and solar radiation data were used, although the number of data points and studies were reduced.

Similar to the ring-porous group, the combination of solar radiation and temperature showed the highest R^2 for the conifer wood group, in which only 895 data points with 3 studies were included. In contrast, incorporating solar radiation and VPD increased the number of data points and studies to 1616 and 4, respectively, even though the R^2 was decreased to only 0.1.

4.4. Discussion

4.4.1 Assumptions and consequential uncertainties

We assumed that the values provided by the Grainer method for each study were correct. However, what needs to be done is a careful analysis of each of the studied papers and how they made the measurement using the Grainer method. Other methods in the heat-pulse technology such as heat-pulse method (Kirkham, 2014) require a wound-response to the invasion by the probes. Heat-pulse technology methods assume that the heater and temperature probes have no effect on the measured heat flow. In reality, however, convection of the heat pulse is disrupted by the presence of heater and temperature probes and by the disturbance of xylem tissue related to their placement. Therefore, these disturbances produce a systematic underestimation in the measured heat pulse velocity (Green et al., 2003). Though, in the evaluated papers, it is not clear if this factor is considered for the tree sap flux measurements. Additionally, Grainer methods assumes a zero sap flux at night times, while, nocturnal sap fluxes can be significantly high (Green et al., 1989).

To extract transpired water data, we faced discrepancies in the reported transpired water since studies measured transpiration for various species utilizing different tactics. Although transpired water was measured for individual species using the sap flux measurement using heat dissipation methods to estimate transpiration, the reported measurements were not always attributed to each certain species. For example, in Peters et al. (2010), an average of different species in the same genus was reported as the genus transpired water. In Rana et al. (2020), measured species were assigned to four main categories (*Olea*, *Citrus* and *Eriobotrya*, Conifers, and Broadleaves), and averaged transpired water over a group of species was stated as a representative for each category. Additionally, the number of sampled trees were not identical

across the studies. Therefore, all these inconsistencies led to uncertainty in our collected data, which, in return, affect the results.

Due to the limited number of field studies in urban areas, the influence of individual studies was strong. Moreover, we were limited to the types of data reported across a sufficient number of studies (Table 4.2). For instance, data from Bush et al. (2008), which were collected in the Salt Lake valley with high values in temperature and VPD, may have substantially impacted our analysis in several ways. For example, only ring and diffuse-porous wood anatomy groupings were studied, and solar radiation was not measured in their work. As a result, the environmental conditions of this study did not affect the conifer wood grouping, when it impacted the other two studied wood groups. Also, since solar radiation was not measured in their study, this variable was not incorporated into multiple linear regression model analyses.

Methods for measuring and reporting soil moisture data also were not consistent among the studies. Studies utilized different reporting methods, including crop water stress index, relative extracted water, soil water content measurement, and declaring whether the crops were irrigated or not. As a result, different assumptions were made for individual studies. For instance, in Pataki et al. (2011), from which relatively low values for sap flux were reported, it was not mentioned whether the plants were water-stressed or not; instead, only plants that were not irrigated throughout the study period were specified. Thus, we assumed that if plants were not labeled "unirrigated," they were not affected by water limitations.

To make a meta-data analysis feasible, we made simplifying assumptions and used equations to unify the variable units across the studies. However, these assumptions and equations inside them carry some uncertainties. For example, Equations 4.2 and 4.3, which were used to scale sap flux measurements taken across the outermost sapwood area to the entire active sapwood

for angiosperms and gymnosperms, respectively, was not an ideal Gaussian fit for the data used to develop these equations. Although the fit was relatively robust, the coefficients of determination were 0.63 and 0.76 for angiosperms and gymnosperms, respectively (Pataki et al., 2011).

We used variables on a daily basis in our analysis. Throughout the day, the value of each variable changes and each variable may experience a different range over different days of measurement. However, for the purpose of simplification, an average of each variable over the day was utilized for analysis purposes. For example, over a day temperature may experience of a range of 18 to 28°C, or 21 to 25°C, while both give an average value of 23. Therefore, considering only an averaged value over the day overlooks its range of variation and the potential effects of it on other variables.

We assigned the value of each independent variable to its corresponding sap flux for each day. However, sap flux may have a lagged response to explanatory variables. Therefore, different daily sap flux values may occur even with the same averaged explanatory-variables magnitude. Similar circumstances exist between independent variables correlation, which leads to more complexity in the sap flux approximation.

4.4.2 Water management

As indicated by their higher median sap fluxes, ring-porous trees showed a higher capability in transpiring water through their stems. Also, based on an analysis in our study, sapwood area showed no meaningful relationship to tree diameter of breast height (DBH) and projected canopy cover (results are not published). This absence of clear relationship indicates increasing DBH does not necessarily lead to an increase in sapwood depth. Therefore, a wise selection of trees with a higher ratio of sapwood depth to DBH can guide to higher transpired water while more surface area is saved. These results imply that in urban areas with runoff issues, type

of tree wood anatomy and sapwood area to DBH rate should be considered for better management decisions.

While ring-porous wood had a higher median of sap flux compared to the other two wood groupings, its range of sap flux variation was much lower. This result agrees with Peters et al. (2010), who found that the sap flux of ring-porous species remained relatively unchanged compared to diffuse-wood and conifer trees. A potential cause of this behavior may correspond to the stomatal regulation of ring-porous wood, because their sizeable earlywood vessels increase the risk of cavitation for this group (Peters et al., 2010; Taneda & Sperry, 2008; Hacke et al., 2006). Although the number of data points that were excluded from the dataset to remove water-limited periods was almost equal across the tree wood groupings, diffuse-porous groups indicated a higher sensitivity to water limitation. However, more research is needed to evaluate the effect of plant water stress and its intensity on the behavior of sap flux in various tree wood groupings.

With temperature representing the most influential independent variable on the sap flux rate, not all wood groups responded equally to this variable. Diffuse-porous showed the most responsiveness to increase in temperature among tree wood groupings, whereas the conifer tree group was the least sensitive. This result helps water managers and policymakers to better select trees in urban areas according to individual area requirements.

In a simple linear regression model, all environmental variables evaluated herein (temperature, VPD, and solar radiation) showed a positive correlation with sap flux while they were also positively correlated to one another. However, in multiple regression models developed for ring-porous trees and with respect to R^2 , solar radiation and VPD did not appear to be influential when incorporated as a variable in the multiple regression model. We should note that in simple linear regression models, the effect of each variable is evaluated through the model, while other

variables are being ignored. In multiple regression models, the coefficient of each variable shows the effect of an assessed variable on the dependent variable while other independent variables are being fixed. Therefore, increases in sap flux by an increase in solar radiation could be due to the positive relationship of solar radiation to temperature and not just its relationship with sap flux as the dependent variable.

In general, no single-variable model did a good job of explaining observed variability in observed sap fluxes (R^2 values ranged from the low of 0.02 to the high of 0.56). In other words, transpiration and associated sap flows are more complicated than being estimated only with variables evaluated in this work. Therefore, other environmental variables (i.e., wind speed, relative humidity, elevation, albedo, pollution, etc.) may influence transpired water as well as the individual tree species characteristics. Additionally, the “best fit” model was different for each wood type, which suggests the importance of wood anatomy in transpiring water.

Although VPD was very positively correlated to temperature, it did not show a significant relationship to sap flux over any of the tree wood anatomy groupings. As the temperature increased, the threshold for VPD values was raised. This result means that a rise in temperature allowed the VPD values to experience wider ranges. Results showed that a 10 °C increase in temperature (for a range of zero to 30 °C) allowed VPD to rise one kPa (for a range of zero to 3 kPa). Although significant relationships were not detected, we observed a unique pattern in the sap flux behavior with changes in VPD. There was almost no sap flux beyond 160 g/cm²/day for VPD values above 2.5 kPa in the ring-porous wood grouping. Similarly, two notable thresholds occurred in the conifer wood grouping. While sap flux ranged up to nearly 400 g/cm²/day for VPD values below 1 kPa, it went down below 220 g/cm²/day for VPD values greater than 1 kPa. The next threshold happened at 2 kPa, beyond which sap flux fell below 100 g/cm²/day. This fact may show

the role that VPD has on stomatal regulation of plants. When VPD reaches specific values in urban settings, it may control stomatal opening.

It is not clear how the simultaneous effect of the different independent variables can affect the magnitude of transpiration. For example, how does the effect of a high temperature and VPD on sap flux differ from the influence of high temperature and a low or moderate VPD? Therefore, additional research with more complex statistical approaches is required to evaluate the aggregate effect of explanatory variables on transpiration.

Although a much larger number of data exist in natural forests, a comparison of this study to an all-inclusive natural forest study (Wullschleger et al., 1998a), with data included from a wide variety of climates and environmental conditions, suggested an almost similar pattern for trees in these two different environments. For 90% of the data in rural forests, the average transpiration was 74.5 (s.d. 52.3) $kg\ H_2O/tree/day$ with a range from 10 to 179 $kg\ H_2O/tree/day$. Similarly, for 90% of the urban tree data analyzed herein, urban trees transpired an estimated 6.5 to 178.5 $kg\ H_2O/tree/day$, with an average of 66 (s.d. 47.8) kg of water per tree per day.

4.5. Conclusion

In an urban-tree review, we investigated the variation of sap flux for different wood anatomy groupings, including diffuse-porous, ring-porous, and conifer trees and how water-limited conditions can affect the sap flux of each group. Ring-porous trees had the highest median sap flux and also the lowest range in variation. The diffuse-porous group was more sensitive to the water-limited conditions compared to the other two groups. Temperature appeared to be the most influential climatic variable in controlling the sap flux variation in urban areas. Although VPD did not exhibit a significant correlation in estimating the sap flux, at certain VPD thresholds, drastic declines in sap flux values occurred in conifer trees. Also, beyond the VPD of 2.5 kPa , the

maximum sap flux was limited to $150 \text{ g/cm}^2/\text{day}$ in the ring-porous wood group. A comparison between the result of this study, which is a review urban trees, and a similar review paper by Wullschleger et al. (1998) in natural forests, did not demonstrate a substantial difference of the range or average transpired water for these two different environments. The outcomes of this study could give stormwater managers and policymakers a better perspective to manage water use and stormwater, while minimizing the impact of increased impervious cover in urban areas.

Chapter 5 - A modeling approach on the role of trees on the urban runoff management: A case study of three small watersheds in the Kansas City metropolitan area

5.1 Introduction

The hydrological impacts of urbanization have been well documented and include increases in the volume, peak rate, duration and frequency of surface runoff with commensurate reductions in infiltration and evapotranspiration (e.g. Kalnay & Cai, 2003). Associated impacts to hydrological regimes and biological integrity of receiving aquatic systems have also been studied (e.g., Booth, 2002; Paul & Meyer, 2001), and have spurred efforts to enhance infiltration and other natural hydrologic processes in urban watersheds through the use of green infrastructure and related technologies (Fletcher et al., 2013; Walsh et al., 2005). Urban forests and trees are broadly recognized as a component of urban green infrastructure networks and, as such, their capacity to reduce surface runoff while providing other environmental benefits is receiving increased attention (e.g., Armson et al., 2013; Puno et al., 2019). Above ground, trees intercept and evaporate incident precipitation to reduce runoff timing and volume. Trees may also reduce runoff by enhancing infiltration processes below ground and subsequently returning water stored in the soil profile to the atmosphere via transpiration. The quantitative synthesis of existing precipitation partitioning and transpiration studies in urban tree canopies presented in Chapters 2 and 4 of this dissertation provide some indication of the potential magnitude of these processes at the tree-scale. For example, urban tree canopies can intercept 15% to 72% of annual precipitation, while daily transpiration rates were found to range from 13 to 464 g H₂O cm⁻² day⁻¹

¹. Others have conducted experimental studies in an attempt to better understand how tree-scale processes may influence hydrologic outcomes at larger spatial scales. For example, at the yard-scale, rainfall interception in 16 residential yards with various tree canopy and understory structure was found to range from 9.1 to 21.4% of annual precipitation (Inkiläinen et al. 2013). At the scale of a small catchment (9 m²), parking lot runoff was reduced by 62% when directed to a tree pit relative to an asphalt surface (Armson et al. 2013b).

Clearly, there is a large gap between the spatial scales at which hydrological processes mediated by trees have been measured and the spatial scales at which stormwater is generally regulated and monitored. Not surprisingly, efforts to quantify the aggregate impact of tree-scale processes at the scale of urban watersheds have relied on a variety of empirical and process-based models. A mechanistic water balance model in which combined effects of canopy interception, infiltration and evapotranspiration (ET) were represented was calibrated and validated using field experiment data to identify tree pit capability on runoff mitigation in small (100 m² to 480 m²), highly impervious urban catchments (Grey et al., 2018). The results of this study revealed that even in heavily urbanized areas with low conductivity soils, a 90% reduction in annual runoff is achievable when tree pits were sized between 2.5% and 8% of the impervious catchment area, depending on pit exfiltration rates (Grey et al. 2018). In this study, tree interception and infiltration were modeled as constant values while ET was modeled using the reference ET method (Allen et al., 1998). Matteo et al. (2006) studied watershed-wide implications of street and riparian buffering through urban forestry and their ability to reduce these impacts. A distributed/lumped parameter watershed model called generalized watershed loading function (GWLF) was used to simulate the watershed processes based on weather data and water balance calculations on a daily time step. In this modeling approach, hydrologic

effects of trees were represented via the curve number method (Cronshey et al., 1985). Results indicated that watershed stormwater runoff would be decreased through location-specific application of riparian and street buffers. Similarly, Yao et al. (2015) applied the curve number method to evaluate the effect of canopy cover increase on runoff reduction on a city scale in Beijing, China. Model results indicated a 30% yearly reduction in runoff by increasing tree canopy cover by approximately 11%. Others have adopted more process-based models to represent the effects of urban trees on urban runoff hydrology at various spatial scales. For example, Mittman (2009) examined the impact of the spatial distribution of vegetation using a spatially distributed GIS based model called Regional Hydro-Ecological Simulation System (RHESys). In this model, tree canopy interception processes are explicitly modeled as a function of rainfall depth, gap fraction, plant area index, and canopy storage capacity. In the case study watersheds to which this model was applied, results indicated that riparian forests may provide better reduction of peak flow than upslope forests, but upslope forests may provide greater reduction of runoff volumes. UFORE-Hydro was run by Wang et al. (2008a) on the Dead Run catchment in Baltimore, Maryland. The study area was 70% pervious, and 30% impervious. In the impervious area, 5% was covered by trees, and in the pervious area 17% was covered by trees, 69% covered by short vegetation and 14% covered by bare soil. The results indicated a 50% increase in total runoff by increasing the existing impervious cover by 50%. Also, a total precipitation of 18 mm (three storms), 7.1 mm (three storms), and 50.3 mm (one storm) for existing watershed condition resulted in 18.9%, 40.8%, and 3.6% of interception, respectively. The effects of different vegetation cover on surface and subsurface hydrology in an urban park located in the Northern Terraces city park in Hradec Králové, Czech Republic was evaluated using a semi distributed, bucket-type model for daily flow simulations model (PERSiST).

Results showed that tree landcover had significantly less surface runoff than park lawn.(Deutscher et al., 2019).

The overview of modeling efforts presented in the preceding paragraph demonstrates the range in approaches used to examine the effects of urban trees on urban hydrology. These approaches vary in terms of their overall complexity in representing hydrological processes, as well as in how trees are represented. The modeling approaches could be categorized as low complexity (e.g. curve number method), moderate complexity (e.g. i-Tree-Hydro; US EPA), and advanced complexity (e.g. SWAT; RHESSys). Among these models i-Tree, Soil and Water Assessment Tool (SWAT), and RHESSys explicitly consider the effect of trees. However, compared to i-Tree the other two models are more complex and require more inputs (Coville et al., 2020).

This overview also reveals several gaps in current understanding of the role of urban trees in regulating urban stormwater runoff. It is not evident how an organized increasing in tree canopy cover over pervious and impervious area affects runoff volume using a model in which the effect of trees is explicitly considered. Also, the extent to which tree phenologic factors, including leaf area index and evergreenness influence runoff volume remains unclear. A systematic study design with a wide range of tree phenologic factor variation is required to fill this gap in the literature. Moreover, while the literature reports the hydrological benefits of increasing canopy cover within urban areas, the relative effect of land cover in enhancing or dampening these benefits has not been widely explored.

In this study, we aimed to address these gaps by adopting a systematic modeling approach implemented in i-Tree Hydro and applied to three different urban watersheds. I-Tree Hydro was selected as the modeling tool in this study because not only it explicitly considers the effect of

trees in the model, but also requires fewer input variables compared to advanced complex models. In addition, we tried to examine the influence of an organized increasing in tree canopy cover for urbanized watersheds. Specifically, we aimed to address the following questions in this study:

- (1) To what extent do different patterns of urbanization influence watershed hydrological response to increases in tree canopy cover and precipitation magnitude?
- (2) What is the effect of tree phenology on runoff response for storm events relevant to urban stormwater management?
- (3) What is the influence of tree phenological patterns on runoff response for different patterns of urbanization on an annual basis?

To answer these questions, calibrated/validated i-Tree hydro models were created for three different urban watersheds, each representing a different pattern and intensity of urban development. Within these models, canopy cover, tree type (evergreen or deciduous), and leaf area index (LAI) was systematically varied within each of the three study watersheds for storm events relevant to stormwater management (i.e., the so-called 25-mm “water quality” storm and the 10-year, 24 hour storm). In addition, a wide range of LAI was applied to each level of urbanized watershed to examine the change in runoff response. Finally, the effects of tree phenology were examined by varying deciduous and evergreen tree cover within a continuous, multi-year simulation period.

5.2 Method

5.2.1 Watershed descriptions

Three sub-watersheds within the Blue River watershed of the Kansas City metro area were selected based on the following criteria: (1) watersheds were located within the same

hydro-physiographic province and exhibited similar slope and soils and (2) watersheds exhibited different levels of imperviousness, tree canopy cover and land use. The first criterion was selected to reduce the influence of topographic features and soil type while the second criterion was intended to enable comparing hydrological responses to increasing tree canopy cover across urban watersheds with differing land cover characteristics. Selected watersheds were known as Turkey Creek @ Quail Creek (TU02), Indian Creek @ Quivira (IN05), and Tomahawk Creek (TH03) and were representative of residential, commercial/industrial, and a mix residential/commercial land use, respectively (Table 5.1; Figure 5.1).

Table 5-1- Study Watershed Characteristics

		Watershed		
		TU02	IN05	TH03
Watershed area	(km ²)	2.7	2.5	4.2
Land Cover (% of total watershed area)	Tree canopy	45	21	14
	Herbaceous/Shrub	14	12	36
	Impervious cover	41	67	45
	Agricultural crop (cultivated)	0	0	5

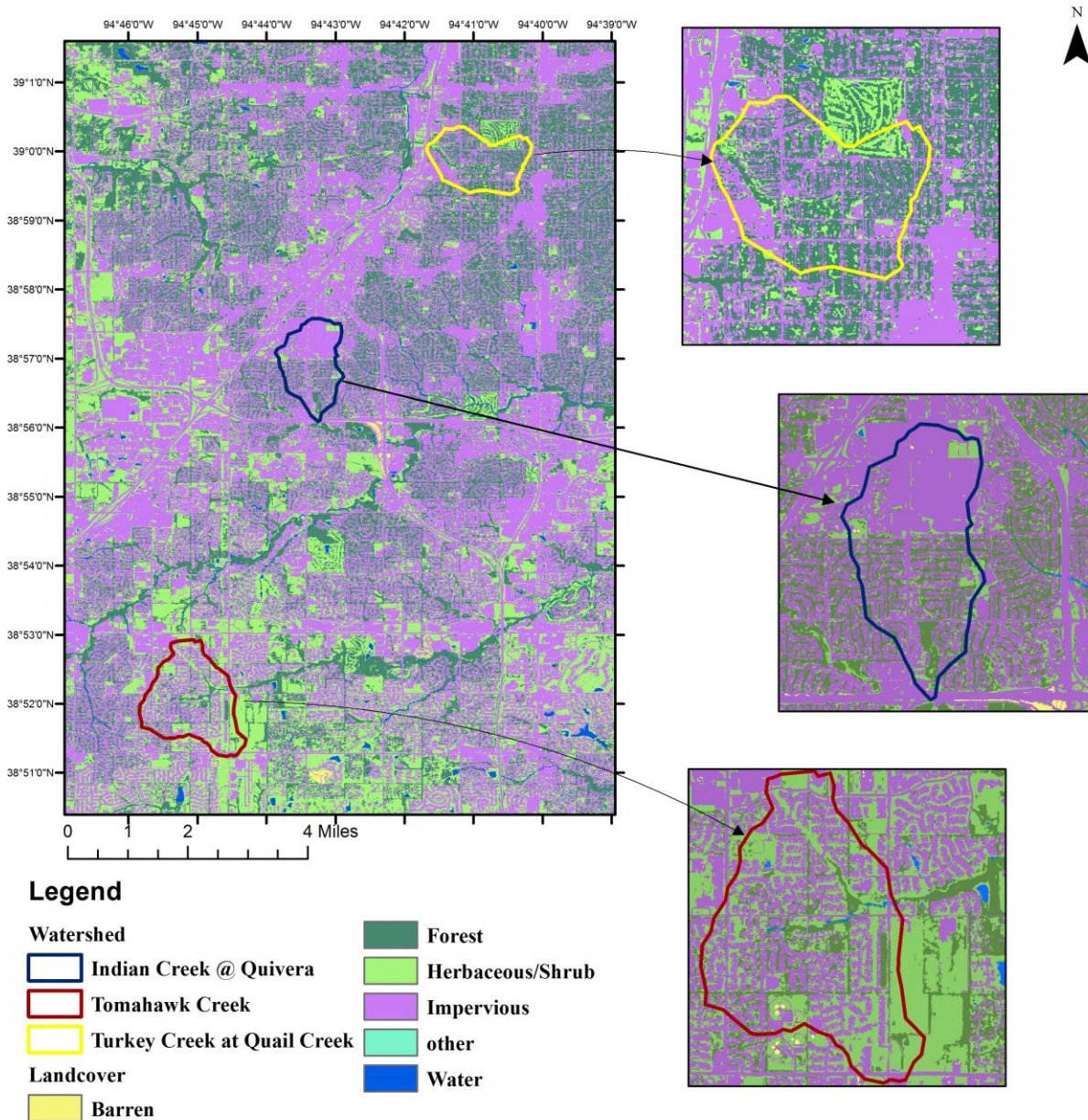


Figure 5-1- Land Cover distribution of surveyed watersheds

5.2.2 i-Tree Hydro model description and data requirements

To estimate the effect of increasing tree canopy cover, decreasing impervious cover, and tree characteristics on urban stormwater runoff, i-Tree hydro has been used as an analytical model tool to simulate the influence of land-cover change on surface runoff in urban areas

(Bautista & Peña-Guzmán, 2019; Nyelele et al., 2019; Soares et al., 2011; X. Wang et al., 2018).

I-Tree Hydro is a semi-distributed, physically-based urban forest hydrological model which utilizes numerous inputs including land-cover, elevation, weather data, soil infiltration properties, and vegetation parameters (Table 5.2). The i-Tree Hydro software package includes pre-uploaded weather and USGS streamflow data for 2005-2012 which can be utilized in model calibration, validation and/or simulation runs.

Interception, evapotranspiration, infiltration, surface runoff generation and other hydrological processes are modeled as described by Wang et al. (2008a). Briefly, the Rutter interception model (Rutter et al., 1975) was used to simulate the interception process as described in Equation 5.1.

Equation 5.1

$$\frac{\Delta C}{\Delta t} = P - R - E$$

In which, C (m) = Depth of water on the unit canopy at time t , P (m/s) = above canopy precipitation, R (m/s) = below canopy throughfall reaching the ground, E (m/s) = Evaporation rate from the wet canopy, Δt = period of simulation.

Based on the work of Deardorff (1978) and Noilhan and Planton (1989) evaporation was modeled using Equation 5.2.

Equation 5.2

$$E = \left(\frac{C}{S}\right)^{2/3} E_p$$

In which S (m) = Storage capacity, and E_p (m/s) = Potential evaporation.

Infiltration rate (i , m/s) was modeled using Green and Ampt (1911) model (Equation 5.3).

Equation 5.3

$$i = \frac{dI}{dt} = \frac{\Delta\Psi + Z}{\int_{z=0}^{z=z} \frac{dz}{Kz}}$$

Variables in Equation 5.3 are defined as: K_z (m/s) = Hydraulic conductivity Z (m) = Soil depth, and $\Delta\Psi$ (m) = Effective wetting front suction.

Evapotranspiration under a range of soil water conditions is represented in i-Tree Hydro via a combination of the Penman-Monteith (Monteith, 1965) potential evapotranspiration model and simulated resistance in the root zone based on the work of Beven et al. (2001) as presented in Equation 5.4.

Equation 5.4

$$ET_a = ET_p \left(1 - \frac{S_r}{S_{max}}\right)$$

Here, S_r (m) is the Root zone storage deficit, S_{max} (m) is the Maximum allowable storage deficit, and ET_p (m/s) is the Potential evapotranspiration.

Model calibration requires hourly climate and streamflow data. Weather and stream stage data collected at the outlet of each study watershed by Johnson County Stormwater, a county-level stormwater program in the study region, were used for model calibration and validation. Data from 2011 to 2013 were used to coincide with the time frame during which land cover data used as input to the model were collected. Both precipitation and streamflow data were recorded on a sub-hourly basis. To format sub-hourly precipitation to hourly, all data recorded 30 minutes before or after each hour were summed and assigned to the corresponding hour. Measured stream stage at the outlet of each study watershed were converted to stream discharge using the Manning Equation (Equation 5.5) with assumed Manning roughness coefficients n (0.02, 0.04, and 0.03) and channel slope S (0.005, 0.0025, and 0.01) consistent with the channel materials and estimated slopes for TU02, IN05, and TH03 respectively. The cross-sectional flow area (A

(m^2) and hydraulic radius ($R (m)$) for a given channel stage were determined from measurements of channel geometry. The channel outlets of IN05 and TU02 were shaped as two box culverts (3 m x 2.5m each) and a rectangular lined channel (5.5 m x 1.8 m), respectively. TH03 was a natural channel with an approximately parabolic geometry as determined from channel cross-sections measured in the field. Therefore, discharge associated with each channel stage of TH03 was estimated using parabolic channel geometric relationships presented by (Mwiya, 2013).

Equation 5.5

$$Q = \frac{1}{n} \cdot A \cdot R^{\frac{2}{3}} \cdot S^{\frac{1}{2}}$$

In which Q is in m^3/s .

Resulting subhourly streamflow data were aggregated to an hourly basis using a time-weighted approach to average data points recorded half an hour before and half an hour after each hourly point. For instance, the recorded data from 2:30 PM to 3:30 PM were assigned to 3:00 PM discharge. If the first recorded data after 2:30 PM occurred at 2:45 PM, then the coefficient discharge weight for the duration of 15 minutes was considered as 0.25 (15 minutes out of 60 minutes).

Table 5-2- Model inputs and related sources

	Model Input	Data source	Description
	Watershed area	Arc-hydro watershed delineation	
	Digital elevation model	National elevation dataset	30m x 30m grid
Model area characteristics	Meteorological data (used in calibration)	Johnson County Stormwatch network (www.stormwatch.com)	sub-hourly data, 2011 - 2013
	Observed streamflow data (used in calibration)		
	Simulation period		Selected to be consistent with desired calibration/validation dataset or scenario run
Land cover parameters	% tree, evergreen tree, shrub, herbaceous,	(Council, 2012)	3 m x 3 m land cover grid

	water, bare soil and impervious cover		
	Leaf area index	i-Tree Eco tree survey data (Nowak et al., 2013)	
	Shrub and herbaceous leaf area index	i-Tree default values	Verified with field values
	% impervious area (total and directly connected)	(Bochis & Pitt, 2009)	Verified with field values
	Pervious/impervious cover beneath tree canopy	(Council, 2012)	Verified with field values
Hydrologic parameters	Soil characteristics: texture, infiltration parameters (wetting front suction, wetted moisture content, surface hydraulic conductivity), initial moisture content	STATSGO soil database ¹ , field infiltration tests (Christianson, unpublished data)	additional adjustment of infiltration parameters through calibration
	Root zone depth	i-Tree default values	
	Leaf phenology and storage: leaf on, off and transition periods	(Carter et al., 2017)	
	Calibration parameters	Model default values used as initial starting point	final values determined through auto-calibration with comparison to available literature values

¹ Soil Survey Staff, Natural Resources Conservation Service, United States Department of Agriculture. Web Soil Survey. Available online at <http://websoilsurvey.nrcs.usda.gov/>. Accessed 10/16/2017.

5.2.3 Model calibration and validation

To accurately simulate the behavior of the surveyed watersheds, each study watershed was calibrated. Initial parameter values were estimated according to characteristics of the watershed along with model default values to begin the calibration process. This initial parameter set was then manipulated with a trial and error method to improve the accuracy of the simulation. Subsequently, the auto-calibration routines built in to i-Tree were applied to the obtained parameter set to optimize model fit. Finally, if needed to keep the range of parameters consistent with the real characteristics of the watershed, another manual adjustment was performed. The

Nash-Sutcliffe efficiency (NSE) coefficient criteria was utilized to judge the fit of the model (Nash & Sutcliffe, 1970). Equation 5.6 presents the definition of NSE.

Equation 5.6

$$NSE = 1 - \frac{\sum_t^T (Q_m^t - Q_o^t)^2}{\sum_t^T (Q_o^t - \overline{Q_o})^2}$$

Here, Q_o is the mean of observed discharges, Q_M is modeled discharge and Q_o^t is observed discharge at time t .

Considering the time frame in which land cover data were generated as well as time periods in which frozen stream conditions likely produced errors in water height measurement, hourly meteorological and stream flow data from May to October 2013 were selected for model calibration for all studied watersheds. Likewise, meteorological and streamflow data from May to October 2011 were chosen for model validation. However, there was an exception for IN05 watershed in which a period of May to September 28th, 2011 was selected for model validation due to availability of the data. Similar to the calibration period, NSE was selected to characterize model fit during the validation period.

5.2.4 Model Scenarios

Following model calibration and validation, model scenarios were designed to address the general questions posed in the introduction. These questions are re-stated here, along with the scenarios designed to address them. These scenarios themselves are then described in the following sections.

- (1) To what extent do different patterns of urbanization influence watershed hydrological response to increases in tree canopy cover and precipitation magnitude? – *Tree canopy cover scenarios*

- (2) What is the effect of tree phenology on runoff response for storm events relevant to urban stormwater management? – *Tree seasonal and evergreenness scenarios*
- (3) What is the influence of tree phenological patterns on runoff response for different patterns of urbanization on an annual basis? – *Tree seasonal and evergreenness scenarios*

5.2.4.1 Tree canopy cover scenarios:

To evaluate the tree canopy cover impact on generated runoff volume, two scenarios were considered. The first scenario (S1) reflected an increase in tree canopy cover while the impervious surface beneath the canopy remained constant. This scenario was intended to represent cases in which canopy expands without a corresponding decrease in impervious surfaces (e.g., as existing trees mature or by planting trees in existing pervious areas) and, as such, isolates the effects of canopy interception processes on downstream runoff volume. However, increasing urban tree canopy cover likely requires planting more trees, and we suspect that such trees have the greatest influence on watershed hydrology when planted in existing impervious surfaces. Therefore, the second scenario (S2) was considered to convert 20% of the surface beneath the added tree canopy cover to permeable surface consistent with the typical area recommended for urban tree plantings. Figure 5.2 provides an example to illustrate the differences between S1 and S2 in the IN05 watershed.

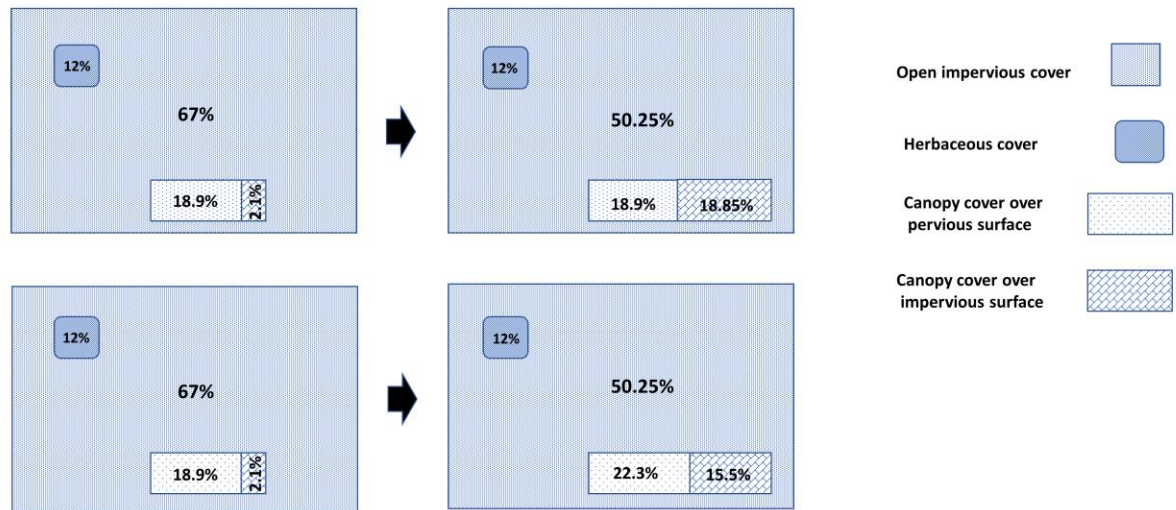


Figure 5-2 Example of IN05 watershed with 25% tree canopy cover increase for an application of scenario 1 (Top panel) and scenario 2 (bottom panel)

As shown in Table 5 1, the existing land cover of this watershed is 67% impervious cover, 12% herbaceous cover, and 21% tree canopy cover. Under S1, increasing canopy cover over impervious surfaces to reduce the amount of open impervious area by 25% (from 69% to 50.3%) increased the amount of canopy overhanging impervious surfaces from 2.1% to 18.9%, but the total amount of impervious surface cover remained constant at approximately 69%. Under S2, increasing the same increase in canopy cover also reduced open impervious area from 69% to 50.3%; however, since a portion of the impervious area below tree canopy was converted to pervious planting area, there was an attendant reduction in total impervious area from 69% to 66%. For each of the S1 and S2 scenarios, four different canopy cover scenarios (25, 50, 75, and 100%) were applied to each of the 3 study watersheds. These scenarios represent the % increase in canopy cover over open impervious surfaces relative to the baseline condition in each

watershed. Additionally, to analyze the difference between the impacts of range of storm event magnitudes with relevance to stormwater management, the so-called water quality event for the region (25mm) and a 10 year, 24hour (140mm) design storm as representatives of a small and large storm respectively, were applied to the model for each individual scenario. The water quality event, which is defined as the storm event that produces less than or equal to 90 percent volume of all 24-hour storms on an annual basis, was determined based on previous analyses of precipitation probability distributions for the region (Council, 2012).

5.2.4.2 Tree seasonal and evergreenness scenarios

As season changes, trees respond differently to the reduction of runoff due to the change in canopy density. Therefore, we hypothesized that tree seasonal factors and species differences, in particular LAI and tree type (evergreen vs deciduous), can impact the total runoff volume at a watershed scale. A water quality design storm event (25mm) as a frequent design storm event was applied to each study watershed to assess the effect of LAI on runoff reduction with respect to different levels of urbanization. In this regard, a sparse canopy was designated with a LAI value of 1, and a highly dense canopy with a LAI of 18 were applied to compare the existing condition (base line) to each level of canopy density for each study watershed.

Also, a pre-loaded continuous weather and streamflow data from 2008 to 2012 were introduced to i-Tree Hydro for each level of urbanized watershed to compare the effect of tree evergreenness on the runoff attenuation. A total volume of each month was extracted for each year and an average over the simulation period for each month was calculated. The current condition of each watershed was set as the baseline and two scenarios with 0% and 100% evergreen tree cover were applied to each watershed, as to be comparable to the baseline. Pre-loaded weather datasets were used from the following stations: BLUE R NR STANLEY, KS

06893080, JOHNSON CO. INDUSTR 724475-93909, and JOHNSON CO EXECUTIVE 724468-03967 were utilized for TU02, IN05, and TH03 watersheds, respectively, based on their relative proximity. Weather data were obtained from National Oceanic and Atmospheric Administration’s (NOAA), and National Climatic Center (NCDC).

5.3 Results

5.3.1 Model calibration and validation

For each study watershed, a combination of i-Tree default values, manual and automatic calibration while considering the characteristics of the study area, resulted in calibrated hydrological parameters presented in Table 5.3.

Table 5-3- hydrologic parameters values attained through calibration process for current watershed conditions

		TU02	TH03	IN05
Model parameters	Annual Average Flow of Project Area (cms)	0.049	0.897	0.045
	<hr/>			
Soil characteristics	Wetting Front Suction (m):	0.06	0.07	0.07
	Wetted Moisture Content (m):	0.45	0.24	0.3
	Surface Hydraulic Conductivity (cm/h):	3.9	2	4
	Depth of Root Zone (m):	0.1	0.08	0.12
	Initial Soil Saturation Condition (%):	10	27.85	9.26
<hr/>				
Vegetation & land cover parameters	Canopy cover (%)	45	14	21
	Evergreen trees (%)	10	4	4
	Leaf Transition Period (days):	28	28	28
	Leaf On Day (Day of year 1-365):	97	97	97
	Leaf Off Day (Day of year 1-365):	297	297	297
	Leaf Area Index:	4.7	4.7	4.7
	Shrub Bark Area Index	0.5	0.5	0.5
	Leaf Storage (mm):	1	1	1
	Pervious Depression Storage (mm):	2.5	2.3	2.5
	Impervious Depression Storage (mm):	1	1	1
	% directly connected impervious area	40	40	40
	% Impervious surface under canopy cover	4.5	1.4	2.1
	% Pervious surface under canopy cover	40.5	12.6	18.9
Scale Parameter of Power Function:	2	2	2	

Surface and subsurface routing parameters	Scale Parameter of Soil Transmissivity:	0.8	1.2	0.9
	Transmissivity at Saturation (m ² /h):	3.32	6.5	3.26
	Unsaturated Zone Time Delay (h):	111	94	129.82
	Soil Macropore Percentage (%):	0.0000003	0.0000002	0.0001
	Sub Surface Flow Routing: B (h):	0.85	0.98	0.65
	Time Constant for Surface Flow: Alpha (h):	239	0.1	123.78
	Time Constant for Surface Flow: Beta (h):	0.4	0.4	0.48
	Watershed Area Where Rainfall Rate can Exceed Infiltration Rate (%):	41	65	67

Nash-Sutcliffe Efficiency (NSE) ratios were used to evaluate the performance of the model. Table 5.4 presents the NSE achieved for the study watersheds.

Table 5-4- Nash-Sutcliffe Efficiency (NSE) ratios attained for study watersheds through model calibration process

	TU02	TH03	IN05
Calibration period	2013-May to October	2013-May to October	2013- May to October
Validation period	2011-May to October	2011-May to October	2011- May to 28 th September
NSE (Calibration)	0.46	0.49	0.72
NSE (validation)	0.41	0.76	0.43

Figures 5-3, and 5-4 illustrate the model predicted water flow (Total flow) in m³/h, the discharge (m³/h), and the rainfall (mm/h) over the evaluated period for the study watersheds for calibration and validation processes respectively.

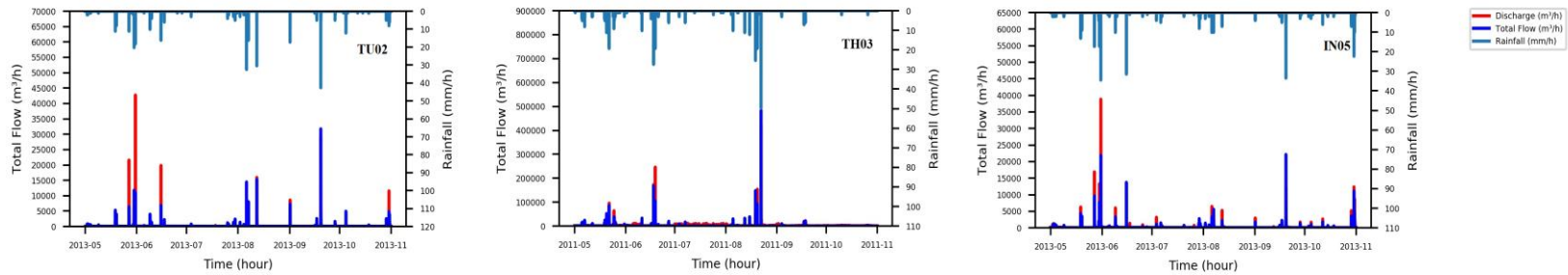


Figure 5-3 Total predicted water flow (m³/h) and discharge (m³/h) for the study watersheds over the calibration time period

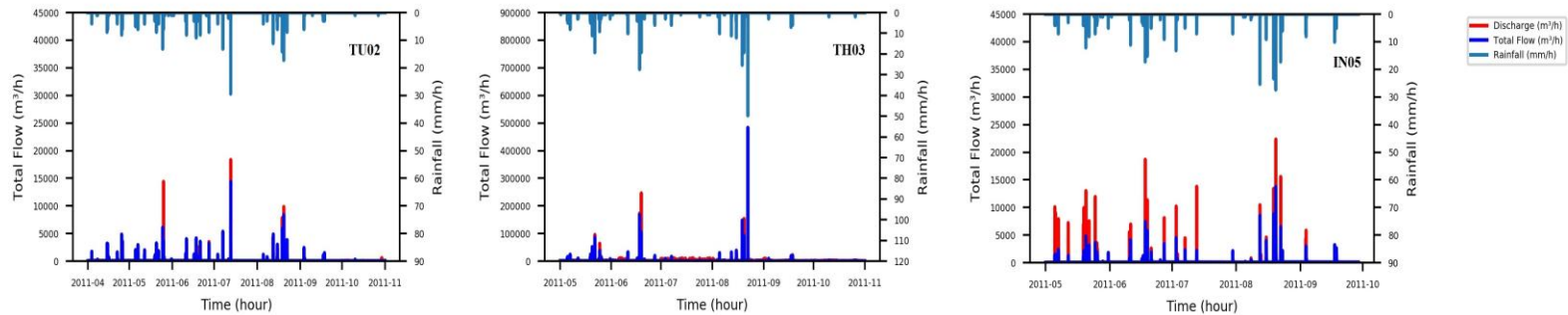


Figure 5-4 Total predicted water flow (m³/h) and discharge (m³/h) for the study watersheds over the validation time period

5.3.2 Tree canopy cover Scenarios

5.3.2.1 Design storm event -Water quality (25mm)

As mentioned in the methods section, scenario1 (S1) was defined as merely an increase in canopy cover and scenario 2 (S2) was defined as increase in canopy cover and decrease in impervious surface. Results of applying a water quality design storm event as a small, frequent event for a range in % increase of canopy cover over open impervious surfaces (25, 50, 75, and 100%) were obtained as follows:

IN05, which represented the most urbanized area, had the highest reduction in total runoff volume with a range of variation from 10 to 38.3% for various rates in increasing tree canopy cover for S2. Likewise, TH03 and TU02 (which represented commercial/residential and residential areas, respectively) behaved very similarly, with runoff reductions ranging from 8.4 to 32.7%. Similar to S2, results for the S1 canopy scenarios followed the same pattern in total runoff volume reduction as IN05 showed the highest reduction, while TH03 and TU02 indicated almost equal variation. However, compared to Scenario 2, total volume reduction was less, and ranged from 7.6 to 28.4% for IN05 watershed in the S1 canopy scenarios. Similarly, the volume reduction varied from almost 6.1 to 24% for TU02 and TH03 watersheds. Figure 5.3 shows the reduction in total stormwater runoff for a water quality design storm event. Various increasing tree canopy cover for both Scenarios 1 and 2 in all levels of urbanization are presented.

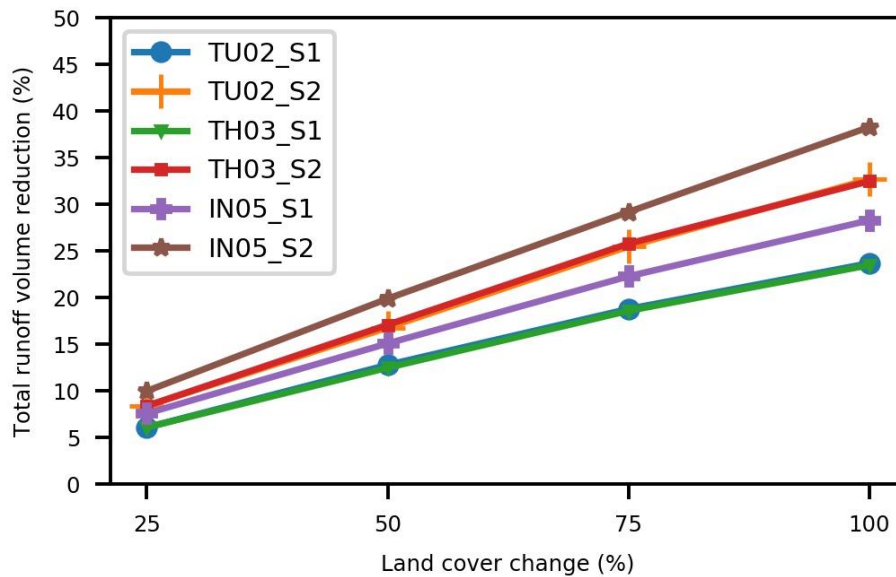


Figure 5-5 Total volume reduction; comparison of watersheds in all levels of urbanization for a water quality (25mm) storm water design event in an application of both Scenario; Note, TU02-S1 underlies TH03_S1, and TU02_S2 underlies TH03_S2

Table 5.5 provides an example of the 100% tree canopy cover over impervious area scenario to illustrate changes in the relative cover of total impervious area, total tree canopy cover, and the fraction of impervious surface cover underlying tree canopy for each of the study watersheds. In this scenario, tree canopy overhanging impervious surfaces was increased such that 100% of the existing impervious surfaces were under tree canopy. As noted previously, in the S1 scenario, the total impervious surface cover (which includes impervious surfaces beneath and outside of the tree canopy cover) remains constant in each of the study watersheds, while in S2, total impervious cover decreased by 8.2%, 9% and 13.4% in TU02, TH03 and IN05, respectively to simulate converting a portion of the existing impervious surface to pervious tree planting areas. While the 100% scenario is extreme and not very realistic, modeling it provides insight to the capacity for urban tree canopy to regulate runoff volume. Under this most extreme scenario, the effect of increasing tree canopy over impervious surfaces was substantial as runoff

reductions of 23.5% to 28.4% were predicted across all study watersheds. Increasing the tree canopy cover from 45% to 86% to completely cover all impervious surfaces along with a 13.4% decrease in imperviousness resulted in 38.3% reduction in total runoff volume for IN05 as the most urbanized watershed. TU02 and TH03 experienced similar absolute changes in total canopy cover (a 41% change in TU02 and a 45% change in TH03) as well as in total impervious surface cover, which resulted in similar total volume reductions for both watersheds.

Table 5-5- Watershed comparison for an example of 100% tree canopy over impervious surface cover for a water quality design storm event in the application of Scenarios 1&2

	TU02		TH03		IN05	
	S1	S2	S1	S2	S1	S2
Total impervious cover, existing condition (%)	45.5	45.5	46.4	46.4	69.1	69.1
Total open impervious cover, existing condition (%)	41	41	45	45	67	67
Total canopy cover, existing condition (%)	45	45	14	14	21	21
Total canopy cover, 100% impervious surface under tree canopy	86	86	59	59	88	88
Total impervious cover, 100% impervious surface under tree canopy	45.5	37.3	46.4	37.4	69.1	55.7
Change in impervious cover compared to existing watershed conditions (%)	0	-8.2	0	-9	0	-13.4
Runoff reduction (%)	23.7	32.7	23.5	32.5	28.4	38.3

5.3.2.2 Design storm event - 10 year/24hour (140mm)

As with the water quality design storm event, a 10 yr, 24hr design storm event was applied for the same scenarios (S1 & S2) and levels of tree canopy cover increase over impervious surfaces (25%, 50%, 75% and 100%). Figure 5.4 demonstrates the reduction in total

runoff volume for a comparison of watersheds in various levels of urbanization for a 10yr, 24hr storm. As can be seen from Figure 5.4, while in the application of scenario1 all watersheds followed a similar pattern, the total volume reduction was negligible. However, decreasing the imperviousness along with increasing tree canopy cover (as represented in S2), caused a total volume reduction ranging from 5 to 20% for IN05 watershed. Although TU02 showed a pretty similar pattern to IN05, the total volume reduction was slightly less in this watershed. Also, TH03 showed a much less total volume reduction compared to the other two watersheds. The volume reduction variation for this watershed ranged from 3 to 10.5% corresponding to various tree canopy cover increasing rate.

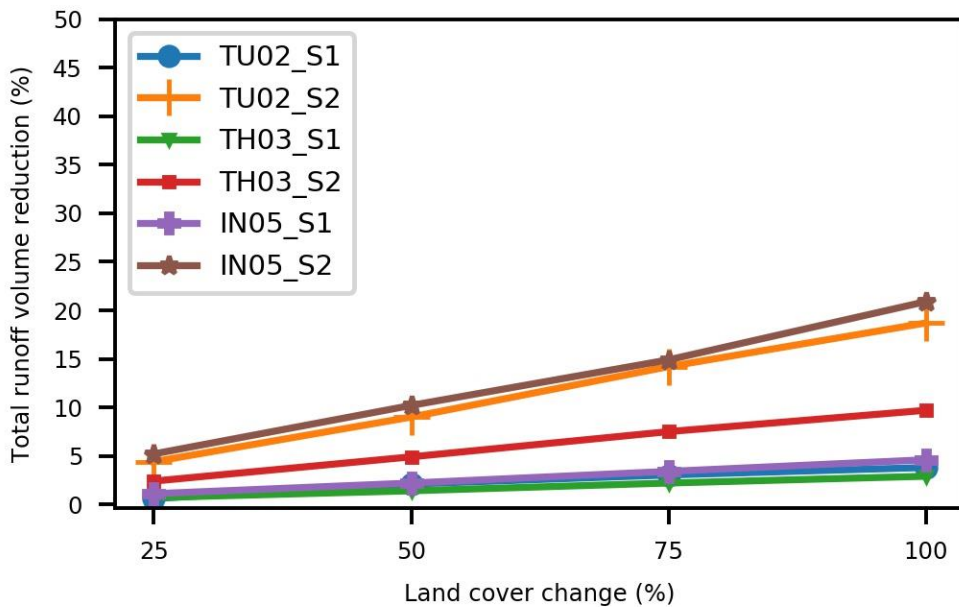


Figure 5-6- Total volume reduction; comparison of watersheds in all levels of urbanization for a 10 year 24 hour (140mm) storm water design event in the application of both Scenario

Similar to Table 5.5, Table 5.6 reviews an example of the 100% tree canopy cover over impervious cover scenario as implemented in each of the study watersheds for a 10yr, 24hr design storm event for both S1 and S2. As for the water quality storm, greater runoff reductions

were achieved under the S2 scenario set, as would be expected given the reduction in impervious surface cover. However, the absolute difference between runoff reductions predicted for the S1 and S2 scenarios tended to be larger under the 10yr, 24hr event (approximately 15% in the case of TU02 and IN05) relative to the smaller water quality event.

Table 5-6 Watershed comparison for an example of 100% tree canopy cover structures for a 10yr/24hr design storm event in the application of Scenario 1&2

	TU02		TH03		IN05	
	S1	S2	S1	S2	S1	S2
Total impervious cover existing condition (%)	45.5	45.5	46.4	46.4	69.1	69.1
Total open impervious cover existing condition (%)	41	41	45	45	67	67
Total canopy cover existing condition (%)	45	45	14	14	21	21
Total canopy cover, 100% canopy cover increase	86	86	59	59	88	88
Total impervious cover, 100% canopy cover increase	45.5	37.3	46.4	37.4	69.1	55.7
Change in impervious cover compared to existing watershed conditions (%)	0	-8.2	0	-9	0	-13.4
Runoff reduction (%)	3.8	18.7	2.9	9.7	4.6	20.9

5.3.3 LAI Scenario

In TU02 as a residential watershed, with 45% tree canopy cover, changing LAI from 4.7 (existing conditions) to 18 caused almost a 10.1% reduction in stormwater runoff volume. However, the effect of applying this wide range of LAI variation on other watersheds was not as extreme. Table 5.7 compares the influence of LAI, for values of 1 and 18, to the existing condition of each study watershed.

Table 5-7 The effect of wide-range variation of LAI in stormwater runoff reduction for various levels of urbanization

	TU02	TH03	IN05
Tree cover (%)	45	14	21
Baseline (Existing condition) LAI	4.7	4.7	4.7
Runoff reduction% (LAI = 1)	-2.7	-1.9	-0.91
Runoff reduction% (LAI = 18)	10.1	6.5	3.4

5.3.4 Tree Evergreenness Scenarios

The existing condition of each watershed was defined as a baseline scenario to be compared to scenarios in which (1) the entire tree canopy was comprised of evergreen trees (evergreen scenarios) and (2) deciduous trees comprised all trees in the watershed (deciduous scenario). Figures 5.5 to 5.7 show the monthly total volume runoff reduction in percentage for TU02, TH03, and IN05 watersheds relative to mean total monthly precipitation over the period of 2008 to 2012 for each watershed. Across all study watersheds, the influence of evergreen trees in enhancing stormwater volume reductions was evident across the months of March, April, and May a period in which precipitation exceeds the monthly average and when deciduous trees have low LAI values. For the predominantly residential watershed with relatively high existing canopy cover (45% in TU02), the corresponding runoff volume reduction from March to May ranged from 11 to 14%. By comparison, the total runoff volume reduction was almost half of this in the TH03 and IN05 watersheds. For the residential/commercial watershed (TH03), November, December, and March produced the highest runoff reduction with a range of variation from 5.5 to 8%. Similarly, in the industrial/commercial watershed (IN05), April, March, and December indicated the most reduction in total runoff volume with a range of variation from 6.5 to 7.5%.

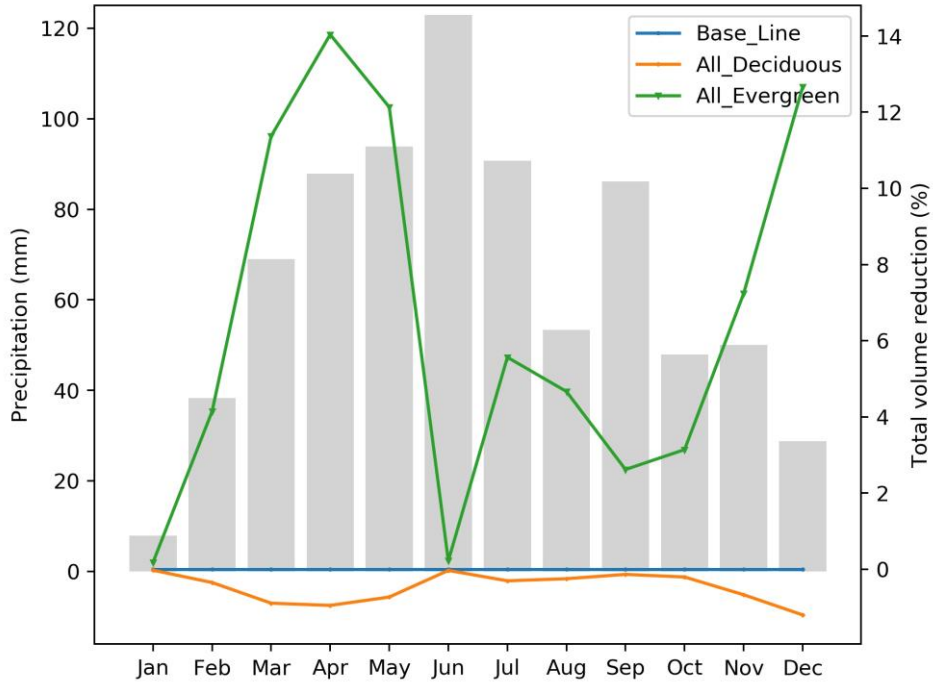


Figure 5-7 Monthly total volume runoff reduction in percentage for residential (TU02) watershed

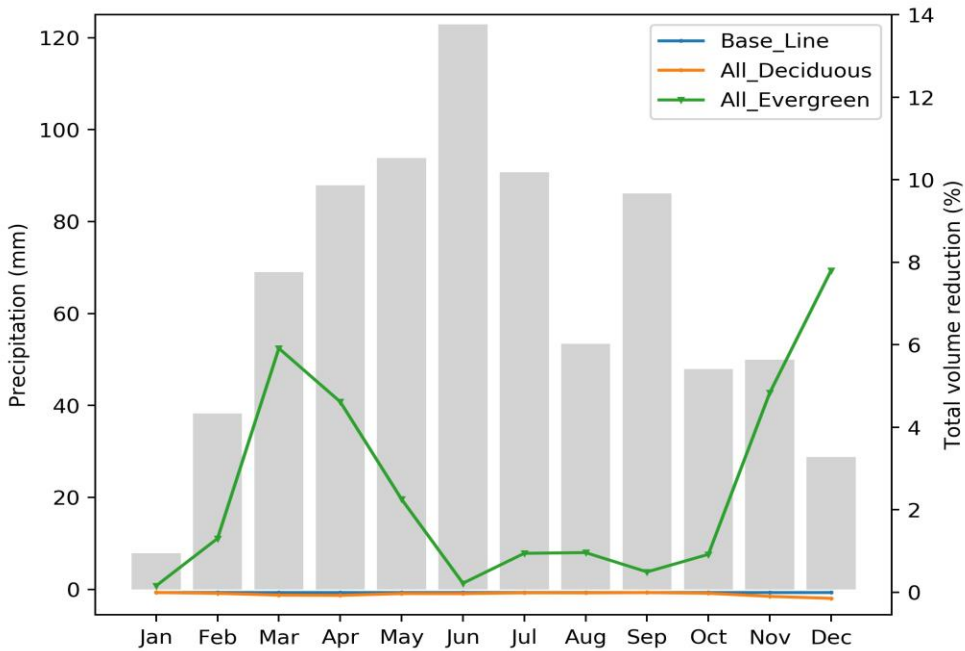


Figure 5-8 Monthly total volume runoff reduction in percentage for residential/commercial (TH03) watershed

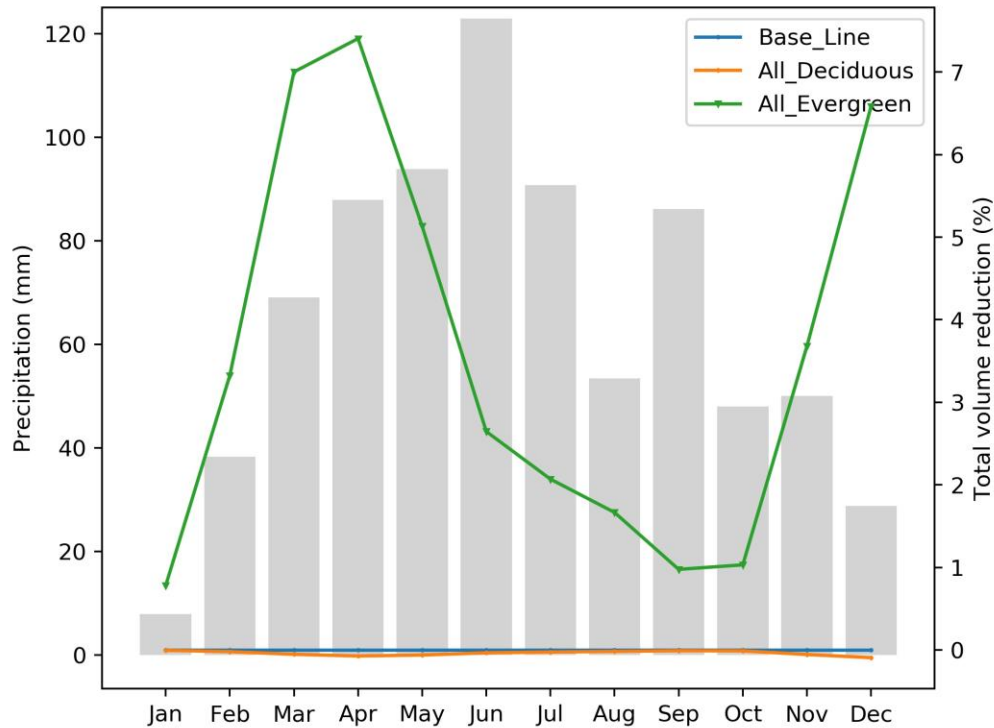


Figure 5-9 Monthly total volume runoff reduction in percentage for industrial/commercial (IN05) watershed

On a yearly basis, the effect of replacing all tree species by evergreen trees as compared to existing condition of each watershed is presented in Table 5.8. Relative to monthly reductions, total annual runoff reductions were not as pronounced.

Table 5-8 Yearly average of total runoff reduction; a comparison of all watershed area covered by evergreen trees with existing condition for the study watersheds

	Tree cover %	Evergreen tree %, existing condition	Predominant watershed landcover (% impervious)	Yearly average of total runoff reduction %
TU02	45	10	Residential (41)	6.7
TH03	14	4	Commercial/Residential (45)	2.3
IN05	21	4	Industrial/Commercial (67)	3.7

5.4. Discussion

As expected, for a small, frequent event (i.e., the 25-mm water quality event), the most urbanized watershed with the highest impervious cover experienced the greatest reduction in the

total runoff volume after in response to tree canopy cover scenarios implemented under S1 (i.e., no change in impervious cover) and S2 (i.e., reduction in impervious cover consistent with new tree planting areas). This analysis indicated that adding canopy cover equals to 25% of open impervious cover (S1) can result in almost 5 to 7% reduction in total runoff volume. In addition, a 20% reduction in the impervious area beneath the added tree canopy (S2) can cause the reduction of runoff up to 10% for a small storm event.

For a large storm event, results indicated a similar pattern to a small storm event. Reduction in runoff volume had the highest sensitivity to increase in tree canopy cover as well as decrease in impervious surface in a predominantly industrial (IN05) watershed. Contrary to the industrial watershed, a residential/commercial watershed (TH03) was less sensitive compared to other two watersheds. Also, for all the studied watersheds, reduction in impervious cover can be more beneficial, as this could reduce the runoff almost four times greater than a mere increase in tree canopy cover. In general, while adding tree canopy cover and impervious cover reduction could both be influential, the extent of effectiveness depends on varying factors including the type of storm and urbanization level of an urban watershed. Roughly though, if the reduction of runoff is pursued and both options of increase in canopy cover and reduction in impervious cover existed, reduction in impervious cover might be more beneficial.

Although, increasing LAI in watersheds with more canopy cover is expected to show more runoff reduction and this was true for TU02, comparing TH03 and IN05 watershed disputes this prospect. While IN05 with 21% tree canopy cover exhibited a 3.4% runoff reduction compared to its existing condition, TH03 with only 14% tree canopy cover illustrates 6.5% of reduction in runoff. This could raise the question of how important, is the characteristics of a watershed and its development as compared to tree characteristics. Therefore, evaluating the

change in runoff on a scale of a watershed might be more affected by existing conditions of the watershed, such as open impervious cover, and tree canopy cover rather than tree characteristics.

The analysis of tree evergreenness and seasonal changes in LAI highlights the importance of considering tree type in management decisions. Based on the results of this study, yearly average runoff reduction by replacing evergreen trees compared to existing condition of each watershed varied between 2 to 7%. However, in months during which deciduous trees were not fully-leafed, this reduction was as high as 14% in a residential watershed with 45% tree canopy cover. Results imply that in areas with the majority of rainfall happening during the leaf off period, planting and/or conserving evergreen trees will be more effective toward urban stormwater management than planting new deciduous trees. If a linear relationship is assumed, it can be deduced from the results that each 10% replacement of deciduous trees with evergreen trees can result in 0.74, 0.24, and 0.38% runoff reduction for TU02, TH03, and IN05 respectively. However, tree canopy cover for aforementioned watersheds are 45, 14, and 21%. Therefore, a normalization through all watersheds indicates that regardless of the watershed application type, if 10% of the existing deciduous tree canopy cover was replaced with evergreen species for urban watersheds in this region, for each 10% replacement, on average 0.17% reduction in runoff volume occurs.

In this work, we tried to underscore the importance of different urban developments on the reduction of runoff when tree canopy cover and corresponding impervious cover are manipulated. To do so, three different urban watersheds representing different levels of urbanization were selected. Although, this study separated urban watersheds based on their functioning, the linked features such as tree canopy, open imperviousness, and sizes are specific. Therefore, while other urban watersheds might in different areas, might be assigned with the

same levels, their conditions and characteristics may differ. Also, this study was performed on three urban watersheds in Kansas City metro area with a humid continental climate.

Consequently, the results might be more advantageous for similar climate and not applicable to different climatic conditions.

Although, i-Tree hydro is a semi-distributed physically-based model in which seasonal variation in LAI is considered, other tree characteristics, such as canopy health, branch angle, or meteorological factors such as wind speed and its direction are not considered in the model. Additionally, even though it considers the directly connected impervious area, the pattern of this connection is overlooked. Similarly, the pattern and the design of the canopy cover in urban watersheds are missing in the i-Tree hydro model. Therefore, a more precise analysis of the effect of trees and imperviousness in urban settings requires considering all above-mentioned factors.

5.5 Conclusion

Overall, while this study evaluated the influence of canopy cover variation and species selection on the reduction of stormwater runoff volume, various urban developments were compared to elucidate the effect of different levels of urbanization in this manner. A water quality design storm event (25mm) and a 10yr, 24hr design storm event (140mm) were selected as representatives of a small and a large rainfall event, respectively. A calibrated/validated i-Tree hydro model was established for three urban watersheds with residential, commercial/residential, and commercial/industrial developments in the Kansas City Metro area. Outcomes of this study unveiled the fact that, for a small rainfall event, the effectiveness of canopy cover and impervious surface change on runoff reduction can significantly be influenced by development classification of an urbanized area.

For a small storm event, canopy cover increasing equals to 25% of the open impervious cover resulted in almost 5 to 7 % reduction in runoff. Also, a 20% reduction in impervious canopy cover beneath the added canopy cover will improve the ability to reduce runoff to the range of 7 to 10%. While in the happening of a large storm event, an increasing canopy cover by 25% of the open impervious cover did not have significant influence on the reduction of runoff, reducing the impervious cover beneath the added canopy cover was able to reduce the runoff volume by up to 6%.

Although, wide range of variation in LAI did not show a significant change in runoff volume reduction, the effect of watershed characteristics and development classification on runoff reduction for varying LAI and other tree characteristics are needed to be further investigated.

A comparison analysis for the assessment of tree type influence (evergreen vs deciduous) on stormwater runoff volume reduction determined the significance of this factor during leaf-off seasons. As an example, in a residential development with 45% tree canopy cover, using trees with all evergreen kind can reduce the amount of runoff by 14% as compared to all trees consisting of deciduous kind. This fact implies that, selecting tree types in areas with more precipitation during leaf-off period should be taken into consideration. However, the extent to which the total runoff volume can be reduced varies due to various types of environments.

This study provides a perspective about the capacity of urban trees in runoff regulation. Due to minimum disturbance to the environment, trees are gaining more attention in stormwater management decisions. Therefore, the extent to which trees and their characteristics can affect the total runoff volume can give a better outlook to stormwater manager and policy makers in order to obtain the maximum proficiency of trees in choosing proper strategies. To achieve this

goal, our study showed that different development levels in urbanized areas should be well-thought-out along with changing in tree canopy cover, imperviousness surface, and tree characteristics. However, the influence of different types of environments on runoff reduction with respect to capacity of trees can be examined in future researches. Overall, results of this work can help environmental managers and policy makers to make a proper decision with respect to strict policies in urban zones. Therefore, it leads to a low impact on environment while gaining a favorable result to attenuate runoff volume in urban areas.

Chapter 6 - Conclusion

Green infrastructure can be utilized as a beneficial solution to address environmental issues linked to urban development. Green infrastructure simulates the behavior of the natural environment, while at the same time promoting cultural and benefits to people living in urban settings. As a component of green infrastructure networks, urban trees play an essential role in providing such benefits. This dissertation focused specifically on the capacity of urban trees to regulate urban water cycles from the tree to the watershed scale as a function of interception and transpiration processes. Although established that urban tree canopy does influence urban hydrology and stormwater runoff, systematic study and synthesis is still needed to better characterize variability in key processes (e.g., interception, transpiration), their relationship to key drivers (e.g., meteorological variables and tree characteristics), and resulting changes in urban runoff. The overall goal of this work was to advance understanding of the role of trees on stormwater runoff management in urban areas. In line with this goal, this dissertation advanced understanding by (1) quantitatively describing how rainfall partitioning and transpiration processes vary in urban environments as well as how meteorological and tree characteristics may influence these two processes through quantitative data syntheses and (2) examining the aggregate hydrologic effects of tree canopy cover, phenology and canopy density on stormwater runoff at the small ($< 10 \text{ km}^2$) urban watershed scale through application of a process-based model. The results of these study components are highlighted in the following sections, followed by a discussion of potential broader applications of this work.

6.1 Meta-analysis

At the tree-scale, meta-analyses of existing datasets were conducted to better characterize the magnitude of interception and transpiration processes as well as relationships between these

processes and key environmental variables and tree attributes. In this work, we investigated the throughfall changes in urban tree canopies with the change in the magnitude of rainfall. To do this, we collected the existing urban studies in the literature in which partitioning of the rainfall was measured for different events. We then classified the collected rainfall data into four main groups, including 0-5 mm, 5-25 mm, 25-50 mm, and above 50 mm. A total of 396 events from 8 different studies with a wide variety of climate were analyzed to develop a linear regression model between rainfall and corresponded throughfall for each rainfall grouping. The impact of bark characteristics and LAI on the magnitude of rainfall that reaches the ground as throughfall was also examined. Results indicated that the throughfall rate was significantly higher for deciduous-leafless trees than evergreen trees for rainfall groupings of 5-25, and 25-50 mm. Likewise, the throughfall rate for deciduous-leafless trees was significantly higher than deciduous-leafed trees in the rainfall group of 5-25 mm. Rough-barked trees had a significantly lower throughfall rate than smooth-barked trees for rainfall events during leafless periods. LAI exhibited an influential role in throughfall rates, and this effect was strongest for rainfall values above 25 mm. An analysis of sensitivity based on a multiple linear regression model revealed the stronger impact of rainfall value for rainfall groupings below 50 mm. In contrast, the LAI effect was stronger for rainfall depths above 50 mm.

We compared the results of this work as a review of open-grown trees to one of the most holistic, stand-scale studies that we know of, in which a similar linear regression model was performed to examine the throughfall rate in a rural hardwood forest of eastern United States (Helvey & Patric, 1965). Different rainfall classifications were not considered in their work, and throughfall regression model coefficients of 0.9 for both summer and winter periods were reported. Therefore, for the purpose of comparison, we averaged the rainfall coefficients over all

rainfall classifications, and results indicated rainfall coefficients of 0.59, 0.63, and 0.79 for evergreen, deciduous-leafed, and deciduous-leafless trees, respectively. The higher throughfall rate of rural forest (implying lower interception and/or stemflow rates) as compared to throughfall rates characterized for urban tree canopies in this work could relate to the difference in microclimate between rural and urban areas or differences in canopy density and architecture typical of open-grown trees in urban areas. However, more comprehensive research is needed to evaluate the potential reasons for this difference and the extent to which urban climate could affect the rainfall partitioning.

Among the limitations of a meta-regression approach is that resulting empirical equations are limited to the conditions represented in the datasets included in the analysis. To confront this limitation, a preliminary performance assessment of partitioning regression equations was conducted. An independent dataset from Smets et al., (2019) was utilized to verify the performance of the three developed models including linear regression, multi-linear regression, and non-linear LAI regression models. Smets et al., (2019) evaluated the efficiency of three mechanistic models (Rutter, Gash, and WetSpa), against a measured rainfall partitioning for two deciduous trees with rainfall values below 20 mm. The linear and multi-linear regression models had R^2 of 0.46, and 0.53, plus RMSE of 1.28 and 2.06, respectively. These results were comparable to the mechanistic models in the study with Rutter ($R^2 = 0.5$; RMSE = 1.05), Gash ($R^2 = 0.6$; RMSE = 0.89), and WetSpa ($R^2 = 0.59$; RMSE = 0.95). Although, the linear and multi-linear regression models did not outperform the mechanistic models, given the much less required inputs (one and two variables compared to more than 10 variables for mechanistic models), they showed satisfactory results on predicting the rainfall partitioning components.

Furthermore, the non-linear LAI regression model provided a better fit to observed interception rates relative to mechanistic models despite its relatively simple form and low input variable requirements.

Transpiration is another primary process through which trees move water from the soil profile to the atmosphere, and therefore, contribute to stormwater management in urban areas. As with to the rainfall partitioning studies, most of the transpiration studies conducted in urban areas have been performed on a tree scale. Nevertheless, studies have been done in a wide range of climate, which resulted in an extensive variability in climate variables. Besides, the way by which transpired water was reported was not consistent across the studies, and it was not evident if trees with various wood anatomies could make any difference in the value of reported transpired water. Therefore, we evaluated the change of sap flux for three various wood anatomy groupings (diffuse-porous, ring-porous, and conifer woods) in a meta-data analysis. The effect of environmental variables, including temperature, solar radiation, and VPD, as well as water-limiting conditions, were analyzed on the rate of sap flux for all the wood anatomy groupings. Results showed the highest median sap flux for the ring-porous group, which also had the least range of variation compared to diffuse-porous and conifers.

In contrast, the average sap flux of the diffuse-porous group showed the most considerable change after the water-limited period was removed, which might imply a higher sensitivity to water-limited conditions, compared to other wood groups. According to the multi-linear regression models and on an R^2 basis, temperature showed the strongest climatic variable controlling the sap flux rate across all the wood anatomy groupings. Even though VPD did not demonstrate a significant correlation to the sap flux rate in any of the wood anatomy groupings (Spearman's $\rho < 0.53$), it served as a threshold for the sap flux rate at specific VPD values for

conifer wood anatomy grouping. Similarly, beyond the VPD value of 2.5 *kPa*, the maximum sap flux rate was restricted to 150 *g/cm²/day* for the ring-porous wood grouping. Although, to the best of our knowledge, this work is by far the most holistic meta-data analysis in assessing the transpiration of urban trees, a larger number of data exist for trees in rural forests. A comparison between the current work and a natural forest study (Wullschleger et al., 1998b) with a wide-ranging climate and a large number of various species indicated no considerable difference in the range and the average transpired water between urban and rural environments.

6.2 Modeling

As mentioned, due to limitations in time, accessible equipment, and energy, if not impossible, it is not justifiable to apply a measured study on a large scale such as a city or a watershed. Therefore, models have been developed to add up the single effect of trees to larger scales. For stormwater management purposes, methods exist to estimate runoff in areas with various land uses. However, not all the models explicitly consider the effect of trees for studied land uses (e.g., rational method, curve number method, SWMM, HSPF). If they do (e.g., SWAT, RHESSys), a high number of data inputs are required as their complexity is categorized under advanced models (Coville et al., 2020). Briefly, rational method is a spatially lumped model that simulates peak runoff rates for the single outlet of a land parcel subjected to a single precipitation event. Curve number method is a spatially lumped model that simulates runoff depth for a land parcel subjected to a single precipitation event. The Storm Water Management Model (SWMM) is a semi-distributed model that simulates runoff quantity and quality for storm sewers and their contributing areas subjected to a single precipitation event or continuous weather. The Hydrological Simulation Program-FORTRAN (HSPF), and The Soil and Water Assessment Tool (SWAT) are spatially semi-distributed model that simulates runoff quantity and quality for

watersheds, sub-watersheds, and interior land segment units with homogeneous hydrologic response, when subjected to continuous weather. The Regional Hydro-Ecological Simulation System (RHESSys) is a spatially semi-distributed model that simulates runoff quantity and quality for small to mid-sized river basins, interior hillslopes, and smaller patches defined as hydrologic response units, when subjected to continuous weather. Among these models, i-Tree hydro explicitly considers the effect of trees on runoff reduction, while it is considered as a moderately complex model. The benefits of increasing canopy cover specifically over impervious surfaces within urban areas and the relative effect of land use in enhancing or dampening these benefits have not been widely explored, nor has the extent to which phenologic factors including LAI and evergreenness influence runoff. Therefore, a set of scenarios in which canopy cover over impervious surfaces was systematically increased, as well as variation on the relative composition of evergreen versus deciduous trees and their respective LAI, were applied to examine the runoff volume change in a residential, commercial/residential, and commercial/industrial watersheds in the Kansas City metro area. Results showed that for a small storm event (25 mm), adding canopy cover over 100% of impervious surfaces caused a 23.7, 23.5, and 28.4% reduction in runoff volume for residential, residential/commercial, and commercial/industrial watersheds, respectively. The same increase in canopy cover plus a 20% conversion of impervious cover to pervious cover beneath the corresponding added canopy cover resulted in 32.7, 32.5, and 38.3% for the same order of urban land use. Similarly, in the case of a large storm event (140 mm), adding canopy cover over 100% of impervious surfaces produced a 3.8, 2.9, and 4.6% reduction in runoff volume for residential, residential/commercial, and commercial/industrial watersheds, respectively. Moreover, only a 20% conversion of impervious

cover to pervious cover beneath the 100% added canopy cover ended up in 18.7, 9.7, and 20.9% reduction in the same order of urban land uses.

A wide range of variation in LAI did not have a substantial impact on the change in runoff volume. In contrast, the evergreenness factor showed an appreciable influence on runoff volume reduction. A replacement of trees for existing conditions (Table 5.8) with all evergreen trees indicated a yearly average runoff reduction of 6.7, 2.3, and 3.7% for residential, residential/commercial, and commercial/industrial watersheds, respectively.

6.3 Stormwater management implications

Overall, from a stormwater management standpoint, in this work, we tried to evaluate the role of trees as a constituent of green infrastructure on the reduction of runoff in urban areas. Although measured studies have mostly been done on the scale of a tree, the meta-data analysis of this work could help stormwater managers and policymakers to have a better understanding of trees behavior on a tree scale. Moreover, the outcomes could be generalized to larger scales such as a city or the watershed.

The fewer inputs in the developed equations in the meta-analysis part of this work may help to have a reasonable estimate of the trees' capacity to reduce runoff while input variables and calculations are minimal. On the other hand, the modeling part of the work could deliver an outlook of how an increasing change in the percentage of canopy cover, together with the influence of reduction in impervious cover, affect the runoff volume in the scale of an urban watershed.

References

- Alberti, M. (2008). Advances in urban ecology: Integrating humans and ecological processes in urban ecosystems. In *Advances in Urban Ecology: Integrating Humans and Ecological Processes in Urban Ecosystems*. <https://doi.org/10.1007/978-0-387-75510-6>
- Allen, R. G., Pereira, L. S., Raes, D., & Smith, M. (1998). Crop evapotranspiration: Guidelines for computing crop requirements. *Irrigation and Drainage Paper No. 56, FAO*, 56, 300. <https://doi.org/10.1016/j.eja.2010.12.001>
- Ankit Rohatgi. (2019). *WebPlotDigitizer*.
- Armson, D., Stringer, P., & Ennos, A. R. (2013). The effect of street trees and amenity grass on urban surface water runoff in Manchester, UK. *Urban Forestry & Urban Greening*, 12(3), 282–286.
- Asadian, Y., & Weiler, M. (2009). A New Approach in Measuring Rainfall Interception by Urban Trees in Coastal British Columbia. *Water Quality Research Journal of Canada*, 44(1), 16–24. <https://doi.org/10.2166/wqrj.2009.003>
- Asadian, Yeganeh, & Weiler, M. (2009). A new approach in measuring rainfall interception by urban trees in coastal British Columbia. *Water Quality Research Journal of Canada*, 44(1), 16–25. <https://doi.org/10.2166/wqrj.2009.003>
- Baptista, M. D., Livesley, S. J., Parmehr, E. G., Neave, M., & Amati, M. (2018). Variation in leaf area density drives the rainfall storage capacity of individual urban tree species. *Hydrological Processes*, 32(25), 3729–3740. <https://doi.org/10.1002/hyp.13255>
- Barbier, S., Balandier, P., & Gosselin, F. (2009). Influence of several tree traits on rainfall partitioning in temperate and boreal forests: a review Article published by EDP Sciences 602 Stéphane Barbier et al. *Ann. For. Sci*, 66, 602. <https://doi.org/10.1051/forest/2009041>
- Baró, F., Calderón-Argelich, A., Langemeyer, J., & Connolly, J. J. T. (2019). Under one canopy? Assessing the distributional environmental justice implications of street tree benefits in Barcelona. *Environmental Science and Policy*, 102, 54–64. <https://doi.org/10.1016/j.envsci.2019.08.016>
- Bautista, D., & Peña-Guzmán, C. (2019). Simulating the hydrological impact of green roof use and an increase in green areas in an urban catchment with i-tree: A case study with the town of Fontibón in Bogotá, Colombia. *Resources*, 8(2). <https://doi.org/10.3390/resources8020068>
- Beidokhti, A. N., & Moore, T. L. (2019). The role of tree phenology on urban stormwater management: A case study of two small watersheds in the Kansas City metropolitan area. *2019 ASABE Annual International Meeting*. <https://doi.org/10.13031/aim.201900860>

- Benedict, M. A. E. T., & McMahon, J. D. (2012). *Green Infrastructure: Smart Conservation for the 21st Century* "Infrastructure-the substructure or underlying foundation...on which the continuance and growth of a community or state depends." www.conservationfund.org.
- Berland, A., Shiflett, S. A., Shuster, W. D., Garmestani, A. S., Goddard, H. C., Herrmann, D. L., & Hopton, M. E. (2017). The role of trees in urban stormwater management. *Landscape and Urban Planning*, *162*, 167–177. <https://doi.org/10.1016/j.landurbplan.2017.02.017>
- Berland, Adam, & Hopton, M. E. (2014). Comparing street tree assemblages and associated stormwater benefits among communities in metropolitan Cincinnati, Ohio, USA. *Urban Forestry & Urban Greening*, *13*(4), 734–741. <https://doi.org/10.1016/j.ufug.2014.06.004>
- Berland, Adam, Shiflett, S. A., Shuster, W. D., Garmestani, A. S., Goddard, H. C., Herrmann, D. L., & Hopton, M. E. (2017). The role of trees in urban stormwater management. In *Landscape and Urban Planning* (Vol. 162, pp. 167–177). Elsevier B.V. <https://doi.org/10.1016/j.landurbplan.2017.02.017>
- Beven, K., & Freer, J. (2001). Equifinality, data assimilation, and uncertainty estimation in mechanistic modelling of complex environmental systems using the GLUE methodology. *Journal of Hydrology*, *249*(1–4), 11–29. [https://doi.org/10.1016/S0022-1694\(01\)00421-8](https://doi.org/10.1016/S0022-1694(01)00421-8)
- Bezak, N., Zabret, K., & Šraj, M. (2018). Application of Copula Functions for Rainfall Interception Modelling. *Water*, *10*(8), 995. <https://doi.org/10.3390/w10080995>
- Bigelow, D. S., Slusser, J. R., Beaubien, A. F., & Gibson, J. H. (1998). American Meteorological Society The USDA Ultraviolet Radiation Monitoring Program. *Source: Bulletin of the American Meteorological Society*, *79*(4), 601–615. <https://doi.org/10.2307/26215058>
- Bijoor, N. S., McCarthy, H. R., Zhang, D., & Pataki, D. E. (2012). Water sources of urban trees in the Los Angeles metropolitan area. *Urban Ecosystems*, *15*(1), 195–214. <https://doi.org/10.1007/s11252-011-0196-1>
- Bochis, C., & Pitt, R. E. (2009). Land use and runoff uncertainty. *Proceedings of World Environmental and Water Resources Congress 2009 - World Environmental and Water Resources Congress 2009: Great Rivers*, *342*, 1314–1324. [https://doi.org/10.1061/41036\(342\)130](https://doi.org/10.1061/41036(342)130)
- Bolund, P., & Hunhammar, S. (1999). Ecosystem services in urban areas. In *Ecological Economics* (Vol. 29). <https://www.sciencedirect.com/science/article/pii/S0921800999000130>
- Booth, R. K. (2002). Testate amoebae as paleoindicators of surface-moisture changes on Michigan peatlands: Modern ecology and hydrological calibration. *Journal of Paleolimnology*, *28*(3), 329–348. <https://doi.org/10.1023/A:1021675225099>
- Bruijnzeel, L. A. (2004). Hydrological functions of tropical forests: Not seeing the soil for the trees? *Agriculture, Ecosystems and Environment*, *104*(1), 185–228. <https://doi.org/10.1016/j.agee.2004.01.015>

- Burns, R. M., & Honkala, B. H. (1990a). *Silvics of North America: Volume 2. Hardwoods. Agriculture Handbook 654*, 2, 877.
- Burns, R. M., & Honkala, B. H. (1990b). *Silvics of North America. Agriculture Handbook 654*, 2, 877.
- Bush, S. E., Pataki, D. E., Hultine, K. R., West, A. G., Sperry, J. S., & Ehleringer, J. R. (2008). Wood anatomy constrains stomatal responses to atmospheric vapor pressure deficit in irrigated, urban trees. *Oecologia*, 156(1), 13–20. <https://doi.org/10.1007/s00442-008-0966-5>
- Cappiella, K., Claggett, S., Cline, K., Day, S., Galvin, M., Macdonagh, P., Sanders, J., Whitlow, T., & Xiao, Q. (2016). *Recommendations of the Expert Panel to Define BMP Effectiveness for Urban Tree Canopy Expansion*. <http://www.saveitlancaster.com/resources/all-about-trees/street-trees/>
- Carlyle-Moses, D. E., Livesley, S., Baptista, M. D., Thom, J., & Szota, C. (2020). *Urban Trees as Green Infrastructure for Stormwater Mitigation and Use* (pp. 397–432). Springer, Cham. https://doi.org/10.1007/978-3-030-26086-6_17
- Carlyle-Moses, D., & Gash, J. (2011). Rainfall Interception Loss by Forest Canopies. In *Forest Hydrology and Biogeochemistry: Synthesis of Past Research and Future Directions* (pp. 407–423). https://doi.org/10.1007/978-94-007-1363-5_20
- Carter, J. M., Orive, M. E., Gerhart, L. M., Stern, J. H., Marchin, R. M., Nagel, J., & Ward, J. K. (2017). Warmest extreme year in U.S. history alters thermal requirements for tree phenology. *Oecologia*, 183(4), 1197–1210. <https://doi.org/10.1007/s00442-017-3838-z>
- Chen, L., Zhang, Z., & Ewers, B. E. (2012). Urban Tree Species Show the Same Hydraulic Response to Vapor Pressure Deficit across Varying Tree Size and Environmental Conditions. *PLoS ONE*, 7(10). <https://doi.org/10.1371/journal.pone.0047882>
- Chen, L., Zhang, Z., Li, Z., Tang, J., Caldwell, P., & Zhang, W. (2011). Biophysical control of whole tree transpiration under an urban environment in Northern China. *Journal of Hydrology*, 402(3–4), 388–400. <https://doi.org/10.1016/j.jhydrol.2011.03.034>
- Clark, J., & Kjelgren, R. (1990). Water as a Limiting Factor in the Development of Urban Trees. *Journal of Arboriculture*, 16(8). https://digitalcommons.usu.edu/psc_facpub/661
- Council, M.-A. R. (2012). *Manual of Best Management Practices for Stormwater Quality*.
- Coville, R., Endreny, T., & Nowak, D. J. (2020). *Modeling the Impact of Urban Trees on Hydrology*. Modeling the Impact of Urban Trees on Hydrology. https://doi.org/10.1007/978-3-030-26086-6_19
- Craul, P. J. (1985). *A DESCRIPTION OF URBAN SOILS AND THEIR DESIRED CHARACTERISTICS 1*.
- Crockford, R. H., & Richardson, D. P. (2000). Partitioning of rainfall into throughfall, stemflow

- and interception: effect of forest type, ground cover and climate. *Hydrological Processes*, 14(16), 2903–2920. <https://doi.org/AID-HYP126>3.0.CO;2-6>
- Cronshey, R. G., Roberts, R. T., & Miller, N. (1985). *URBAN HYDROLOGY FOR SMALL WATERSHEDS (TR-55 REV.)*. 1268–1273.
- Deardorff, J. W. (1978). Efficient prediction of ground surface temperature and moisture, with inclusion of a layer of vegetation. *Journal of Geophysical Research*, 83(C4), 1889. <https://doi.org/10.1029/jc083ic04p01889>
- Depietri, Y., Renaud, F. G., & Kallis, G. (2012). Heat waves and floods in urban areas: A policy-oriented review of ecosystem services. In *Sustainability Science* (Vol. 7, Issue 1, pp. 95–107). Springer. <https://doi.org/10.1007/s11625-011-0142-4>
- Deutscher, J., Kupec, P., Kučera, A., Urban, J., Ledesma, J. L. J., & Futter, M. (2019). Ecohydrological consequences of tree removal in an urban park evaluated using open data, free software and a minimalist measuring campaign. *Science of the Total Environment*, 655, 1495–1504. <https://doi.org/10.1016/j.scitotenv.2018.11.277>
- Dietz, J., Hölscher, D., Leuschner, C., & Hendrayanto. (2006). Rainfall partitioning in relation to forest structure in differently managed montane forest stands in Central Sulawesi, Indonesia. *Forest Ecology and Management*, 237(1–3), 170–178. <https://doi.org/10.1016/j.foreco.2006.09.044>
- Dobbs, C., Kendal, D., & Nitschke, C. R. (2014). Multiple ecosystem services and disservices of the urban forest establishing their connections with landscape structure and sociodemographics. In *Ecological Indicators* (Vol. 43, pp. 44–55). <https://doi.org/10.1016/j.ecolind.2014.02.007>
- Fair, B. A. ;, Metzger, J. D., & Vent, J. (2012). Characterization of physical, gaseous, and hydrologic properties of compacted subsoil and its effects on growth and transpiration of two maples grown under greenhouse conditions. *Arboriculture & Urban Forestry*, 38, 151–159. <https://www.cabdirect.org/cabdirect/abstract/20123266512>
- Fang, C. F., & Ling, D. L. (2003). Investigation of the noise reduction provided by tree belts. *Landscape and Urban Planning*, 63(4), 187–195. [https://doi.org/10.1016/S0169-2046\(02\)00190-1](https://doi.org/10.1016/S0169-2046(02)00190-1)
- Fletcher, T. D., Andrieu, H., & Hamel, P. (2013). Understanding, management and modelling of urban hydrology and its consequences for receiving waters: A state of the art. *Advances in Water Resources*, 51, 261–279. <https://doi.org/10.1016/j.advwatres.2012.09.001>
- Ford, C. R., McGuire, M. A., Mitchell, R. J., & Teskey, R. O. (2004). Assessing variation in the radial profile of sap flux density in Pinus species and its effect on daily water use. In *Tree Physiology* (Vol. 24, Issue 3). Oxford Academic. <https://doi.org/10.1093/TREEPHYS/24.3.241>
- Galenieks, A. (2017). Importance of urban street tree policies: A Comparison of neighbouring

- Southern California cities. *Urban Forestry and Urban Greening*, 22, 105–110.
<https://doi.org/10.1016/j.ufug.2017.02.004>
- Gash", J. H. C., Lloyd, C. R., & Lachaudb, G. (1995). Estimating sparse forest rainfall interception with an analytical model. In *Journal of Hydrology* (Vol. 170).
- Gash, J. (1979). An Analytical Model of Rainfall Interception by Forests. *Quarterly Journal of the Royal Meteorological Society* Vol.105, No.443, p 43-55, January 1979.3 Fig, 1 Tab, 22 Ref, 105(443).
- Gotsch, S. G., Draguljić, D., & Williams, C. J. (2018). Evaluating the effectiveness of urban trees to mitigate storm water runoff via transpiration and stemflow. *Urban Ecosystems*, 21(1), 183–195. <https://doi.org/10.1007/s11252-017-0693-y>
- Granier, A. (1987). Evaluation of transpiration in a Douglas-fir stand by means of sap flow measurements. *Tree Physiology*, 3(4), 309–320.
<https://doi.org/10.1093/TREEPHYS/3.4.309>
- Green, S., Clothier, B., & Jardine, B. (2003). Theory and Practical Application of Heat Pulse to Measure Sap Flow. *Agronomy Journal*, 95(6), 1371–1379.
<https://doi.org/10.2134/agronj2003.1371>
- Green, S. R., McNaughton, K. G., & Clothier, B. E. (1989). Observations of night-time water use in kiwifruit vines and apple trees. *Agricultural and Forest Meteorology*, 48(3–4), 251–261.
[https://doi.org/10.1016/0168-1923\(89\)90072-5](https://doi.org/10.1016/0168-1923(89)90072-5)
- Green, W. H. (1911). GA Ampt. *Studies in Soil Physics, J. Agric. Sci*, 4, 1–24.
- Gregory McPherson, E. (1992). Accounting for benefits and costs of urban greenspace. *Landscape and Urban Planning*, 22(1), 41–51. [https://doi.org/10.1016/0169-2046\(92\)90006-L](https://doi.org/10.1016/0169-2046(92)90006-L)
- Grey, V., Livesley, S. J., Fletcher, T. D., & Szota, C. (2018). Tree pits to help mitigate runoff in dense urban areas. *Journal of Hydrology*, 565, 400–410.
<https://doi.org/10.1016/j.jhydrol.2018.08.038>
- Guevara-Escobar, A., González-Sosa, E., Véliz-Chávez, C., Ventura-Ramos, E., & Ramos-Salinas, M. (2007). Rainfall interception and distribution patterns of gross precipitation around an isolated *Ficus benjamina* tree in an urban area. *Journal of Hydrology*, 333(2–4), 532–541. <https://doi.org/10.1016/j.jhydrol.2006.09.017>
- Hacke, U. G., Sperry, J. S., Wheeler, J. K., & Castro, L. (2006). Scaling of angiosperm xylem structure with safety and efficiency. *Tree Physiology*, 26(6), 689–701.
<https://doi.org/10.1093/TREEPHYS/26.6.689>
- Hahs, A. K., McDonnell, M. J., McCarthy, M. A., Vesk, P. A., Corlett, R. T., Norton, B. A., Clemants, S. E., Duncan, R. P., Thompson, K., Schwartz, M. W., & Williams, N. S. G. (2009). A global synthesis of plant extinction rates in urban areas. *Ecology Letters*, 12(11),

1165–1173. <https://doi.org/10.1111/j.1461-0248.2009.01372.x>

- Helvey, J. D., & Patric, J. H. (1965). Canopy and litter interception of rainfall by hardwoods of eastern United States. In *Water Resources Research* (Vol. 1, Issue 2, pp. 193–206). <https://doi.org/10.1029/WR001i002p00193>
- Hepcan, C. C., & Hepcan, S. (2017). Assessing ecosystem services of the inciralti urban forest. *13th International MEDCOAST Congress on Coastal and Marine Sciences, Engineering, Management and Conservation, MEDCOAST 2017, 1*, 535–546.
- Hölscher, D., Koch, O., Korn, S., & Leuschner, C. (2005). Sap flux of five co-occurring tree species in a temperate broad-leaved forest during seasonal soil drought. *Trees - Structure and Function*, *19*(6), 628–637. <https://doi.org/10.1007/s00468-005-0426-3>
- Huang, J. Y., Black, T. A., Jassal, R. S., & Lavkulich, L. M. L. (2017). Modelling rainfall interception by urban trees. *Canadian Water Resources Journal*, *42*(4), 336–348. <https://doi.org/10.1080/07011784.2017.1375865>
- James, S. A., Clearwater, M. J., Meinzer, F. C., & Goldstein, G. (2002). Heat dissipation sensors of variable length for the measurement of sap flow in trees with deep sapwood. In *Tree Physiology* (Vol. 22, Issue 4). Oxford Academic. <https://doi.org/10.1093/TREEPHYS/22.4.277>
- Jim, C. Y., & Chen, W. Y. (2008). Assessing the ecosystem service of air pollutant removal by urban trees in Guangzhou (China). *Journal of Environmental Management*, *88*(4), 665–676. <https://doi.org/10.1016/j.jenvman.2007.03.035>
- Kabisch, N. (2015). Ecosystem service implementation and governance challenges in urban green space planning-The case of Berlin, Germany. *Land Use Policy*, *42*, 557–567. <https://doi.org/10.1016/j.landusepol.2014.09.005>
- Kalnay, E., & Cai, M. (2003). Impact of urbanization and land-use change on climate. *Nature*, *423*(6939), 528–531. <https://doi.org/10.1038/nature01675>
- Kim, H. W., & Park, Y. (2016). Urban green infrastructure and local flooding: The impact of landscape patterns on peak runoff in four Texas MSAs. *Applied Geography*, *77*, 72–81. <https://doi.org/10.1016/j.apgeog.2016.10.008>
- Kirkham, M. (2014). *Principles of soil and plant water relations*. <https://books.google.com/books?hl=en&lr=&id=Y5r8AgAAQBAJ&oi=fnd&pg=PP1&dq=principles+of+soil+and+plant+water+relations&ots=kaxeG5v8ys&sig=Y1Pw1NhwbCeW4C6t624AqaOkD4w>
- Kjelgren, R., & Montague, T. (1998). Urban tree transpiration over turf and asphalt surfaces. *Atmospheric Environment*, *32*(1), 35–41. [https://doi.org/10.1016/S1352-2310\(97\)00177-5](https://doi.org/10.1016/S1352-2310(97)00177-5)
- Kottek, M., Grieser, J., Beck, C., Rudolf, B., & Rubel, F. (2006). World map of the Köppen-Geiger climate classification updated. *Meteorologische Zeitschrift*, *15*(3), 259–263.

<https://doi.org/10.1127/0941-2948/2006/0130>

- Kuehler, E., Hathaway, J., & Tirpak, A. (2017). Quantifying the benefits of urban forest systems as a component of the green infrastructure stormwater treatment network. *Ecohydrology*, *10*(3), e1813.
- Levia, D. F., Nanko, K., Amasaki, H., Giambelluca, T. W., Hotta, N., Iida, S., Mudd, R. G., Nullet, M. A., Sakai, N., Shinohara, Y., Sun, X., Suzuki, M., Tanaka, N., Tantasirin, C., & Yamada, K. (2019). Throughfall partitioning by trees. *Hydrological Processes*, *33*(12), 1698–1708. <https://doi.org/10.1002/hyp.13432>
- Linhoss, A. C., & Siegert, C. M. (2016). A comparison of five forest interception models using global sensitivity and uncertainty analysis. *Journal of Hydrology*, *538*, 109–116. <https://doi.org/10.1016/j.jhydrol.2016.04.011>
- LITVAK, E., MCCARTHY, H. R., & PATAKI, D. E. (2011). Water relations of coast redwood planted in the semi-arid climate of southern California. *Plant, Cell & Environment*, *34*(8), 1384–1400. <https://doi.org/10.1111/j.1365-3040.2011.02339.x>
- Liu, X., & Chang, Q. (2019). The Rainfall Interception Performance of Urban Tree Canopy in Beijing, China. In *Green Energy and Technology*. https://doi.org/10.1007/978-3-319-99867-1_8
- Liu, Y. B., & De Smedt, F. (2004). *WetSpa Extension, A GIS-based Hydrologic Model for Flood Prediction and Watershed Management Documentation and User Manual*.
- Livesley, S. J., Baudinette, B., & Glover, D. (2014). Rainfall interception and stem flow by eucalypt street trees - The impacts of canopy density and bark type. *Urban Forestry and Urban Greening*, *13*(1), 192–197. <https://doi.org/10.1016/j.ufug.2013.09.001>
- Livesley, S. J., McPherson, G. M., & Calfapietra, C. (2016). The urban forest and ecosystem services: Impacts on urban water, heat, and pollution cycles at the tree, street, and city scale. *Journal of Environmental Quality*, *45*(1), 119–124. <https://doi.org/10.2134/jeq2015.11.0567>
- Lockaby, G., Nagy, C., Vose, J., Ford, C., ... G. S.-... : U.-F. S., & 2013, U. (2013). Forests and water. *Fs.Usda.Gov*. <https://www.fs.usda.gov/treearch/pubs/download/44214.pdf>
- Macinnis-Ng, C. M. O., Flores, E. E., Müller, H., & Schwendenmann, L. (2014). Throughfall and stemflow vary seasonally in different land-use types in a lower montane tropical region of Panama. *Hydrological Processes*, *28*(4), 2174–2184. <https://doi.org/10.1002/hyp.9754>
- Maco, S. E., & Mcpherson, E. G. (2002). ASSESSING CANOPY COVER OVER STREETS AND SIDEWALKS IN STREET TREE POPULATIONS. In *Journal of Arboriculture*. *28*(6): 270-276 (Vol. 28, Issue 6).
- Magliano, P. N., Whitworth-Hulse, J. I., & Baldi, G. (2019). Interception, throughfall and stemflow partition in drylands: Global synthesis and meta-analysis. In *Journal of Hydrology* (Vol. 568, pp. 638–645). <https://doi.org/10.1016/j.jhydrol.2018.10.042>

- Marin, C. T., Bouten, W., & Sevink, J. (2000). Gross rainfall and its partitioning into throughfall, stemflow and evaporation of intercepted water in four forest ecosystems in western Amazonia. *Journal of Hydrology*, 237(1–2), 40–57. [https://doi.org/10.1016/S0022-1694\(00\)00301-2](https://doi.org/10.1016/S0022-1694(00)00301-2)
- Martin, T. A., Brown, K. J., Cermák, J., Ceulemans, R., Kucera, J., Meinzer, F. C., Rombold, J. S., Sprugel, D. G., & Hinckley, T. M. (1997). Crown conductance and tree and stand transpiration in a second-growth *Abies amabilis* forest. In *Can. J. For. Res* (Vol. 27).
- Matteo, M., Randhir, T., & Bloniarz, D. (2006). Watershed-Scale Impacts of Forest Buffers on Water Quality and Runoff in Urbanizing Environment. *Journal of Water Resources Planning and Management*, 132(3), 144–152. [https://doi.org/10.1061/\(ASCE\)0733-9496\(2006\)132:3\(144\)](https://doi.org/10.1061/(ASCE)0733-9496(2006)132:3(144))
- McDonnell, M., Pickett, S., Groffman, P., Bohlen, P., Pouyat, R., Zipperer, W., Parmelee, R., Carreiro, M., & Medley, K. (1997). Ecosystem processes along an urban-to-rural gradient. *Urban Ecosystems*, 1(1), 21–36. <https://doi.org/1014359024275>
- McPherson, E. Gregory, Simpson, J. R., Xiao, Q., & Wu, C. (2011). Million trees Los Angeles canopy cover and benefit assessment. *Landscape and Urban Planning*, 99(1), 40–50. <https://doi.org/10.1016/j.landurbplan.2010.08.011>
- McPherson, E.G., Simpson, J. R., Xiao, Q., & Wu, C. (2011). Million trees Los Angeles canopy cover and benefit assessment. *Landscape and Urban Planning*, 99(1), 40–50. <https://doi.org/10.1016/j.landurbplan.2010.08.011>
- McPherson, G. E., Simpson, J. R., Xiao, Q., & Chunxia, W. (2008). Los Angeles 1-Million tree canopy cover assessment. In *Gen. Tech. Rep. PSW-GTR-207*. Albany, CA: U.S. Department of Agriculture, Forest Service, Pacific Southwest Research Station. 52 p (Vol. 207). <https://doi.org/10.2737/PSW-GTR-207>
- Mittman, T. S., Band, L. E., Berke, P. R., & Dolye, M. W. (2009). *Assessing the Impact of the Urban Tree Canopy on Streamflow Response: An Extension of Physically Based Hydrologic Modeling to the Suburban Landscape*.
- Monteith, J. L. (1965). Evaporation and environment. In *Symposia of the Society for Experimental Biology* (Vol. 19, pp. 205–234). <https://repository.rothamsted.ac.uk/item/8v5v7/evaporation-and-environment>
- Mwiya, R. M. (2013). Parabolic Channel Design. *International Journal of Scientific & Engineering Research*, 4(4). <http://www.ijser.org>
- Nanko, K., Hotta, N., & Suzuki, M. (2006). Evaluating the influence of canopy species and meteorological factors on throughfall drop size distribution. *Journal of Hydrology*, 329(3–4), 422–431. <https://doi.org/10.1016/j.jhydrol.2006.02.036>
- Nash, J. E., & Sutcliffe, J. V. (1970). River flow forecasting through conceptual models part I - A discussion of principles. *Journal of Hydrology*, 10(3), 282–290.

[https://doi.org/10.1016/0022-1694\(70\)90255-6](https://doi.org/10.1016/0022-1694(70)90255-6)

- Niemelä, J. (1999). Ecology and urban planning. *Biodiversity and Conservation*, 8(1), 119–131. <https://doi.org/10.1023/A:1008817325994>
- Noilhan, J., & Planton, S. (1989). A simple parameterization of land surface processes for meteorological models. *Monthly Weather Review*, 117(3), 536–549. [https://doi.org/10.1175/1520-0493\(1989\)117<0536:ASPOLS>2.0.CO;2](https://doi.org/10.1175/1520-0493(1989)117<0536:ASPOLS>2.0.CO;2)
- Nowak, D. J., Bodine, A. R., Hoehn, R. E., Crane, D. E., Ellis, A., Endreny, T. A., Yang, Y., Jacobs, T., & Shelton, K. (2013). Assessing Urban Forest Effects and Values : the Greater Kansas City Region. In *fs.usda.gov*. <https://www.fs.usda.gov/treearch/pubs/42931>
- Nowak, D. J., & Crane, D. E. (2002). Carbon storage and sequestration by urban trees in the USA. *Environmental Pollution*, 116(3), 381–389. [https://doi.org/10.1016/S0269-7491\(01\)00214-7](https://doi.org/10.1016/S0269-7491(01)00214-7)
- Nyelele, C., Kroll, C. N., & Nowak, D. J. (2019). Present and future ecosystem services of trees in the Bronx, NY. *Urban Forestry and Urban Greening*, 42, 10–20. <https://doi.org/10.1016/j.ufug.2019.04.018>
- Nytch, C. J., Meléndez-Ackerman, E. J., Pérez, M.-E., & Ortiz-Zayas, J. R. (2019). Rainfall interception by six urban trees in San Juan, Puerto Rico. *Urban Ecosystems*, 22(1), 103–115.
- Pataki, D. E., McCarthy, H. R., Litvak, E., & Pincetl, S. (2011). Transpiration of urban forests in the Los Angeles metropolitan area. *Ecological Applications*, 21(3), 661–677. <https://doi.org/10.1890/09-1717.1>
- Paul, M. J., & Meyer, J. L. (2001). Streams in the Urban Landscape. *Annual Review of Ecology and Systematics*, 32(1), 333–365. <https://doi.org/10.1146/annurev.ecolsys.32.081501.114040>
- Peters, E. B., McFadden, J. P., & Montgomery, R. A. (2010). Biological and environmental controls on tree transpiration in a suburban landscape. *Journal of Geophysical Research*, 115(G4). <https://doi.org/10.1029/2009JG001266>
- Rana, G., De Lorenzi, F., Mazza, G., Martinelli, N., Muschitiello, C., & Ferrara, R. M. (2020). Tree transpiration in a multi-species Mediterranean garden. *Agricultural and Forest Meteorology*, 280, 107767. <https://doi.org/10.1016/j.agrformet.2019.107767>
- Riikonen, A., Järvi, L., & Nikinmaa, E. (2016). Environmental and crown related factors affecting street tree transpiration in Helsinki, Finland. *Urban Ecosystems*, 19(4), 1693–1715. <https://doi.org/10.1007/s11252-016-0561-1>
- Risken, H. (1996). *Fokker-Planck Equation* (pp. 63–95). Springer, Berlin, Heidelberg. https://doi.org/10.1007/978-3-642-61544-3_4

- Roth, B. E., Slatton, K. C., & Cohen, M. J. (2007). On the potential for high-resolution lidar to improve rainfall interception estimates in forest ecosystems. *Frontiers in Ecology and the Environment*, 5(8), 421–428. <https://doi.org/10.1890/060119.1>
- Rutter, A. J., Kershaw, K. A., Robins, P. C., & Morton, A. J. (1971). A predictive model of rainfall interception in forests, 1. Derivation of the model from observations in a plantation of Corsican pine. *Agricultural Meteorology*, 9(C), 367–384. [https://doi.org/10.1016/0002-1571\(71\)90034-3](https://doi.org/10.1016/0002-1571(71)90034-3)
- Rutter, A. J., Morton, A. J., & Robins, P. C. (1975). A predictive model of rainfall interception in forests. II. Generalization of the model and comparison with observations in some coniferous and hardwood stands. *Journal of Applied Ecology*, 367–380.
- Sadeghi, S. M. M., Attarod, P., Van Stan, J. T., & Pypker, T. G. (2016). The importance of considering rainfall partitioning in afforestation initiatives in semiarid climates: A comparison of common planted tree species in Tehran, Iran. *Science of the Total Environment; Science of the Total Environment*, 568, 845–855. <https://doi.org/10.1016/j.scitotenv.2016.06.048>
- Sanders, R. A. (1986). Urban vegetation impacts on the hydrology of Dayton, Ohio. *Urban Ecology*, 9(3–4), 361–376. [https://doi.org/10.1016/0304-4009\(86\)90009-4](https://doi.org/10.1016/0304-4009(86)90009-4)
- Santos Alves, et all. (2014). Forest Biology and Biogeochemistry. In *Igarss 2014* (Issue 1). <https://doi.org/10.1007/s13398-014-0173-7.2>
- Schellekens, J. (2000). The interception and runoff generating processes in the Bisley catchment, luquillo experimental forest, Puerto Rico. *Physics and Chemistry of the Earth, Part B: Hydrology, Oceans and Atmosphere*, 25(7–8), 659–664. [https://doi.org/10.1016/s1464-1909\(00\)00081-2](https://doi.org/10.1016/s1464-1909(00)00081-2)
- Seitz, J., & Escobedo, F. (2008). Urban Forests in Florida: Trees Control Stormwater Runoff and Improve Water Quality. *EDIS*, 2008(5).
- Service, F., McPherson, E. G., Simpson, J. R., Xiao, Q., & Wu, C. (2008). United States Department of Agriculture Los Angeles 1-Million Tree Canopy Cover Assessment. In *fs.usda.gov*. <https://www.fs.usda.gov/treesearch/pubs/29402>
- Smets, V., Wirion, C., Bauwens, W., Hermy, M., Somers, B., & Verbeiren, B. (2019). The importance of city trees for reducing net rainfall: comparing measurements and simulations. *Hydrol. Earth Syst. Sci*, 23, 3865–3884. <https://doi.org/10.5194/hess-23-3865-2019>
- Soares, A. L., Rego, F. C., McPherson, E. G., Simpson, J. R., Peper, P. J., & Xiao, Q. (2011). Benefits and costs of street trees in Lisbon, Portugal. *Urban Forestry & Urban Greening*, 10(2), 69–78.
- Šraj, M., Brilly, M., & Mikoš, M. (2008). Rainfall interception by two deciduous Mediterranean forests of contrasting stature in Slovenia. *Agricultural and Forest Meteorology*, 148(1), 121–134. <https://doi.org/10.1016/j.agrformet.2007.09.007>

- Staelens, J., De Schrijver, A., Verheyen, K., & Verhoest, N. E. C. (2008). Rainfall partitioning into throughfall, stemflow, and interception within a single beech (*Fagus sylvatica* L.) canopy: influence of foliation, rain event characteristics, and meteorology. *Hydrological Processes*, 22(1), 33–45. <https://doi.org/10.1002/hyp.6610>
- Stovin, V. R., Jorgensen, A., & Clayden, A. (2008a). Street trees and stormwater management. *Arboricultural Journal*, 30(4), 297–310. <https://doi.org/10.1080/03071375.2008.9747509>
- Stovin, V. R., Jorgensen, A., & Clayden, A. (2008b). Street trees and stormwater management. *Arboricultural Journal*, 30(4), 297–310. <https://doi.org/10.1080/03071375.2008.9747509>
- Tan, Z., Lau, K. K. L., & Ng, E. (2016). Urban tree design approaches for mitigating daytime urban heat island effects in a high-density urban environment. *Energy and Buildings*, 114, 265–274. <https://doi.org/10.1016/j.enbuild.2015.06.031>
- Taneda, H., & Sperry, J. S. (2008). A case-study of water transport in co-occurring ring- versus diffuse-porous trees: contrasts in water-status, conducting capacity, cavitation and vessel refilling. *Tree Physiology*, 28(11), 1641–1651. <https://doi.org/10.1093/TREEPHYS/28.11.1641>
- Tavakol, A., Rahmani, V., & Harrington, J. (2020a). Changes in the frequency of hot, humid days and nights in the Mississippi River Basin. *International Journal of Climatology*, joc.6484. <https://doi.org/10.1002/joc.6484>
- Tavakol, A., Rahmani, V., & Harrington, J. (2020b). Evaluation of hot temperature extremes and heat waves in the Mississippi River Basin. *Atmospheric Research*, 239, 104907. <https://doi.org/10.1016/j.atmosres.2020.104907>
- Taylor, M. S., Wheeler, B. W., White, M. P., Economou, T., & Osborne, N. J. (2015). Research note: Urban street tree density and antidepressant prescription rates—A cross-sectional study in London, UK. *Landscape and Urban Planning*, 136, 174–179. <https://doi.org/10.1016/j.landurbplan.2014.12.005>
- Tirpak, R. A., Hathaway, J. M., & Franklin, J. A. (2018). Evaluating the influence of design strategies and meteorological factors on tree transpiration in bioretention suspended pavement practices. *Ecohydrology*, 11(8). <https://doi.org/10.1002/eco.2037>
- Tobaa, T., & Ohtaa, T. (2005). An observational study of the factors that influence interception loss in boreal and temperate forests. In *Journal of Hydrology* (Vol. 313, Issues 3–4, pp. 208–220).
- Van Stan, J. T., Levia, D. F., & Jenkins, R. B. (2015a). Forest Canopy Interception Loss Across Temporal Scales: Implications for Urban Greening Initiatives. *The Professional Geographer*, 67(1), 41–51. <https://doi.org/10.1080/00330124.2014.888628>
- Van Stan, J. T., Levia, D. F., & Jenkins, R. B. (2015b). Forest Canopy Interception Loss Across Temporal Scales: Implications for Urban Greening Initiatives. *Professional Geographer*, 67(1), 41–51. <https://doi.org/10.1080/00330124.2014.888628>

- Van Stan, J. T., Van Stan, J. H., & Levia, D. F. (2014). Meteorological influences on stemflow generation across diameter size classes of two morphologically distinct deciduous species. *International Journal of Biometeorology*, *58*(10), 2059–2069. <https://doi.org/10.1007/s00484-014-0807-7>
- Véliz-Chávez, C., Mastachi-Loza, C. A., González-Sosa, E., Becerril-Piña, R., & Ramos-Salinas, N. M. (2014). Canopy Storage Implications on Interception Loss Modeling. In *American Journal of Plant Sciences* (Vol. 05, Issue 20, pp. 3032–3048). <https://doi.org/10.4236/ajps.2014.520320>
- Walker, J. S., Grimm, N. B., Briggs, J. M., Gries, C., & Dugan, L. (2009). Effects of urbanization on plant species diversity in central Arizona. *Frontiers in Ecology and the Environment*, *7*(9), 465–470. <https://doi.org/10.1890/080084>
- Walsh, C. J., Fletcher, T. D., & Ladson, A. R. (2005). Stream restoration in urban catchments through redesigning stormwater systems: Looking to the catchment to save the stream. *Journal of the North American Benthological Society*, *24*(3), 690–705. <https://doi.org/10.1899/04-020.1>
- Wang, H., Ouyang, Z., Chen, W., Wang, X., Zheng, H., & Ren, Y. (2011). Water, heat, and airborne pollutants effects on transpiration of urban trees. *Environmental Pollution*, *159*(8–9), 2127–2137. <https://doi.org/10.1016/j.envpol.2011.02.031>
- Wang, H., Wang, X., Zhao, P., Zheng, H., Ren, Y., Gao, F., & Ouyang, Z. (2012). Transpiration rates of urban trees, *Aesculus chinensis*. *Journal of Environmental Sciences (China)*, *24*(7), 1278–1287. [https://doi.org/10.1016/S1001-0742\(11\)60937-6](https://doi.org/10.1016/S1001-0742(11)60937-6)
- Wang, J., Endreny, T. A., & Nowak, D. J. (2008a). Mechanistic simulation of tree effects in an urban water balance model. *Journal of the American Water Resources Association*, *44*(1), 75–85. <https://doi.org/10.1111/j.1752-1688.2007.00139.x>
- Wang, J., Endreny, T. A., & Nowak, D. J. (2008b). Mechanistic Simulation of Tree Effects in an Urban Water Balance Model ¹. *JAWRA Journal of the American Water Resources Association*, *44*(1), 75–85. <https://doi.org/10.1111/j.1752-1688.2007.00139.x>
- Wang, X., Yao, J., Yu, S., Miao, C., Chen, W., & He, X. (2018). Street trees in a Chinese forest city: Structure, benefits and costs. *Sustainability*, *10*(3), 674.
- Wang, Z. H., Zhao, X., Yang, J., & Song, J. (2016). Cooling and energy saving potentials of shade trees and urban lawns in a desert city. *Applied Energy*, *161*, 437–444. <https://doi.org/10.1016/j.apenergy.2015.10.047>
- Whitford, V., Ennos, A. R., & Handley, J. F. (2001). “City form and natural process” - Indicators for the ecological performance of urban areas and their application to Merseyside, UK. *Landscape and Urban Planning*, *57*(2), 91–103. [https://doi.org/10.1016/S0169-2046\(01\)00192-X](https://doi.org/10.1016/S0169-2046(01)00192-X)
- Wullschlegel, S. D., Meinzer, F. C., & Vertessy, R. A. (1998a). A review of whole-plant water

- use studies in tree. *Tree Physiology*, 18(8_9), 499–512.
<https://doi.org/10.1093/treephys/18.8-9.499>
- Wullschleger, S. D., Meinzer, F. C., & Vertessy, R. A. (1998b). A review of whole-plant water use studies in tree. *Tree Physiology*, 18(8–9), 499–512.
<https://doi.org/10.1093/TREEPHYS/18.8-9.499>
- Wullschleger, S. D., Wilson, K. B., & Hanson, P. J. (2000). Environmental control of whole-plant transpiration, canopy conductance and estimates of the decoupling coefficient for large red maple trees. *Agricultural and Forest Meteorology*, 104(2), 157–168.
[https://doi.org/10.1016/S0168-1923\(00\)00152-0](https://doi.org/10.1016/S0168-1923(00)00152-0)
- Xiao, Q. (2000). A new approach to modeling tree rainfall interception. *Journal of Geophysical Research Atmospheres*, 105(D23), 29173–29188. <https://doi.org/10.1029/2000JD900343>
- Xiao, Q., & McPherson, E. (2011a). Rainfall interception of three trees in Oakland, California. *Urban Ecosystems*, 14(4), 755–769. <https://doi.org/10.1007/s11252-011-0192-5>
- Xiao, Q., & McPherson, E. G. (2011). Performance of engineered soil and trees in a parking lot bioswale. *Urban Water Journal*, 8(4), 241–253.
<https://doi.org/10.1080/1573062X.2011.596213>
- Xiao, Q., & McPherson, E. G. (2016). Surface Water Storage Capacity of Twenty Tree Species in Davis, California. *Journal of Environmental Quality*, 45(1), 188–198.
<https://doi.org/10.2134/jeq2015.02.0092>
- Xiao, Q., McPherson, E. G., Ustin, S. L., Grismer, M. E., & Simpson, J. R. (2000). Winter rainfall interception by two mature open-grown trees in Davis, California. *Hydrological Processes*, 14(4), 763–784. [https://doi.org/10.1002/\(SICI\)1099-1085\(200003\)14:4<763::AID-HYP971>3.0.CO;2-7](https://doi.org/10.1002/(SICI)1099-1085(200003)14:4<763::AID-HYP971>3.0.CO;2-7)
- Xiao, Q., & McPherson, G. G. (2011b). Rainfall interception of three trees in Oakland, California. *Urban Ecosystems*, 14(4), 755–769. <https://doi.org/10.1007/s11252-011-0192-5>
- Yang, B., Lee, D. K., Heo, H. K., & Biging, G. (2019). The effects of tree characteristics on rainfall interception in urban areas. *Landscape and Ecological Engineering*, 15(3), 289–296. <https://doi.org/10.1007/s11355-019-00383-w>
- Yao, L., Chen, L., Wei, W., & Sun, R. (2015). Potential reduction in urban runoff by green spaces in Beijing: A scenario analysis. *Urban Forestry and Urban Greening*, 14(2), 300–308. <https://doi.org/10.1016/j.ufug.2015.02.014>
- Zabret, K., Rakovec, J., & Šraj, M. (2018). Influence of meteorological variables on rainfall partitioning for deciduous and coniferous tree species in urban area. *Journal of Hydrology*, 558, 29–41. <https://doi.org/10.1016/j.jhydrol.2018.01.025>
- Zabret, K., & Šraj, M. (2018). Spatial variability of throughfall under single birch and pine tree canopies. *Acta Hydrotechnica*, 1–20. <https://doi.org/10.15292/acta.hydro.2018.01>

Zabret, K., & Šraj, M. (2019). Rainfall Interception by Urban Trees and Their Impact on Potential Surface Runoff. *Clean - Soil, Air, Water*, 47(8).
<https://doi.org/10.1002/clen.201800327>

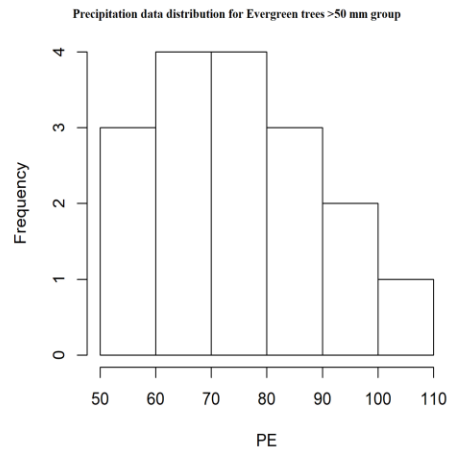
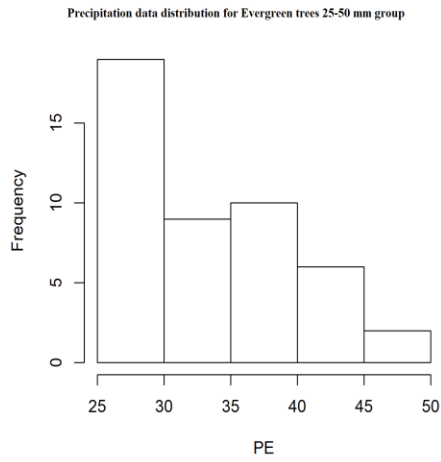
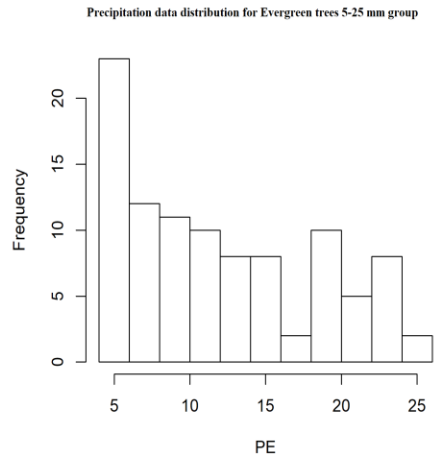
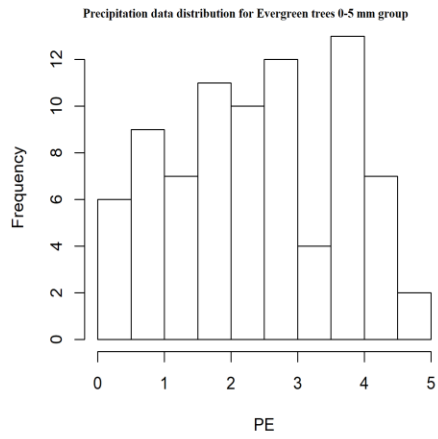
Appendix A - Rainfall partitioning: Characterization of rainfall events, and additional information on canopy structure of the studied trees and their surrounding area

1. Rainfall event characterization

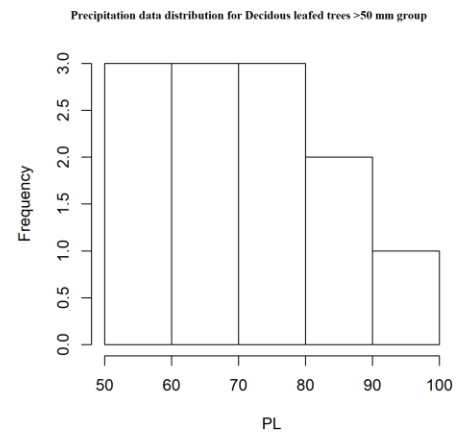
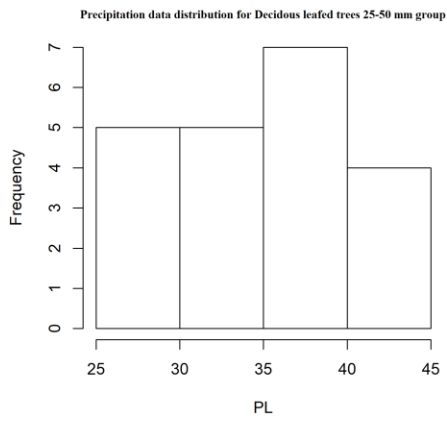
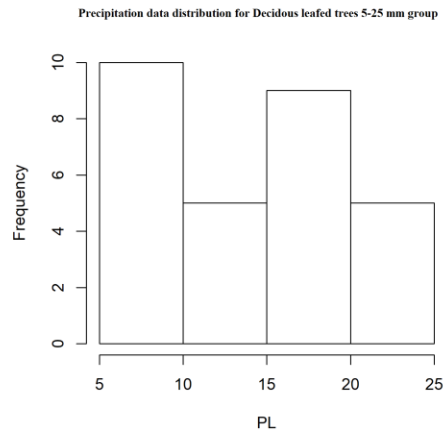
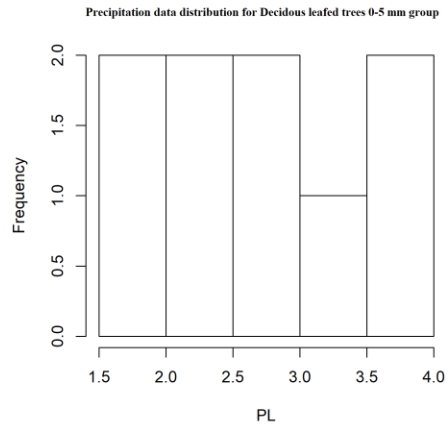
Figure to illustrate the distribution of rainfall events compiled in the analysis to help support the selection of rainfall classes.

a) Data distribution histograms

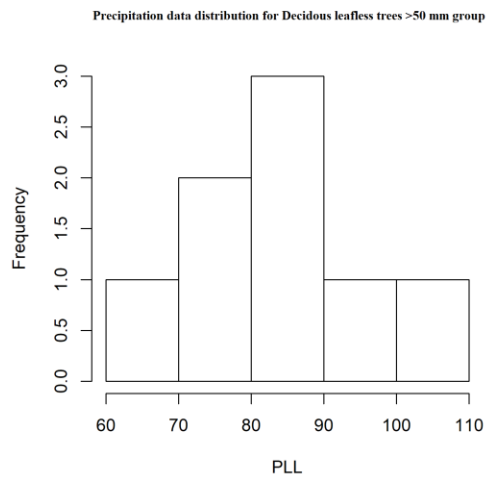
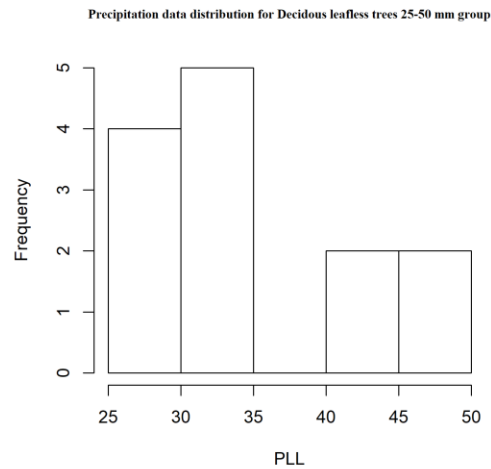
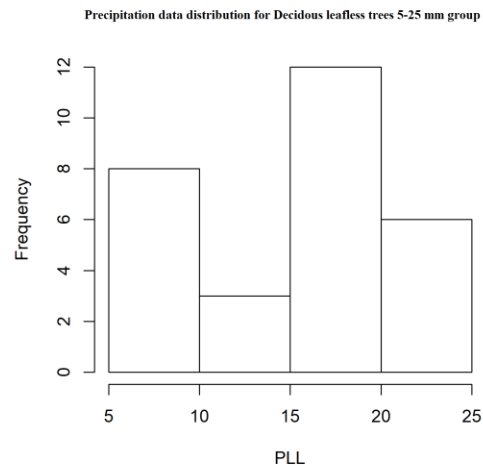
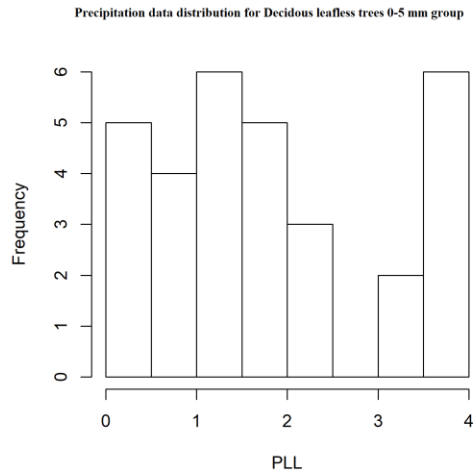
Note: In the graphs below PE is a short form of precipitation events for Evergreen trees, PL is a short form of precipitation for deciduous Leafed trees, and PLL is a short form of precipitation for deciduous leafless trees



Histograms of precipitation data distribution for evergreen trees



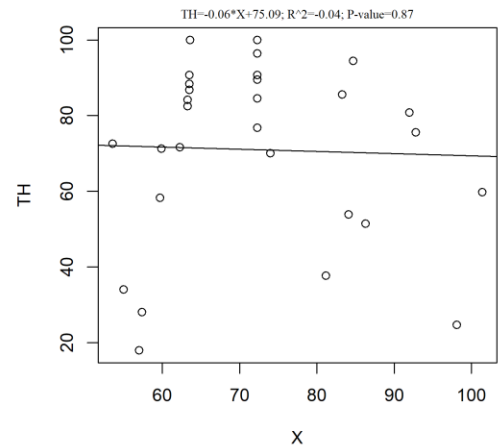
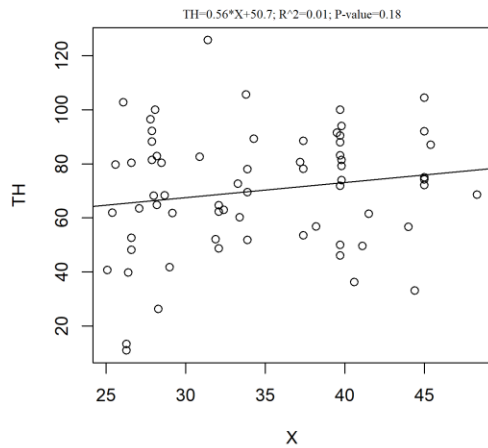
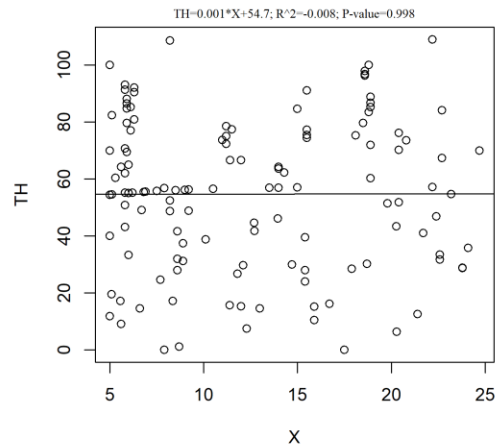
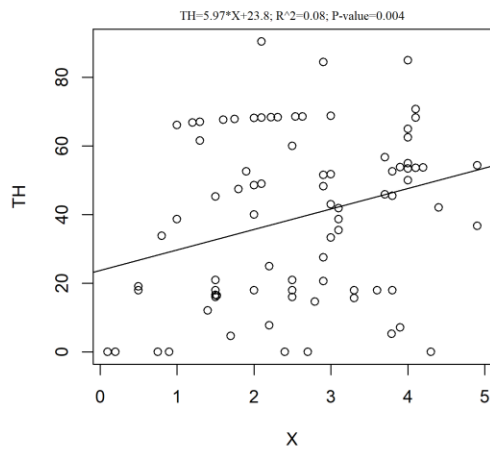
Histograms of precipitation data distribution for deciduous leafed trees



Histograms of precipitation data distribution for deciduous leafless trees

- b) Description of regression analysis completed to ensure that there was no significant relationship between % throughfall and precipitation depth for each rainfall class.

A plotted throughfall-precipitation rate versus precipitation depth and an applied linear regression model indicated a non-significant p-value (except for rainfall group of 0-5 mm) along with near to zero coefficient for all the linear regression lines. The coefficient of determination (R^2) and p-values for 0-5, 5-25, 25-50, and above 50mm were ($R^2=0.08$, $p=0.003$), ($R^2=-0.008$, $p=0.99$), ($R^2=0.01$, $p=0.18$), and ($R^2=-0.04$, $p=0.87$) respectively. This result supported the proper selection of rainfall classes in the study and was also used for LAI analysis in section 3.2.



Precipitation (X) against precipitation to throughfall percentage (TH) for each rainfall class. The equations, R squared, and p-values are provided on the top of each graph for the associated group

- Summary of rainfall and throughfall attributes, canopy structure characteristics, the landscape, the type of species and tree phenology type for each precipitation partitioning dataset included in this analysis.

Table A.6-1 - Canopy structure, landscape, and rainfall features of final selected studies based on an event-based rainfall evaluation

Study	Species	Tree type group	No. of assessed events	Canopy structure			Landscape condition	Rainfall & throughfall summary			
				Leaf Area Index	Bark & branches characteristics	Leaf characteristics		Total rainfall (mm)	Total throughfall (mm)	Maximum rainfall (mm)	Minimum rainfall (mm)
Xiao et al. 2000	Pear (<i>Pyrus calleryana</i>)	Deciduous-leafless	19	0	*Rough bark, 22 cm (DBH)	Paraboloid crown	UC Davis campus, located in Central Valley California	39.4	23.45	9	0.2
Xiao et al. 2000	Oak (<i>Quercus suber</i>)	Evergreen	37	3.4	*Rough bark 12.5 cm (DBH)	Paraboloid crown	UC Davis campus, located in Central Valley California	169.3	92.1	15	0.1
Guevara-Escobar et al. 2007	<i>Ficus Benjamina</i>	Evergreen	19	N_M	22.4 (Crown diameter) Smooth bark, glabrous branches	Oblong, elliptic, lanceolate, ovate leaf shape	Urban zone of Queretaro City, Mexico, surrounded by several buildings (13 to 100m distance)	151.6	57.8	29.2	0.9
Asadian & Weiler. 2009	<i>Pseudotsuga menziesii</i> & <i>Thuja plicata</i>	Evergreen	12	N_M	*Rough bark 69.3-70.7 cm (DBH)	Structural integrity including tree	Highly urbanized area of North and	334.4	148.7	39.7	22.6

						crown and foliage density was assessed as two groups of poor and good	West Vancouver, residential, industrial and commercial area				
Xiao et al. 2011	<i>Ginko bibola</i> & <i>Liquidambar styraciflua</i>	Deciduous-leafless	29	0	*Rough bark 18.6 – 64.7 cm (DBH)	Paraboloid	Street tree of a residential area in Oakland, California	556.8	409.8	86.3	0.5
Xiao et al. 2011	<i>Ginko bibola</i> & <i>Liquidambar styraciflua</i>	Deciduous leafed	18	4.7-5.2	*Rough bark 18.6 – 64.7 cm (DBH)	Paraboloid	Street tree of a residential area in Oakland, California	349.8	211.7	45	1.5
Xiao et al. 2011	Lemon (<i>Citrus limon</i>)	Evergreen	23	3	*Smooth bark 10.1 cm (DBH)	Paraboloid	Street tree of a residential area in Oakland, California	441.2	260.8	86.3	0.5
Livesely et al. 2014	<i>Eucalyptus saligna</i> & <i>E. nicholii</i>	Evergreen	41	3.03-3.88	Smooth, grey bark to deeply thick, fissured bark	Leaves ranging from 1-2 cm wide to 6-123 cm wide	Burnley campus, University of Melbourne, Victoria, Australia	183.3	110.8	14.3	1
Véliz-Chávez et al. 2014	<i>Ficus Benjamina</i>	Evergreen	21	N_M	22.4 cm Crown diameter), Smooth bark, glabrous branches	Oblong, elliptic, lanceolate, ovate leaf shape	Urban zone of Queretaro City, Mexico, surrounded by several	203.35	55.35	28.3	0.75

							buildings (13 to 100m distance)				
Zabert et al. 2018	Birch (<i>Betula pendula Roth</i>)	Deciduous-leafless	33	0.8	17.9 cm (DBH), smooth bark, , upward branch inclination	Storage capacity 0.7 mm	Located in a park, Ljubljana, Slovenia	2010.8	1482	101.7	0.5
Zabert et al. 2018	Birch (<i>Betula pendula Roth</i>)	Deciduous leafed	23	2.6	17.9 cm (DBH), smooth bark, , upward branch inclination	Storage capacity 0.7 mm	Located in a park, Ljubljana, Slovenia	879.6	576.4	92	8.7
Zabert et al. 2018	Pine (<i>Pinus nigra Arnold</i>)	Evergreen	52	3.9	19cm (DBH), rough, thick, absorbent surface, downward branch inclination	Storage capacity 3.5 mm,	Located in a park, Ljubljana, Slovenia	1858.2	1158.2	101.4	4.3
Nytch et al. 2019	<i>Albizia procera</i>	Deciduous leafed	30	1.5	Smooth bark, 33.7 cm (DBH)	Sparse canopy with long, Bi-pinnate leaves	Highly urbanized watershed, North Botanical Garden of University of Puerto Rico-Rio Piedras San Juan, Puerto Rico	778.2	666	72.3	2.9
Nytch et al. 2019	<i>Calophyllum antillanum</i>	Evergreen	39	1.97	Rough bark, 28.2 cm (DBH)	Rounded canopy with elliptical leaves	Highly urbanized watershed, North Botanical	950.3	826.2	72.3	2.9

							Garden of University of Puerto Rico-Rio Piedras San Juan, Puerto Rico				
--	--	--	--	--	--	--	--	--	--	--	--

*= Bark texture not provided in study; was assigned using tree field guides and other literature sources; N_M = Not Measured in the study

Appendix B - Supplemental data for rainfall partitioning analysis

(double-click chart to link to complete data table in Microsoft Excel)

Precipitation deciduous leafless	Throughfall deciduous leafless	Precipitation deciduous leafed	Throughfall deciduous Leafed	Precipitation evergreen	Throughfall evergreen	Precipitation	Throughfall	Tree Group Type
27.3	25	45	33.75	26.6	21.36	27.3	25	TLL
28.3	26.3	33.9	23.5605	26.6	12.82	28.3	26.3	TLL
28.8	27.5	32.1	20.7366	39.7	19.85	28.8	27.5	TLL
29.7	27.5	45	33.39	39.7	18.26	29.7	27.5	TLL
30.7	27.5	33.9	17.5602	28.2	23.35	30.7	27.5	TLL
31.2	28.8	32.1	19.9983	28.2	18.25	31.2	28.8	TLL
31.2	30.6	27.9	24.6	26.3	2.87	31.2	30.6	TLL
31.2	32.5	27.9	22.7	26.3	3.5	31.2	32.5	TLL
31.7	33.2	39.8	31.5	29.18	18	31.7	33.2	TLL
40.3	36.9	39.7	34.9	45	32.445	40.3	36.9	TLL
43.2	38.1	39.5	36.1	33.9	26.442	43.2	38.1	TLL
46	38.1	39.8	37.4	32.1	15.6327	46	38.1	TLL
48.4	38.1	25.4	15.7	27.9	25.7	48.4	38.1	TLL

Appendix C- Supplemental data for transpiration analysis

(double-click chart to link to complete data table in Microsoft Excel)

		Js1	Sap flux	Solar radiation	Temperature
	136	133.2407	#NAME?	217.1166998	
	137	144.7147	144.7147	312.3446023	
	138	139.8583	139.8583	273.0253006	
	139	129.7053	129.7053	244.1771279	
	140	59.5274	59.5274	136.8927802	
	141	119.3304	119.3304	239.0354947	
	142	111.1638	111.1638	165.1408882	
	143	66.8054	66.8054	114.3622181	
	144	35.4672	35.4672	112.1865478	
	145	118.6625	118.6625	271.2304598	
	146	84.6761	84.6761	207.6096581	15.19845129
	147	119.7629	119.7629	334.4491434	16.2049697

Note: Data in Columns highlighted in yellow were used for analysis